Household Energy System Sizing Technique to Minimise Household Energy Cost and Estimate Optimal System Size

Brett J. Donnellan

March 29, 2022

Thesis submitted for the degree of
Doctor of Philosophy
in
Electrical Engineering
at The University of Adelaide
Faculty of Engineering, Computer and Mathematical Sciences
School of Electrical and Electronic Engineering

THE UNIVERSITY
of ADELAIDE

Contents

Abstract

The goal of this research is to analytically optimise a Household Energy System (HES), consisting of solar PV generation and energy storage, such that the household's annual energy cost is minimised for a given capital investment. The household's annual energy cost is shown to depend only on the amount of energy it is supplied from the grid, called grid sourced energy (GSE). Note if it is assumed that PV generation will first be used to supply the load, then it can be shown that any excess energy the PV system would feed-into the grid is related to the grid sourced energy (GSE).

The analytical solution for optimal HES size is derived from two equations: i) a closed-form equation for the GSE in terms of storage capacity for a fixed PV rating, and ii) an estimation equation of the sensitivity of the GSE to variations in PV rating.

The relationship between GSE and storage capacity, for a fixed PV rating, is found by identifying that the GSE is a piecewise-linear function of storage capacity, under the given assumptions. A piecewise-linear function can be expressed, in closed form, as a finite series where the series partial sums consists of both a constant term and a variable term (storage capacity). For the relationship between the GSE and storage capacity these constant terms are called the critical capacities and are found using a technique developed in Chapter 2. This technique and the piecewise-linear equation is validated against a conventional numerical approach and the two methods are shown to produce identical results. However the piecewise-linear equation provides a faster computational solution compared to the conventional approach. The critical capacities identified in Chapter 2 also provides analytical insight into the trade-off between storage capacity and annual energy cost for a given PV rating.

There currently does not exist a closed-form equation between GSE and PV rating and hence no closed-form equation exists for the sensitivity of GSE to variation in PV ratings. This sensitivity is important since it can be used to find the optimal HES size for a given investment. However by using the GSE to storage capacity equation and the critical capacities, an equation is constructed in Chapter 2 which describes the GSE to PV rating relationship for a discrete set of PV ratings. By using this constructed equation and the sensitivity of GSE to variations in PV rating can be estimated for a given set of assumptions.

The GSE to storage capacity relationship and the sensitivity of the GSE to

variations in PV rating can be combined to derived an equation which estimates the optimal HES size, for a given investment. The estimation of the optimal HES size is validated against the conventional search based solutions and it is shown that the approximation provides a reasonably accurate but computationally faster solution. The estimation equation can also provide useful insights into the sensitivity of the optimal HES size to variations in the cost parameters.

Signed Statement

I certify that this work contains no material which has been accepted for the award of any other degree or diploma in my name, in any university or other tertiary institution and, to the best of my knowledge and belief, contains no material previously published or written by another person, except where due reference has been made in the text. In addition, I certify that no part of this work will, in the future, be used in a submission in my name, for any other degree or diploma in any university or other tertiary institution without the prior approval of the University of Adelaide and where applicable, any partner institution responsible for the joint-award of this degree.

I give permission for the digital version of my thesis to be made available on the web, via the University's digital research repository, the Library Search and also through web search engines, unless permission has been granted by the University to restrict access for a period of time.

I acknowledge the support I have received for my research through the provision of an Australian Government Research Training Program Scholarship.

Signed: ..... Date: .....

Acknowledgements

I would like to thank my two supervisors, Wen Soong and David Vowles, for their invaluable help with producing this thesis.

I acknowledge the financial support from the Australian Government Research Training Program Scholarship. I would also like to acknowledge the University of Adelaide for providing me the opportunity to carry out this research.

Finally I thank my family for their encouragement and support through this time in my life.

Glossary

Benefit The reduction in the household's annual electricity bill due to the use of PV generation and/or energy storage. The sum of both: i) the cost saving from GEO and ii) the income from GFI. Commonly normalised to the household's annual energy cost such that a benefit of 1 pu means the household has no net cost for purchasing energy, noting there is still the capital cost of their HES system.

CCA (Critical capacity analysis) This is the main proposed method in this thesis. Critical capacities are identified from the net generation time series and are used to determine the trade-off between storage capacity and GSE.

Critical capacities The combination of the load critical capacities and the generation critical capacities.

Generation critical capacities The storage capacities associated with breakpoints on the GFI versus storage capacity curve.

GEO (Grid Energy Offset) The combination of energy sourced from the HES, i.e. PV generated energy and stored energy, which is supplied to the load and offsets the need for GSE (grid sourced energy).

GEO$_S$ The component of Grid Energy Offset from the stored energy. Note this stored energy was generated by the PV system.

GEO$_{PV}$ The component of Grid Energy Offset directly from PV generation.

GFI (Grid feed-in) Energy which is sold to the grid at times when both: i) load power is satisfied, and ii) storage is full.

GSE (Grid Sourced Energy) The portion of a household's load energy which is sourced from the power grid. In a HES the GSE refers to the remaining load energy not supplied by GEO.

HES (Household energy system) This refers to the combination of PV generation and energy storage. The HES size refers to a given combination of: i) peak PV power rating (kW$_p$) and ii) energy storage capacity (kWh).

Household Annual Energy Cost The cost the household pays to purchase their annual load energy from the grid.

Load critical capacities The storage capacities associated with breakpoints on the GSE versus storage capacity curve.

MBI (Maximum Benefit per Investment) For a given capital investment there is an optimal HES size resulting in the maximum reduction in the household annual energy cost, i.e. the maximum benefit.

SoC The state of charge of storage. This state of charge refers to the amount of energy remaining in the storage device. This can be expressed in kWh or as a percentage of the nominal storage capacity. The nominal storage capacity refers to when storage is full, when no more energy can be stored.

USE Unserved Energy refers to the percentage of annual load energy demand which is not supplied during a given year. In the literature this is sometimes called either Loss of Load Expectation (LOLE) or Expected Energy not Supplied (EENS).

List of Symbols

Sign	Description	Unit
$B[\mathbf{E_h}, \mathbf{E_f}]$	The household benefit (annual "profit") for the given HES size, note E_h and E_f are in bold to represent that they both functions of $[E_s, P]$.	\$
C_E	Price of storage capacity per kWh.	$\frac{\$}{\text{kWh}}$
C_P	Price of PV per kW_p.	$\frac{\$}{\text{kW}_p}$
C_a	A household's annual energy cost.	\$
$E_L[E_s, P]$	The total load energy supplied by the critical capacities larger than the given storage capacity E_s.	kWh
$E_U[E_s, P]$	The total load energy supplied by the critical capacities smaller than the given storage capacity E_s.	kWh
$E_f[E_s, P]$	GFI for storage capacity E_s and PV rating P.	kWh
$E_g[E_s, P]$	GSE for storage capacity E_s and PV rating P.	kWh
$E_g[E_s, P_0]$	The GSE (E_g) in terms of the given storage capacity (E_s) for a fixed PV rating P_0. The $E_g[E_s, P_0]$ curve refers to the trade-off curve between GSE and storage capacity for a fixed PV rating.	kWh
$E_h[E_s, P]$	Total energy supplied to the load by the HES for storage capacity E_s and PV rating P.	kWh
$E_n(t)$	The net generation energy time series i.e. difference between the generation and load time series.	kWh

Sign	Description	Unit
E_s	Energy storage capacity (kWh)	kWh
$E_{g0}[P]$	The GSE for a given HES size if the contribution of storage capacity is ignored, also called GEO_{PV}.	kWh
$G(t)$	The generation power time series for a given location.	kW
G_1	The total annual energy generated per kW_p of PV rating.	kWh
$I[E_s, P]$	Capital investment into a HES for storage capacity E_s and PV rating P.	\$
L	The household's annual load energy.	kWh
$L(t)$	The load power time series for a given household.	kW
P	PV rating.	kW_p
PV_L	The theoretical upper bound of PV rating which causes the critical capacities to reach their minimum magnitudes and list length (number of critical capacities).	kW_p
$S(t)$	The current SoC time series considering the limits of the storage device.	kWh
$S'(t)$	The current SoC time step ignoring the limits (full/empty) of the storage device.	kWh
$\boldsymbol{C}[\boldsymbol{P}]$	The list of critical capacities for PV rating P, sorted in descending order.	kWh
λ	The Lagrange multiplier.	
c_f	Price of selling energy to the grid. Also called the grid feed-in tariff.	$\frac{\$}{\text{kWh}}$
c_g	Price of purchasing grid energy. Also called the grid supply tariff.	$\frac{\$}{\text{kWh}}$
c_x	The critical capacity at index (x) in the critical capacity list, note this list is sorted in descending order.	kWh
$n[E_s, P]$	A given index in the $\boldsymbol{C}[\boldsymbol{P}]$ list of critical capacities for PV rating P where n is such that $c_n \leq E_s$ for the chosen storage capacity E_s.	
$n_{opt}[P]$	The index in the critical capacity list for PV rating P where the critical capacity at this index is the optimal storage capacity associated with maximum benefit for a given PV rating or investment.	

Chapter 1

Introduction

1.1 Objective

The falling cost of PV systems [1] and battery storage [2,3] has made the combination of PV generation and energy storage an affordable option to reduce a household's annual energy cost in exchange for a capital investment. A challenge is selecting the optimal sizes of both the PV rating and storage capacity to minimise the annual energy cost for a given capital investment and the focus of this research is to develop analytical solutions for these optimal sizes.

The economic analysis presented is simple and does not consider: i) the return on investment, ii) the net present value or iii) the levelised cost of energy. The optimal annual energy cost refers to the smallest annual cost the household would pay for their given energy demand for a given capital investment. Since a new method of sizing storage is proposed the simple analysis provides a reference point to compare this new method to existing methods.

1.2 Household Energy System (HES)

A household energy system (HES) describes the combination of PV generation and energy storage which operates to reduce a household's annual energy cost. The size of the HES refers to a specific combination of PV rating (P) and storage capacity (E_s) which defines its capital investment. The concept of a HES is illustrated in Fig. 1.1a where it operates to supply the load and hence offset grid-energy requirements. Note the generation convention is used, hence positive power represents generation and negative power represents load, and this convention will be used throughout this thesis unless otherwise stated.

The capital investment $I[E_s, P]$ of a HES described in (1.1) depends on the combination of the PV cost and storage cost. The storage cost is given by the storage capacity in kWh and the price (C_E) per kWh. The PV cost is given by the PV rating in kW_p, which is the peak PV output under standard test conditions, and the price (C_P) per kW_p.

$$I[E_s, P] = E_s \times C_E + P \times C_P \tag{1.1}$$

The annual energy cost (C_a) of a HES, under the assumption of a single fixed tariff for purchasing grid energy, is described by (1.2) where C_a depends on the amount of energy purchased from the grid, E_g, called the grid sourced energy (GSE), and the amount of energy sold to the grid, E_f, called grid feed-in (GFI). The fixed grid supply and feed-in tariffs are respectively c_g and c_f. Note the symbols E_g and E_f are both bold to represent that they are functions of the variables E_s and P.

$$C_a[\mathbf{E_g}, \mathbf{E_f}] = E_g[E_s, P] \times c_g - E_f[E_s, P] \times c_f \tag{1.2}$$

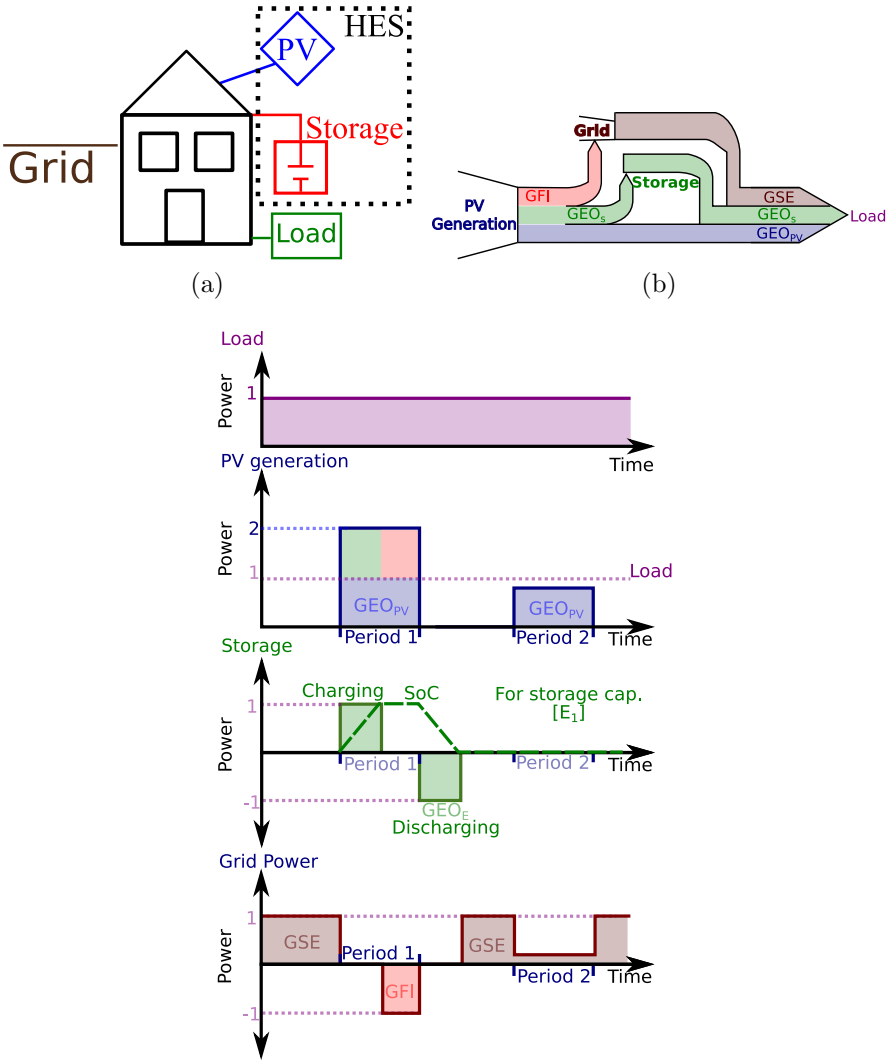

Figure 1.1: Conceptual illustration of a household energy system (HES) and its operation: a) the HES components, b) the energy flows within the HES and c) time series of power flows using the chosen HES operating technique.

The GSE and the GFI both depend on the energy storage capacity E_s and the PV rating P and the focus of this research is to develop a closed-form equation for $E_g[E_s]$ and $E_f[E_s]$ for a given P and to approximate the sensitivity of $E_g[P]$ and $E_f[P]$ to variations in PV rating for a given E_s. The development of the closed-form equations depend on how the HES operates to supply the load. An example of the HES and its operation is illustrated in Fig. 1.1b and Fig. 1.1c.

The energy flows within a HES is illustrated in Fig. 1.1b and are described by the following:

1. GSE is purchased from the grid to supply the load that cannot be supplied by either solar PV directly or from storage.

2. GFI is the excess PV generation that cannot be stored and consequently sold to the grid.

3. The component of grid energy offset directly from PV (GEO_{PV}) is the portion of PV generation which directly supplies the load and offsets an equivalent amount of GSE.

4. The component of grid energy offset from the stored energy (GEO_S) is the portion of PV generation which is stored and then supplied to the load at a later time. The GEO_S also offsets an equivalent amount of GSE.

The energy flows are shown by the shaded areas in the four power time series in Fig. 1.1c. The four power time-series in Fig. 1.1c, in descending order, are: 1) the load time series describing the power demand of the load, 2) the PV generation time series describing the HES PV power generation, 3) the storage time series where positive power represents a flow of power into the storage and negative power represents flows from storage, and 4) the grid power where a positive power represents a flow from the grid (to load) and a negative power represents flows to the grid.

The two periods of positive PV generation, labeled period 1 and period 2, in the illustrated time series can be used to describe the HES behaviour in Fig. 1.1c. Prior to period 1, the storage is empty and there is no PV generation so load is supplied by GSE, hence the grid power is positive. During period 1 the PV generation exceeds the load and the excess energy is transferred to storage until storage is full. Any remaining energy is then sold to the grid as GFI. Between period 1 and period 2, with no PV generation then storage supplies the load until it is empty at which time GSE supplies the load. During period 2, PV power does not exceed load power and storage is empty. Hence GSE supplies the difference between PV power and the required load. After period 2 the load is supplied by only GSE as there is no PV generation and the storage is empty.

There is a fourth potential energy flow, not illustrated in Fig. 1.1b, which connects the grid and storage allowing energy flow between these elements. However this research does not consider this fourth flow as the assumption of a fixed energy price means this energy flow does not assist in reducing the annual energy cost.

There are two key relationships between the energy flows in Fig. 1.1b which can be derived since the fourth energy flow is ignored. These two relationships are as follows:

1. The combination of GEO_{PV} and GEO_S describes the total amount of GEO the HES provides (E_h), and the GEO is related to the GSE and the energy consumed annually by the load (L) through (1.3a).

2. The GFI (E_f) is related to the GEO and the annual amount of energy generated per kW_p of PV (G_1) through (1.3b), where $E_P[P]$ is the annual solar PV energy production.

$$E_g[E_s, P] = L - E_h[E_s, P] \tag{1.3a}$$

$$E_f[E_s, P] = E_P[P] - E_h[E_s, P] = E_P[P] - L + E_g[E_s, P] \tag{1.3b}$$

$$E_P[P] = G_1 \times P$$

There are many potential strategies for coordinating the energy flows in Fig. 1.1c. For the analysis in this thesis the chosen strategy is that the HES will operate to satisfy the load's energy demand throughout the year and the energy will be supplied from one of three sources, which in priority order are: i) the PV system if there is sufficient solar irradiation for generation, ii) the storage device if there is sufficient stored energy or iii) the grid-connection.

Fig. 1.1c demonstrates the priority order in period 1. The load is directly supplied by PV energy in the form of GEO_{PV} with any excess generation being used to first charge storage until it is full and then any remaining energy is sold to the grid. Between period 1 and period 2 there is no PV generation so load is first supplied from the storage device until storage is empty and the grid supplies the remaining load. In period 2 the PV generation supplies as much of the load as possible and then the remaining load energy is supplied from the grid, since storage is empty prior to this period.

The operation of a HES provides the household with a benefit, an amount of income derived from the combination of selling energy to the grid and from offsetting the need to purchase grid energy. An optimal HES sized which minimize the annual energy cost also describes the optimal HES size which maximises the benefit. Hence the HES optimisation of finding the minimum annual energy cost for a given investment is equivalent to finding the maximum benefit for a given investment. The benefit (B) is described in (1.4) as the savings derived by avoiding grid energy consumption ($E_h \times c_g$) and the income from selling energy to the grid ($E_f \times c_f$).

$$B[\mathbf{E_h}, \mathbf{E_f}] = E_h[E_s, P] \times c_g + E_f[E_s, P] \times c_f \tag{1.4}$$

Note in B the symbols E_h and E_f are in bold representing that they are functions of the variables E_s and P. The remainder of the thesis will use this notation, when a function's terms is written in bold then that terms is itself a function of the variables E_s and P.

The remainder of this thesis will focus on the benefit as the resulting plots of benefit to investment are simpler to understand since benefit is always positive, while total annual energy cost can transition from positive to negative.

1.3 Literature Review

The literature review shows how the HES, the focus of this thesis, fits within the broader area of energy storage sizing. The three main aspects of energy storage sizing are: i) the location of energy storage (Section 1.3.1), ii) the application or function of energy storage (Section 1.3.2) and, iii) the technique used to select storage size (Section 1.3.3). A summary of these aspects and examples of their content is seen in Fig. 1.2.

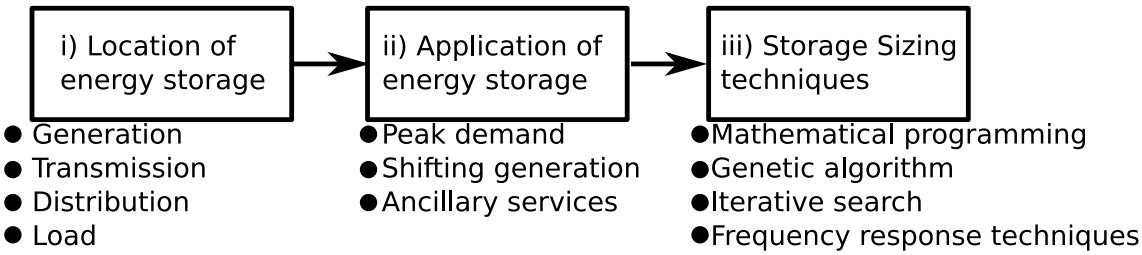

Figure 1.2: A summary of the three main aspects of storage sizing and for each aspect a number of examples are listed.

Tables 1.1 and 1.2 categorise literature relevant to these three topics prior to their discussion. Firstly, Table 1.1 lists literature references relative to the location and application of storage. Secondly, Table 1.2 categorise storage sizing techniques depending on the cost function and optimisation method.

1.3.1 Energy Storage Location

Energy storage in power systems can be located at four distinct levels: i) generation, ii) transmission, iii) distribution and, iv) load, as shown in Fig. 1.3. At each of these levels there is the potential to install storage for one or more of the applications discussed in Section 1.3.2.

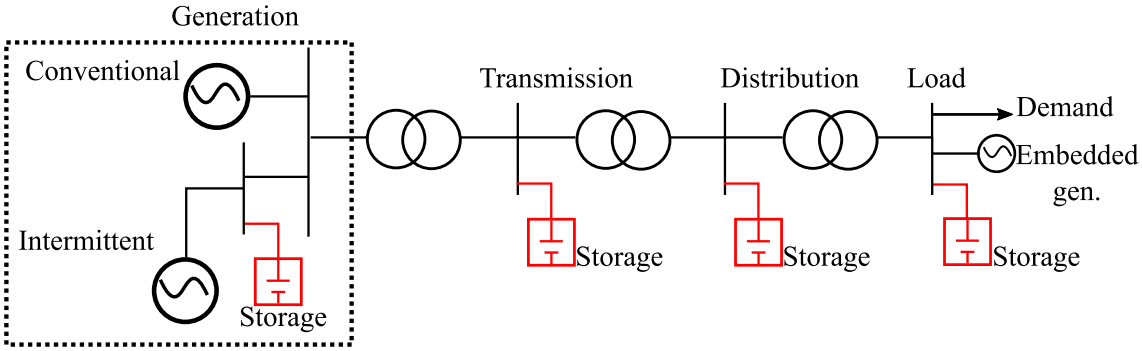

Figure 1.3: A simplified overview of a power system, where energy storage may be installed at different levels in the network. The load refers to consumer (e.g. a household or a industry customer), who have a demand for energy and may have embedded generation such as solar PV.

The generation level refers to main grid-connected generation and includes conventional sources of generation (e.g. coal, gas) and the intermittent sources of gen-

eration (e.g. large scale wind or solar etc). The goal of storage at this level is to smooth the variation in renewable generation and allow generators to produce a controllable output, e.g. by temporally shifting intermittent generation.

At the transmission and distribution levels, storage can be used to increase the effective capacity of parts of the network. The transmission/distribution level storage can provide a source of effective generation at a point in the network that can be scheduled to reduce demand on upstream network elements, such as transformers and transmission lines, that may otherwise be overloaded, thereby avoiding or deferring upgrades to these elements, as seen in [4–6].

The load level consists of a power demand, and may also include a source of embedded generation (e.g. PV generation for a HES) and/or a storage element. The use of storage at this level can function as part of a HES which reduces the household's energy cost by temporally shifting intermittent generation. Other functions at this level could include reducing the household's peak power demand if their energy retailer charges additional fees for peak consumption, such as in [7, 8].

1.3.2 Energy Storage Application

The four broad applications of energy storage are:

1. Peak demand reduction
2. Energy arbitrage through time shifting intermittent generation (the focus of this thesis)
3. Ancillary services, including voltage control, frequency control and synthetic inertia.
4. Backup power

Storage for peak demand reduction is located on the demand side of the network element. Energy is stored when the demand is below a threshold and it supplies energy when demand is above a threshold. The objective for this application depends on where the storage is installed. At the transmission or distribution level, storage can avoid or defer network upgrades by reducing peak demand on network elements, such as in [4–6]. At the load level it can reduce peak demand charges, such as in [7,8].

Energy arbitrage involves time shifting intermittent generation. In the context of a HES, the storage device is charged when output from the intermittent generation source is high and it supplies energy when the output from the source is low. This can also apply to larger scale intermittent generators (e.g. wind) seeking to smooth out their net output, such as in [9]. The objective for this application is to leverage the difference in energy cost at different times (energy arbitrage) to obtain a higher value from the intermittent generation, since the output of an intermittent generator may be high when energy cost is low and vice-versa.

The ancillary services include providing voltage, frequency and synthetic inertia. Voltage or frequency control involves installing additional control elements on the storage device to allow it to provide this functionality, such as in [10]. For voltage control an automatic voltage regulator is fitted to the storage device to control the reactive power output from the storage medium via its grid-connected power-electronic converter so as to regulate the voltage at an appropriate point in the network. This may be useful in distribution feeders with high levels of embedded PV generation which are subject to voltage fluctuations due to variations in solar irradiance. For frequency control an automatic frequency regulator, with an appropriate droop setting, is fitted to the storage device to control the (net) power output from the storage device to assist in the control of system frequency. The behaviour is similar to that of a governor fitted to a synchronous generator. Synthetic inertia involves storage momentarily changing power output to prevent rapid changes in frequency, such as in [11]. It is assumed that the suppliers of such ancillary services will be remunerated for providing these services.

Storage for backup power maintains maximum charge and is discharged only when energy cannot be sourced from the grid connection and is similar to an emergency power supply. The objective for this application is to minimise both the occurrence and duration power loss. This value of backup power providing by storage has received little separate attention and is commonly considered alongside a different application, such as in [12] where the reduction of wind spillage (time shifting intermittent generation) is considered in combination with back-up energy.

Summary of the Literature Concerning the Location and Application of Energy Storage

References to literature about storage location and its application are shown in Table 1.1. Since there is significant overlap for the storage application at both the transmission and distribution levels, these are combined into a single group in Table 1.1. The column of "not specified" refers to studies where the location of storage is either not specified or if the technique could be applied to any level of storage.

Table 1.1: Literature references about energy storage application at different levels in the network.

Application	Generation	Trans. & Dist.	Load	Not specified
Peak demand Reduction		[4–6]	[7, 8]	
Temporal shifting intermittent Generation	[12–21]	[6]	[7, 22–30]	[31–35]
Ancillary services	[9–12, 36–38]	[4]		

1.3.3 Storage Sizing Techniques and Objectives

Table 1.2 categorises literature on sizing techniques according to costing and optimisation methodologies.

Fig. 1.4 illustrates the storage sizing process and highlights the areas in which this thesis contributes. The first row in the figure is a flow chart showing how storage sizing starts with time-series data and through analysis results in a desired solution. The second row depicts examples of commonly used figures in each stage of the process. The last row provides examples for implementing each process.

Fig. 1.4 is best described in reverse, starting with the solution. The goal is to specify storage size which satisfies a chosen objective under a range of assumptions on how storage will operate. When storage is operated to shift intermittent generation, such as in this thesis, the solution will involves a trade-off between storage capacity and generation size. The desired objective can be either: i) to minimize cost such as in [5, 6, 25, 26, 32], or ii) to achieve a desired technical characteristic such as minimising peak power demand as in [4].

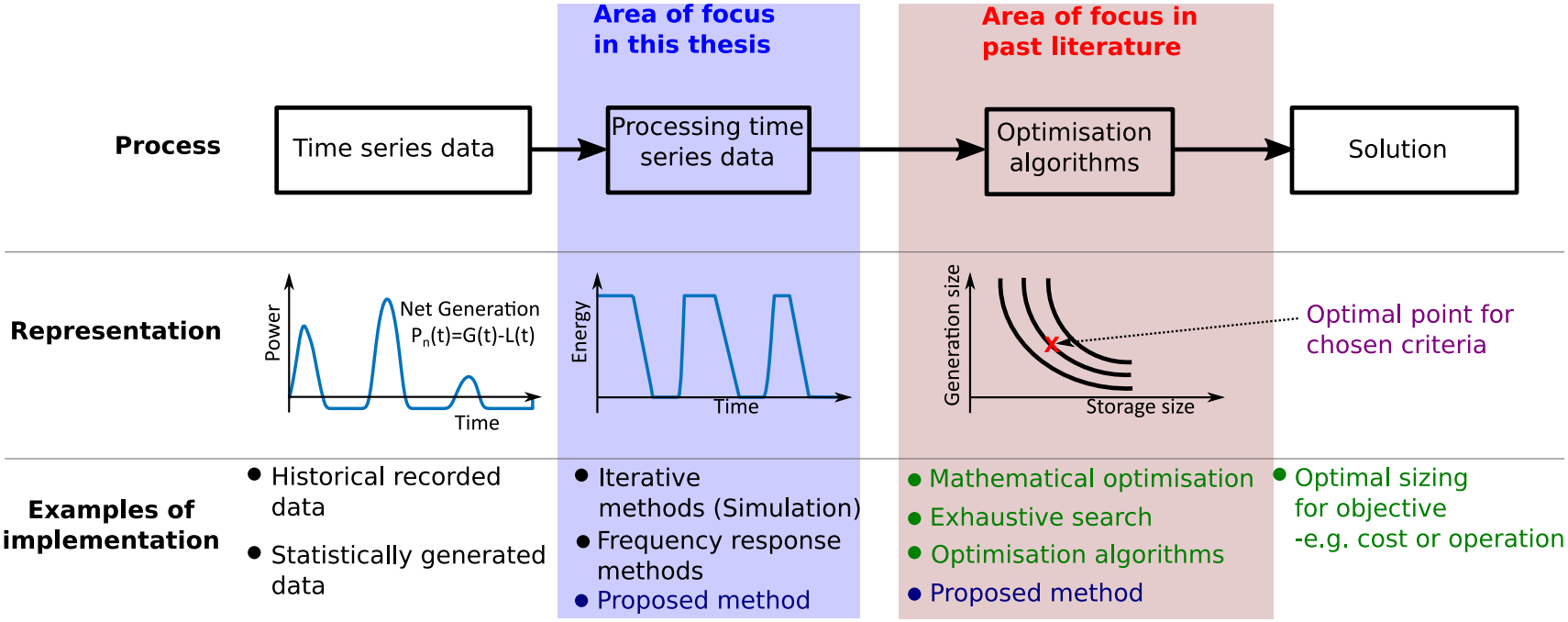

Figure 1.4: Overview of literature topics. The first row depicts the storage sizing process. The second row depicts each step in this process using a generic plot. The third row shows examples of how each process is implemented.

To find this solution, an optimisation algorithm or technique is used to find the optimal solution. The selection of the optimisation algorithm has been a significant focus in the literature. Commonly a range of combined storage sizes and generation sizes are considered. The optimal combination is found by examining the performance of each combination based on a given set of criteria, this performance is commonly to minimize the required grid sourced energy (GSE) such as in [4, 13, 22] and also in this thesis. The performance of each storage and generation combination is found by processing the time series data.

The processing of the time series data has received little attention in the literature. This commonly involves extracting the performance (GSE) for the selected combination of generation size and storage size by processing the time-series data. The common method seen in the literature involves iterative techniques where the GSE of each storage/generation combination is found by simulating the state of charge (SoC) of storage at each time step. The main focus of this thesis is to develop an improved technique for processing this time-series data to extract the GSE information. The goal is to simplify the optimization algorithm.

Finally the time-series data in Fig. 1.4 is derived from either historical data or from a stochastic model.

Summary of Review

Table 1.2: Summary of the literature references about the objective functions and optimisation techniques used in storage sizing studies

	Optimisation Techniques				
Objective function	Math. Optim.	MILP	MILNLP	MOLP	Misc. algorithm
Benefit maximisation	[5, 6, 23, 25, 26, 32]	[10, 19]	[28]	[8]	[7]
Cost recovery				[16]	[33]
Levelised cost of energy	[17]				
Net Present value	[14, 22, 30, 31]				[27, 29]
Function Specific	[4, 15, 24]				[11, 18, 20, 34, 35, 37]

Table 1.2 categorises literature references according to the objective function and optimisation method used to determine storage size. Note the references in this table have used the iterative methods to process the time series data. This is the simplest process to understand but has both: i) higher computational cost and, ii) makes it difficult to obtain insight into the potential solution when compared to the new methods developed in this thesis. There are techniques which do not use iteration, such as [9, 12, 21, 33, 36, 38] which use frequency response analysis in their

storage sizing algorithm.

The following describes the columns (techniques) and rows (cost objective) seen in Table 1.2.

The various techniques are:

1. Mathematical optimisation - these describe a broad range of techniques. However they all have a single optimisation objective, usually cost, and are subject to a number of constraints. An example of this is seen in both eq. (1.4) and in Chapter 4 by (4.2).

2. MILP (mixed-integer linear programming) - is a specific form of mathematical optimization where both: i) some (or all) constraints are assumed to be integer values and, ii) the other non-integer constraints and the sizing objective are assumed to be linear. This technique may be used for representing the charging or discharging state of storage using a binary number (an integer), such as in [10]. Another case is given a mix of PV generation, storage and other generating sources then the state of the other sources can be represented by a binary number [19].

3. MILNLP (mixed-integer non-linear programming) - is the same as the above with the exception that the objective function and constraints are assumed to be non-linear. The reason why this technique may be employed instead of MILP is when one of the constraints is no longer linear, for example in [28] the cost of energy was assumed to be non-linear, where the tariff paid depended on how much energy had previously been purchased from the grid.

4. MOLP (Multi-objective linear programming) - This is a form of mathematical optimisation where there are, i) multiple optimisation objectives, and ii) the objectives and constraints are assumed to be linear.

5. Misc. algorithm - This comprises a broad collection of algorithms that are either novel or not commonly used in storage sizing. Examples of these techniques include: i) particle swarm algorithm, ii) model predictive control, iii) genetic algorithm, iv) artificial neural networks and, v) machine learning techniques.

The various sizing objectives in Table 1.2 are:

1. Benefit maximisation - This describes the broad range of techniques which attempt to maximise the income derived from the combination of the generation source and storage while constrained by its capital cost. This analysis usually considers optimising the annual benefit.

2. Cost recovery - The objective here is similar to the benefit maximisation however instead the amount of time until the system recovers its capital investment

is minimised. This is either in the form of payback period, such as [16], or other cost recovery factor, such as in [33].

3. Levelised cost of energy - The objective is to minimise the levelised cost of energy which is the ratio of the lifetime cost to the total energy produced over the lifetime. Note that storage cannot produce energy hence this levelised cost of energy refers to the combination of both the generation source and of storage.

4. Net Present value - This is an extension to benefit maximisation where the income and cost for future years are converted to a present day value.

5. Function Specific - This row describes techniques which the solutions are not optimal cost but rather are optimal for a given technical function. For example in [11] the optimisation objective is to achieve a desired level of grid inertial response by appropriately sizing storage.

The objective function employed in this thesis, in Chapter 4, is classified as "Benefit maximisation using mathematical optimisation" (first row, first column in Table 1.2). The literature shown in Table 1.2 iterate the demand time-series data over a grid of generation and storage capacities. This thesis eliminates the need to iterate through storage capacities. It is however still necessary to iterate over a set of generation capacities. The advantage this provides is a greater understanding of how the constraint of storage capacity affects the optimisation problem. Note that while the objective function in Chapter 4 is specifically for the benefit maximisation, the underlying process described in Chapter 2 (CCA) can be used for any of the objective functions shown in Table 1.2.

1.3.4 List of publications

The concepts presented in Chapter 2 and Chapter 4 in this thesis have been presented by the candidate and his advisers in the following publications:

1. B. J. Donnellan, W. L. Soong, and D. J. Vowles, 'Critical Capacity Analysis for Optimal Sizing of PV and Energy Storage for a Household', in 2018 IEEE Energy Conversion Congress and Exposition (ECCE), Sep. 2018, pp. 5125–5132, doi: 10.1109/ECCE.2018.8557833.

Other publications produced during the development of this thesis are listed below:

1. B.J. Donnellan, D.J. Vowles, and W.L. Soong, 'A Review of Energy Storage and its Application in Power System', presented at the 2015 Australasian Universities Power Engineering Conference (AUPEC), Sep. 2015.

1.4 Contributions

This thesis contains three key contributions:

1. The recognition of the piece-wise linear (PWL) relationship between a household's GSE and the storage capacity for a given PV rating.

2. The development of an analytical method which calculates the parameters required to write the PWL function as a single closed-form equation between GSE and storage capacity.

3. The derivation of an approximate optimal HES size which achieves the maximum benefit for a given capital investment using the closed-form equation between GSE and storage capacity developed above.

1.4.1 Recognising the Piece-wise Linear Relationship

Previous work by [4,14,23] has presented plots of the GSE to storage capacity, shown in Fig. 1.5, for a given PV rating but these works have not commented on the curve's features. These plots of GSE (or Unserved Energy (USE)) and storage capacity all have a common shape. Note the USE of stand-alone HES is the counterpart of the GSE of an grid-connected HES. Also the vertical axes in Fig. 1.5 have different but equivalent terms to USE and hence GSE. These terms are: i) the loss of load expectation (LOLE) and, ii) the expected energy not served EENS,) to describe the USE.

The first contribution of this thesis is the recognition that GSE is a PWL function of storage capacity and hence it contains two key features: i) linear segments where the relationship between GSE and storage is defined by the slope of that linear segment, and ii) breakpoints corresponding to values of energy storage where the linear segments intersect and the slope changes. By calculating the energy storage breakpoints and slopes of each linear segment it is possible to express the GSE and storage relationship as a closed form equation.

Note this closed form equation between GSE and Storage capacity is applicable to any form of non-controllable generation, e.g. PV or wind generation.

A canonical form for a single variable PWL function has been derived by [39,40] which provides a closed form equation for a PWL function when both the breakpoints and slopes of each linear segments are known.

1.4.2 Defining the Piece-wise Linear Relationship

The second contribution of this thesis is the development of the Critical Capacity Analysis (CCA) method which identifies the energy storage breakpoints, called Critical Capacities, of the GSE-Storage relationship and shows that the slope of the linear segments varies by an integer amount at each critical capacity. The origin of

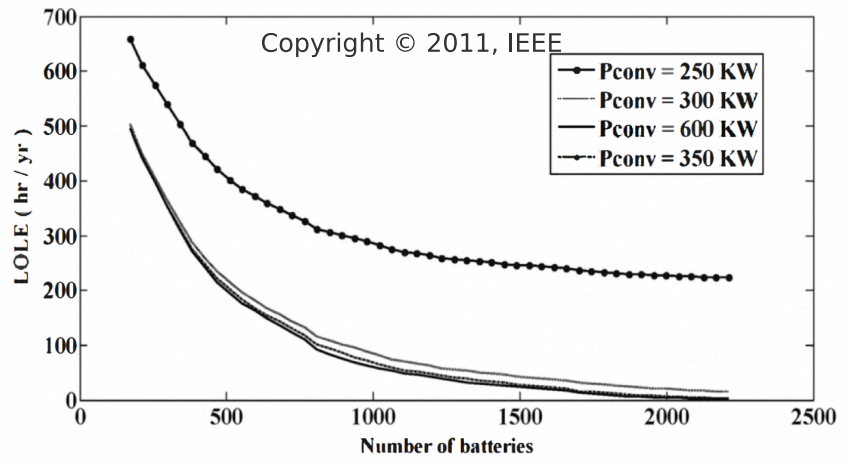

(a)

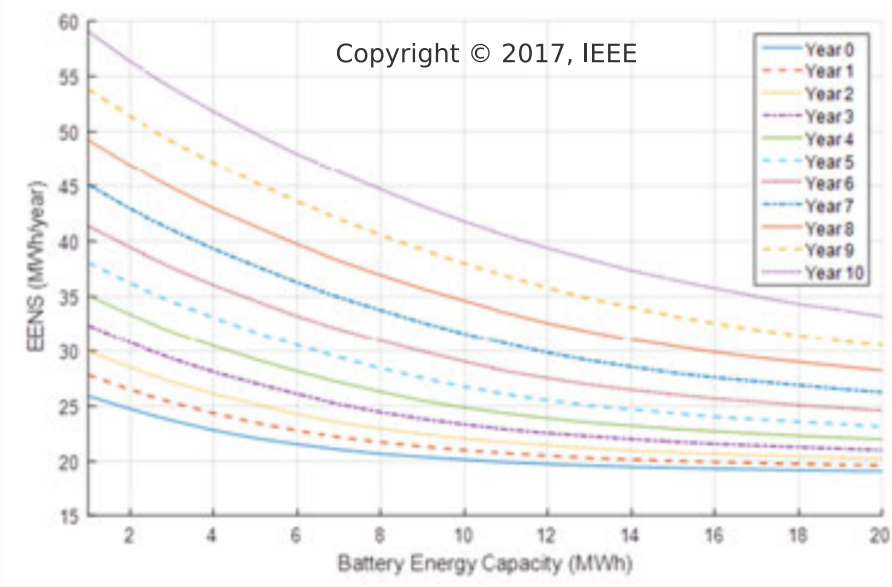

(b)

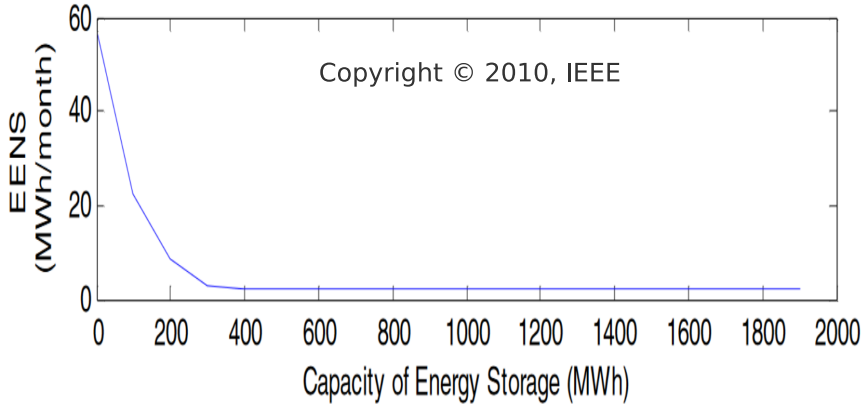

(c)

Figure 1.5: Results from previous work presenting USE versus storage capacity curves. These curve all appear to be piecewise linear however this has not been identified in the respective studies. Sources: a) [14], b) [4], c) [15]

the critical capacities is observed in a household's annual net generation for a given PV rating by plotting power versus energy time-series and noting the closed cycles within this plot, discussed in Chapter 2, and these cycles represent the charging and discharging of the storage. The critical capacities are found by modifying the rainflow algorithm which was originally developed for material fatigue analysis [41–43]. These critical capacities are sorted in ascending order and the linear segment between two critical capacities has a slope given by the index of the smaller critical capacity. The closed-form equation developed using CCA is validated through a case study where the GSE is found for a range of storage capacities and the closed-form equation results are compared to the conventional simulation methods under the same set of assumptions. Compared to the conventional simulation method the CCA approach provides an improvement in computational speed and greater analytical understanding of the relationship between GSE and storage capacity.

1.4.3 Approximate Optimal HES for Maximum Benefit per Investment

By expressing the GSE-Storage function in a closed form for a given PV rating the benefit of the HES is also expressed in a closed form in terms of storage capacity for a given PV rating. For small values of storage capacity the GSE-Storage function provides an approximation of the relationship between the change of benefit and the PV rating. The third contribution of this thesis is to provide an approximate optimal solution for the HES size which maximises the household benefit for a given capital investment. This approximate solution uses the closed-form equation between benefit and storage and the approximate equation between benefit and the PV rating. The conventional approach used by [26, 44–47] finds the optimal solution by searching a number of HES sizes for the maximum benefit for each investment. This thesis proposes an approximate optimal solution which estimates the index n_{opt} in the critical capacity list for a given PV rating which corresponds to the storage capacity at which maximum benefit occurs for a given investment. The proposed method derives an equation for n_{opt} in terms of the cost/value of energy (c_g and c_f) and the capital costs (C_E and C_P) which allows the sensitivity of the maximum benefit to variations in these costs to be directly observed.

A case study is used to compare the approximate optimal solution to the exact optimal solution obtained from the conventional search-based method used by [26, 44–47]. The case study compared the estimated and exact solutions for both the base case and for variations in: i) the cost of energy, ii) the capital costs, iii) the load data by considering a base case household and a number of different households, and iv) the year of generation data. For the base-case household the estimated method results was less than 1% different from the exact solution and the accuracy was similar for the listed variations. An observation made is the existence of two

key points in the optimal solution, point(A) which describes the PV rating at which to begin investing in storage capacity to improve the benefit and point(B) which describes the storage capacity beyond which further investment in storage does not significantly improve the benefit. These two points are used to describe when the household obtains the majority of their benefit from either offsetting their GSE or from GFI. The advantage of the approximation method is its ability to provide a fast estimate for the optimal HES size corresponding to maximum benefit for a given investment. This may have applications for future work.

1.5 Thesis Structure

An overview of Chapters 1-4 and their connections is shown in Fig. 1.6.

The remainder of Chapter 1 discusses the assumptions made for the analysis in this thesis and the case study data used to validate the proposed methods. Chapter 2 will discuss the development of the Critical Capacity Analysis (CCA) method used to derive the closed-form equation between GSE and storage capacity for a given PV rating. Chapter 3 will discuss the key properties of the CCA method, its benefits and will use the case study data to validate the CCA method by comparison with the conventional simulation sizing technique. Chapter 4 derives the estimation equation for the optimal HES size which provides the maximum benefit for a given investment and will validate this estimation equation. Finally, Chapter 5 provides the conclusions and identifies potential areas of further research.

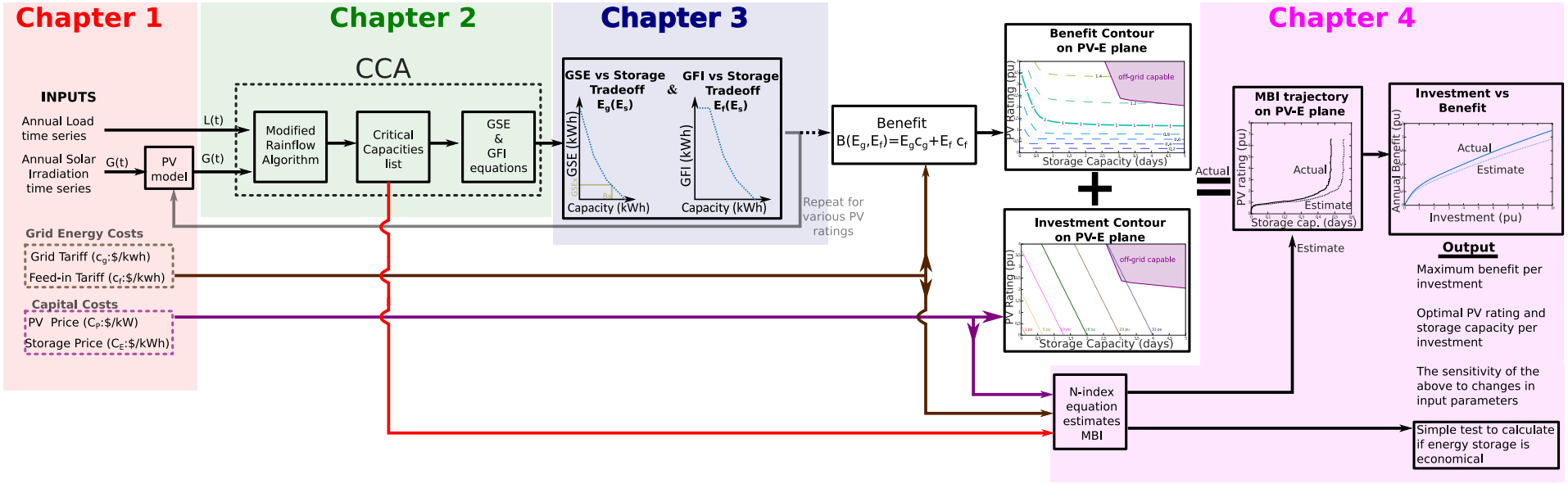

Figure 1.6: An overview of the various chapters and their connections.

1.6 Assumptions

This research makes a number of assumptions on the HES operation and the economics.

The assumptions on the economics and sizing of HES are:

1. The PV and Storage capital costs of the HES are linearly proportional to their rating and the baseline values are shown in Table 1.3.

2. There is a fixed single tariff for buying grid energy and a fixed single tariff for selling energy to the grid, and the baseline values of these tariffs are shown in Table 1.3.

A sensitivity study of the cost in Table 1.3 is performed in Section 4.6.2

Table 1.3: Summary of the HES capital costs and grid tariffs.

Capital costs		Grid Tariffs	
Storage capacity (C_E)	1000 \$/kWh	Grid supply tariff (c_g)	0.35 \$/kWh
PV (C_P)	1500 \$/kW$_p$	Grid feed-in tariff (c_f)	0.06 \$/kWh

The assumptions on the HES operation are:

1. The storage device has the following power limits: it is assumed storage can supply the maximum household power demand and absorb the maximum PV power output (See Section 3.1.1: Power limit).

2. The storage device is assumed to be full at the start of the time series. (See Section 3.1.2: Initial SoC)

3. Transferring energy into and out of storage is 100% efficient. (See Section 3.1.3: Efficiency)

4. No minimum or maximum state of charge limit of the storage device is considered, that is it can operate from 0% to 100% of its nominal capacity. (See Section 3.1.4: SoC limits)

5. It is assumed that the battery capacity does not degrade over time due to aging effects.

The full detail of these assumptions is discussed in Section 3.1.

1.7 Case Study Data

The CCA method and the estimation of optimal HES size are validated against the conventional simulation technique using a number of different household's load data and a number of different years of generation data. The details of this data and the

base case selected as the first case presented to illustrate the concepts and features of the CCA and estimation method are outlined below.

The Household load time series were obtained from the "Smart grid smart city" [48] trial of smart meters for households located in Sydney for the year 2013. The generation data was derived from solar irradiation data from the Australian Bureau of Meteorology one minute interval solar irradiation datasets [49] for the year 2005. Note the closest location with available irradiation data was Wagga Wagga which is approximately 460 km away from the load data (Sydney) and hence there may be differences between the weather in Wagga Wagga and the weather in Sydney. The year of generation data and the year of load data are difference due to the limited data available when this data was accessed. Hence any correlation between weather and load data cannot be considered for this case study however this does not have an impact on the CCA method or the proposed optimal HES sizing.

The solar irradiation data was processed using the PV model from the software "SAM" [50] which converted the solar irradiation time series into a generation time series for a 1 kW_p PV system. The generation time series can then be scaled by multiplying by the desired PV rating to obtain the generation data for that given PV rating. The panel were assumed to be facing north and tilted (relative to ground level) by the angle of latitude for Wagga Wagga of approximately 35.1 degrees. The SAM software provided a default power loss of approximately 10% of PV output, which was separated into approximately 4% for the inverted and approximately 6% for the panels (for effects such as shading, soiling and connections). Hence for a 1 kW_p panel the maximum output possible was 0.9 kW_p.

1.7.1 Normalization

When discussing case study data, the HES size is normalized based on the load data:

1. The PV rating is normalised such that 1 pu corresponds to the PV kW_p rating such that the annual energy produced is equal to the annual average household demand.

2. The storage capacity is normalized such that 1 pu corresponds to the daily average energy consumed by the household which is the total annual energy consumed divided by 365.

1.7.2 Base Case Household

The generation and load data for the base case household is shown in Fig. 1.7. The generation time-series shown is for a 5.4 kW_p or 1 pu PV system and with the assumed 10% loss the maximum PV output is 4.86 kW_p. The year of this data is 2005 and is taken from [48, 49]. The household's annual load is approximately 8.6 MWh, hence 1 pu storage capacity would be 23.5 kWh, and the annual generation per kW_p

is approximately 1.6 MWh, hence the annual energy production of a 5.4 kW_p PV system would equal the annual load. This data has 30 minute time resolution and hence for the year there is 17,520 points of data for both generation and load.

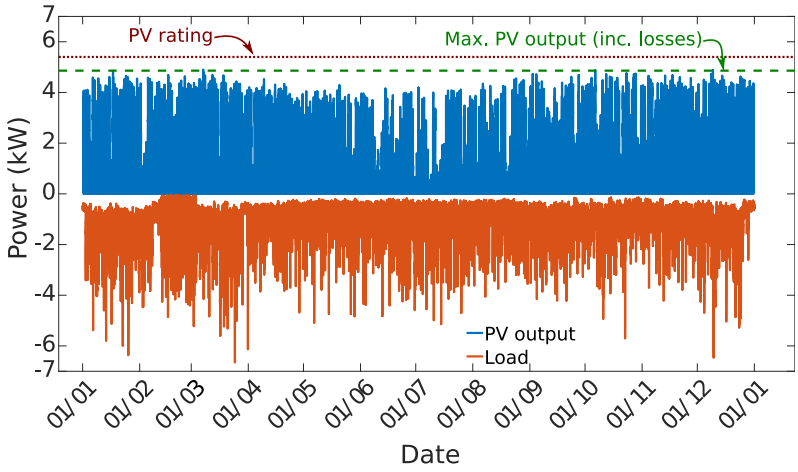

(a)

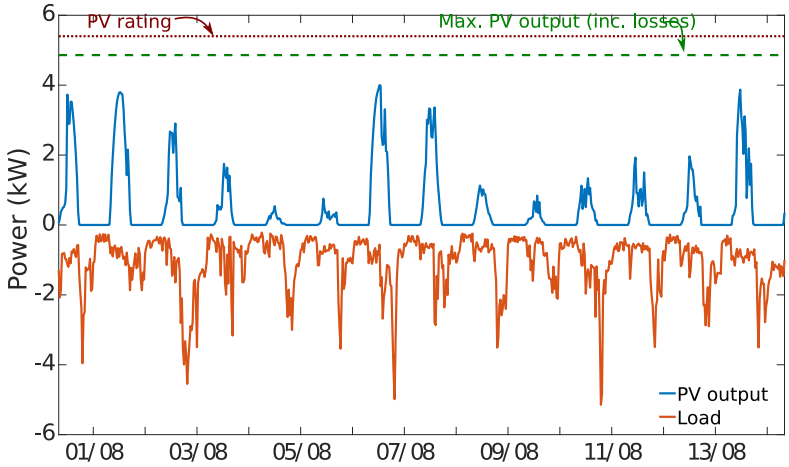

(b)

Figure 1.7: The generation and the load time series data for the base case household which is in the southern hemisphere, (a) for one year, (b) for two weeks in winter. The dotted (brown) curve shows the PV rating of 5.4 kW_p and the dashed (green) curve shows the maximum PV power output (including the 10% loss).

The trends of the generation data is shown by averaging for different seasons of the year and the trends of load is shown by separating the average daily trend between weekdays and weekends.

The base case household residents are generally not at home during the day on weekdays and hence are likely to have higher activity on weekend, i.e. higher energy demand. The daily variation of load in the weekends versus weekdays in Fig. 1.8 plots each day of the year on a single 24 hour period with the blue lines representing the 365 individual days. The black line represents the annual average at each time step and the red lines represents one standard deviation from this average. The weekdays have a large peak in the morning around 7am, the load is mostly flat during the middle of the day and then peaks again in the early evening when the

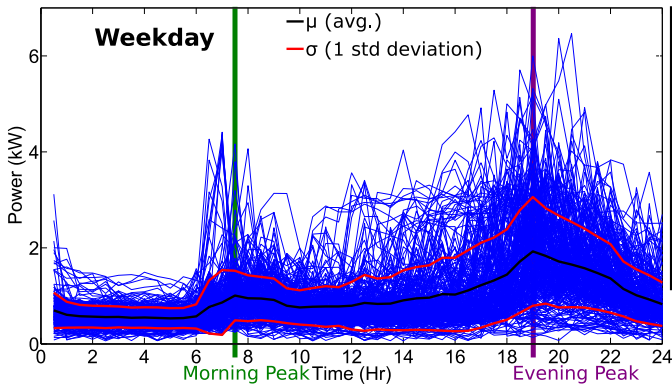

Weekday	Std. dev. lower	Mean	Std. dev. upper
Morning Peak (7.5hr)	0.5 kW	1 kW	1.5 kW
Evening Peak (19hr)	0.8 kW	1.9 kW	3 kW
Min.	0.2 kW	0.5 kW	0.7 kW
Daily Energy	10.1 kWh	23.3 kWh	36.5 kWh

(a)

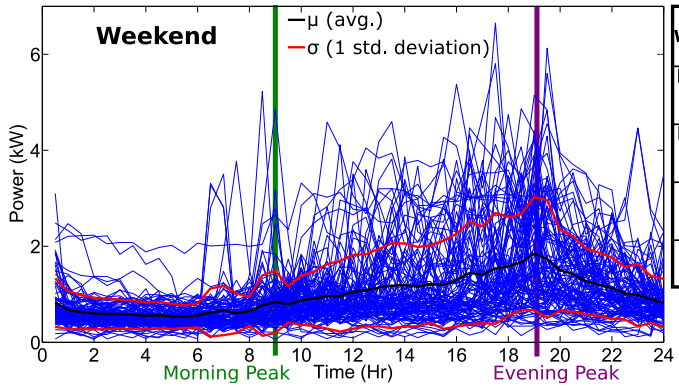

Weekend	Std. dev. lower	Mean	Std. dev. upper
Morning Peak (9hr)	0.2 kW	0.8 kW	1.5 kW
Evening Peak (19hr)	0.7 kW	1.8 kW	3 kW
Min.	0.1 kW	0.5 kW	0.8 kW
Daily Energy	8.5 kWh	23.9 kWh	39.3 kWh

(b)

Figure 1.8: Load data for every weekend and weekday overlaid onto a single day. a) Weekdays, b) Weekends. A summary of the plot key parameters i shown in their adjacent tables which highlights the difference between weekday load and weekend load.

residents return home. The weekend behavior is somewhat different, with a smaller morning peak with a larger variation in the mean during the midday period and a peak in the afternoon. Power consumed during the period from early morning to late afternoon is somewhat higher on weekends compared to weekdays.

The solar irradiation and hence generation data varies seasonally, e.g. there is less sunlight in winter compared to summer. The daily variation of generation data for the four seasons is considered in Fig. 1.9 where the blue, red and black lines have the same meaning as in Fig. 1.8. The average lines and one standard deviation lines vary rather significantly between seasons, for example in summer the average midday peak is approximately 4 kW compared to the winter average peak of approximately 3 kW. Examining the standard deviation lines for each season reveals that both winter and autumn have much higher variability in the data, i.e. each day can vary rather significantly compared to the other days during these seasons, which is likely due to the greater occurrence of cloudy days during these seasons. Thus in summer and spring the PV output is likely to be fairly consistent between each given day while during winter and autumn the PV output will vary rather significantly between each day.

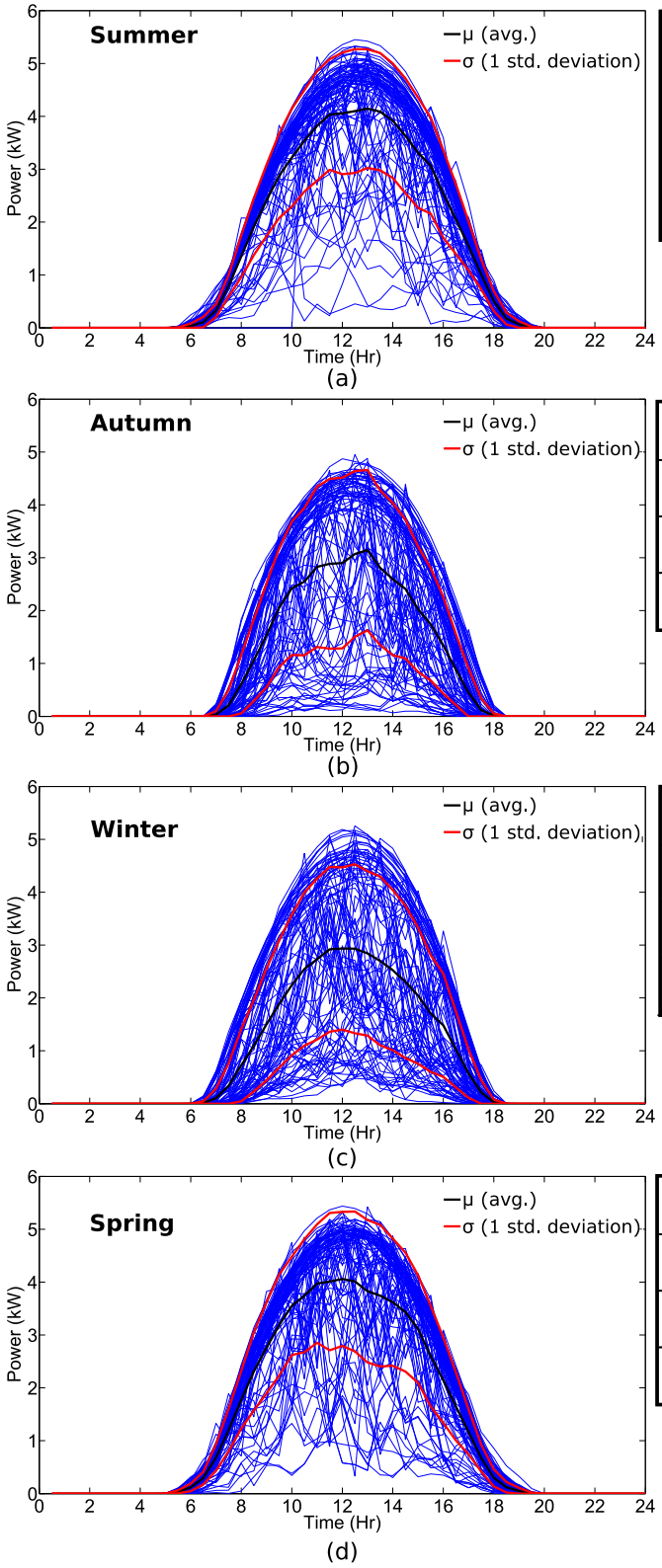

	Std. dev. lower	Mean	Std. dev. upper
Peak kW	3.0 kW	4.1 kW	5.3 kW
Output >50% of pk.	7.5 hr	7.5 hr	8 hr
Daily Energy	22.2 kWh	31.7 kWh	41.1 kWh

	Std. dev. lower	Mean	Std. dev. upper
Peak kW	2.4 kW	3.7 kW	5.1 kW
Output >50% of pk.	6.5 hr	7.5 hr	7.5 hr
Daily Energy	14.2 kWh	25.4 kWh	36.6 kWh

	Std. dev. lower	Mean	Std. dev. upper
Peak kW	1.1 kW	2.7 kW	4.2 kW
Output >50% of pk.	5.5 hr	6.5 hr	7.5 hr
Daily Energy	5.7 kWh	17.0 kWh	28.5 kWh

	Std. dev. lower	Mean	Std. dev. upper
Peak kW	2.3 kW	3.7 kW	5.2 kW
Output >50% of pk.	7.5 hr	8 hr	8 hr
Daily Energy	16.5 kWh	27.8 kWh	39.5 kWh

Figure 1.9: Generation data for each season in the year overlaid onto a single day for a 5.5kW PV rating, a) Summer, b)Autumn, c) Winter, d) Spring. A summary of the key parameters are shown in the adjacent tables which highlights the difference between each season's solar generation.

1.7.3 Household Cases

The annual load data for a number of different households from [48] is shown in Fig. 1.10. These smoothed curves are a rolling 7 day average showing the general trends of the various households' load. H1 refers to the base case household and H2 to H6 refers to the other households whose characteristics are detailed in Table 1.4. Fig. 1.10 demonstrates two key features: i) the similarities between households, and ii) the unique nature of the household loads.

The similarities of the household load behaviour is observed during the summer months, with the peaks and troughs for all household loads occurring at approximately the same times which suggests there is a common trend in the load for the households, e.g. households may all be using air conditioning during similar times. During spring there is also similarities of the peak/troughs of the household loads. During winter and autumn there appears to be a lower coincidence of the household peaks/troughs, e.g. some households have a peak while other households have troughs. The key outlier in Fig. 1.10 is household H3, which has significantly higher winter load compared to the other households and hence it is expected will require a larger HES system.

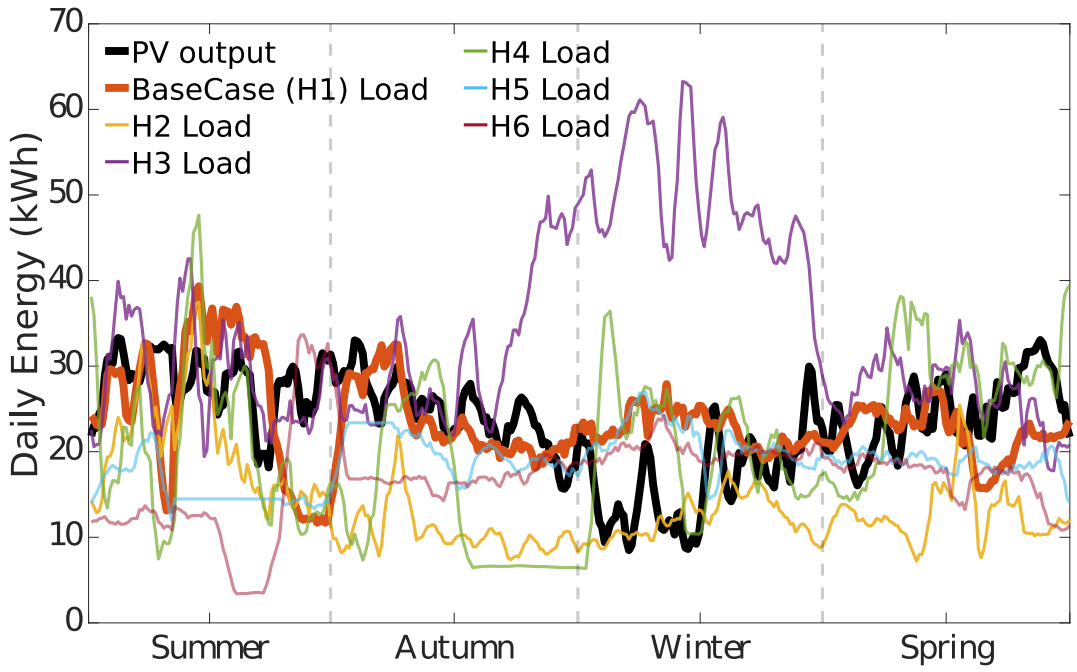

Figure 1.10: Daily generation and load data over a year for various households using 5.5 kW of PV and a rolling 7 day average

Fig. 1.11 lists the total annual load of each household and shows the load duration curve for each household indicating that households H1, H4, H5 and H6 have similar annual load and similar load behavior. Household H3 has the largest annual load and the largest load for 50% of the load duration curve while household H2 has the smallest annual load and has the lowest load duration curve.

Table 1.4: Details on the household loads. Dashed entries are unknown

House-hold	Avg. Daily Load	Gas Heat-ing	Gas Hot-water	Gas Cook-ing	Home in day-time	Air Con. Type	Num. of Occu-pants
H1	23.5 kWh	No	Yes	Yes	No	Split System	4
H2	14.0 kWh	Yes	No	Yes	No	Split System	2
H3	34.1 kWh	No	No	No	No	Ducted	4
H4	20.6 kWh	Yes	No	No	No	Ducted	3
H5	18.9 kWh	-	-	-	Yes	Split System	-
H6	9.8 kWh	-	-	-	Yes	Split System	-

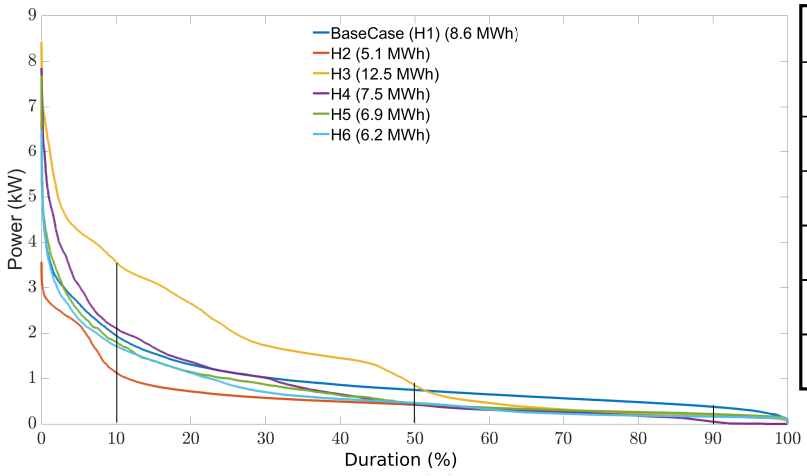

H#	Load Exceeds # for:		
	10%	50%	90%
H1	1.95 kW	0.75 kW	0.38 kW
H2	1.13 kW	0.42 kW	0.17 kW
H3	3.57 kW	0.85 kW	0.19 kW
H4	2.11 kW	0.43 kW	0.05 kW
H5	1.81 kW	0.46 kW	0.22 kW
H6	1.71 kW	0.46 kW	0.16kW

Figure 1.11: Load Duration Curves for the 6 household cases are shown. This curve is summarised in the adjacent table which shows the kW amount that the households load exceeds for i) 10%, ii) 50% and iii) 90% of the year.

1.7.4 Generation Years

The 6 different years of solar irradiation are shown using the generation-duration curves in Fig. 1.12. For the given location the annual generation G_1 varies between 1.5-1.7 MWh/kW$_p$ and the overall generation duration curves are similar with the 2002 year having a slightly higher generation output. The base case year is chosen as 2005.

1.7.5 Base Case: Net Generation

The net generation power time series (i.e. generation minus load) for the base case with a PV rating of 1.1 pu is shown in Fig. 1.13 with positive power being exported to the grid and negative power being imported from the grid. Integrating the net generation power time series provides the net generation energy time series which is

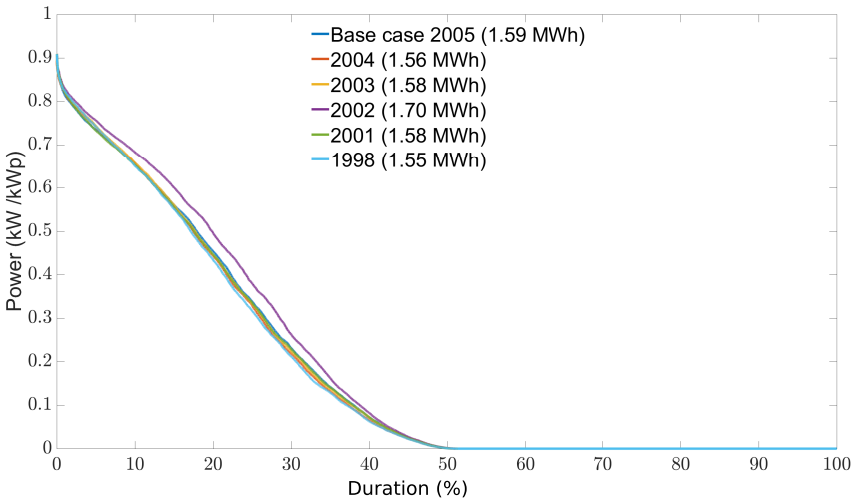

Figure 1.12: Generation Duration Curves for the 6 different years of solar irradiation

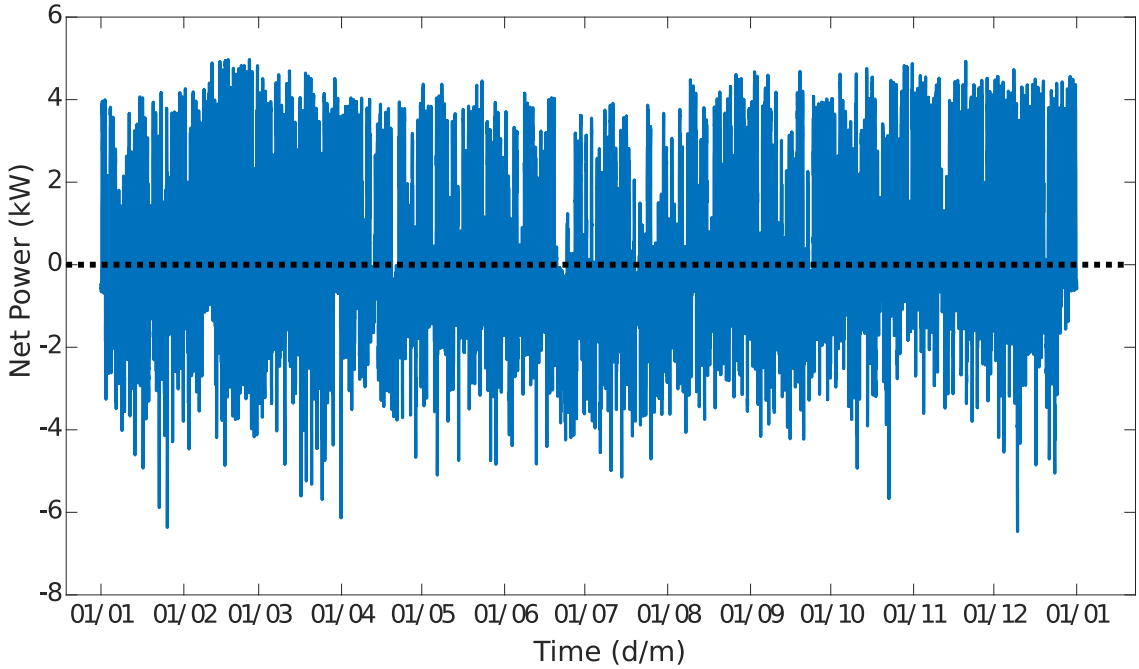

Figure 1.13: Net generation power time series over one year for the household H1 with PV rating 1.1 pu

shown in Fig. 1.14.

Note the net generation energy in Fig. 1.14 falls below zero during the 2nd and 8th month however this has no impact on analysis since storage is assumed to initially be full as discussed in Section 3.1.2 shown in Fig. 3.4.

1.7.6 Base Case: Power-Energy loops

Plotting the power versus energy for the net generation time series (Fig. 1.13 against Fig. 1.14) reveals loops which are seen in Fig. 1.15. The significance of these loops are discussed in Chapter 2. The difference in energy between the start and end of the lower half of each loop represents an important storage capacity, called a critical capacity. These lower-half loops are the foundation for the CCA method used to

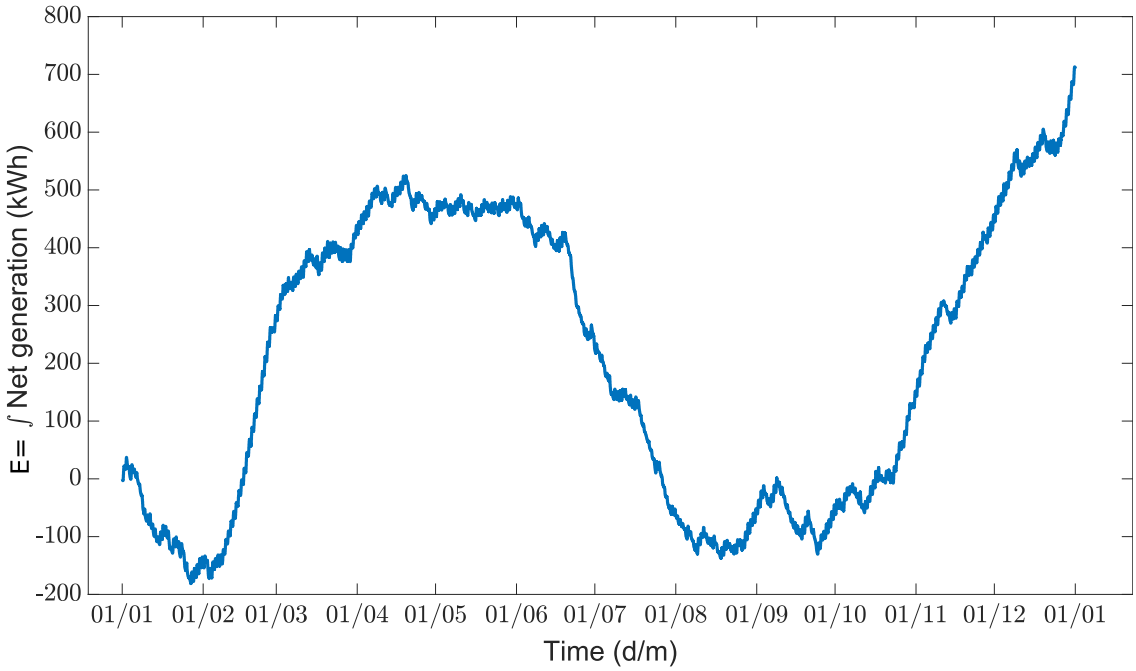

Figure 1.14: Net generation energy time series for the household H1 with PV rating 1.1 pu

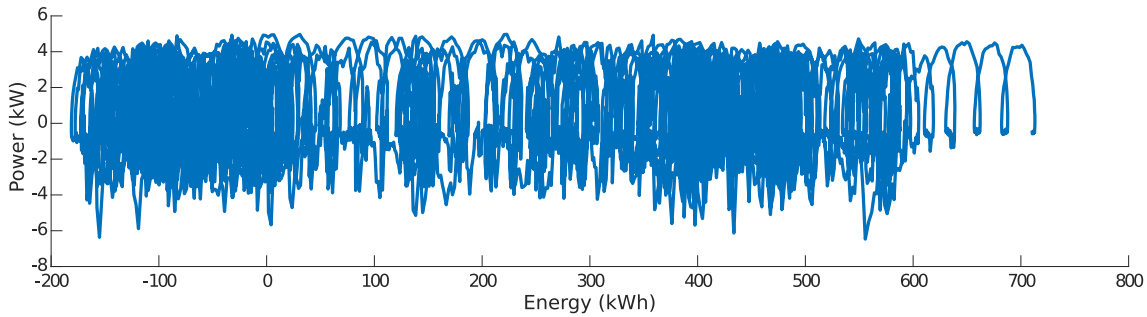

(a)

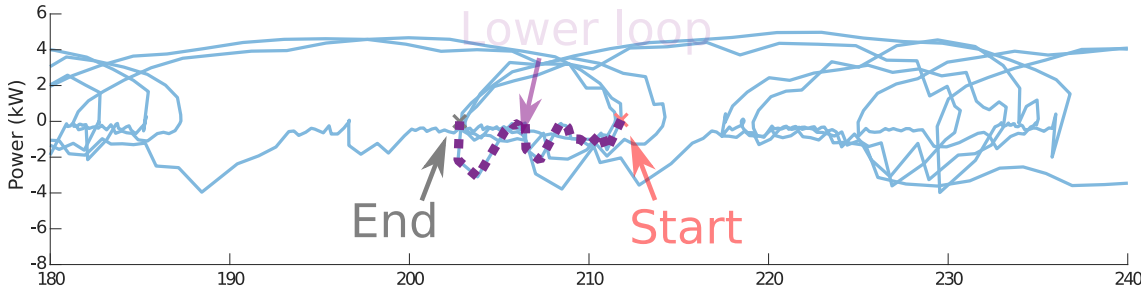

(b)

Figure 1.15: Power-energy plot of the net generation time series for 1 pu PV rating demonstrating a) the entire time series, b) a shorter section of time

analyse and select the optimal HES storage capacity. Fig. 1.15a shows the energy-power plot for the entire time series to illustrate the complexity involved with these loops. Fig. 1.15b shows a short segment of the energy-power curve to show the detail of these loops.

The marked points in Fig. 1.15b demonstrates an example of a critical capacity for the given PV rating, where the energy change between the start and end of the

lower part this loop is about 9 kWh. Note these loops are traversed in a clockwise direction.

Chapter 2

Critical Capacity Analysis: Derivation

The purpose of a HES is to reduce a household's annual energy cost and this cost reduction is called the benefit. As described in Section 1.2, this benefit depends on the total energy which the household buys (GSE) and sells (GFI) from/to the grid and there is a relationship between the HES size and the GSE and GFI. This chapter derives two important equations:

1. The relationship between GSE and storage capacity.

2. The relationship between the GSE and PV rating.

The first equation is a closed-form expression for the GSE in terms of storage capacity ($E_g[E_s, P_0]$) for a given PV rating (P_0). It is used in Chapter 4 to estimate the MBI. The second equation describes the relationship between GSE and PV rating ($E_g[E_{s0}, P]$) for a given storage capacity (E_{s0}) and is composed of three key terms. These key terms are used in Chapter 4 to estimate the MBI.

The HES benefit in (1.4) contains two key components, the cost saving by avoiding grid energy consumption ($E_h \times c_g$) and the income from selling energy to the grid ($E_f \times c_f$). Section 1.2 discusses these terms in detail and highlights that E_h and E_f are related to the GSE (E_g) through (1.3). Hence the benefit can be written in terms of: i) a single function which varies with HES size $E_g[E_s, P]$, ii) the PV rating, and iii) a number of other constants which are discussed later. The reason for writing the benefit in this way is that a closed-form equation for the GSE allows a closed-form equation for the benefit to be derived. Note the bold symbols for $\mathbf{E_h}$ and $\mathbf{E_f}$ are used to represent that these terms are a function of storage capacity and PV rating.

$$B[\mathbf{E_h}, \mathbf{E_f}] = E_h[E_s, P] \times c_g + E_f[E_s, P] \times c_f \qquad \text{(1.4 repeated)}$$

The benefit equation can be rewritten in (2.1) which contains the GSE $E_g[E_s, P]$, the PV rating P and the constants: L is the energy consumed annually by the load, G_1 is the annual amount of generated energy per kW_p of PV, c_g is the grid supply tariff and, c_f is the feed-in tariff.

$$B[\mathbf{E_g}] = (L - \mathbf{E_g}[\mathbf{E_s}, \mathbf{P}])c_g + (G_1 \times P - L + \mathbf{E_g}[\mathbf{E_s}, \mathbf{P}])c_f \qquad (2.1)$$

A special case of (2.1) is when there is no GSE ($E_g = 0$) which implies that the annual load is supplied by only the HES hence:

$$B[\mathbf{E_g} = 0] = L \times c_g + (G_1 \times P - L)c_f$$

In this case the benefit's two parts are: i) the cost savings ($L \times c_g$), and ii) the income derived from selling energy into the grid ($(G_1 \times P - L)c_f$). The cost saving is equal to the cost of annual load since the HES supplies all the load's energy demand (i.e. no GSE). The amount of energy available to be sold to the grid, at the feed-in

tariff rate of c_f, is equal to the total annual generation ($G_1 \times P$) less the annual energy supplied to the load (L).

As mentioned above, a closed-form equation for GSE implies a closed form benefit equation. The GSE can be written as a closed-form equation for a given PV rating (P_0) and variable storage capacity (E_s) in the form of $E_g[E_s, P_0]$. This closed-form GSE equation is derived from the canonical expression of a piece-wise linear (PWL) function and recognising that the GSE and storage capacity ($E_g[E_s, P_0]$) curve have PWL properties for a constant PV rating. The recognition that the $E_g[E_s, P_0]$ curve contains PWL characteristics is a contribution of this thesis as discussed in Section 1.4.1.

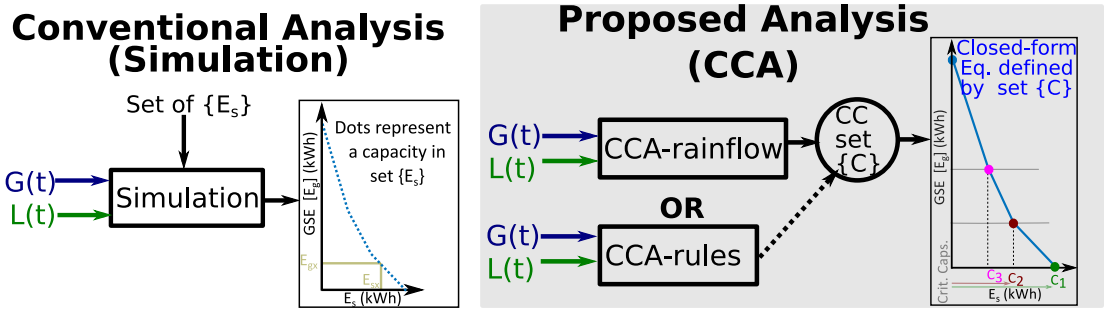

(a) (b)

Figure 2.1: Overview of the conventional and proposed analysis method, a) the conventional analysis (simulation), b) the proposed analysis (CCA) solved using either a heuristic-based algorithm or rainflow-based algorithm

The conventional analysis in [4,13–15,22–24,51] numerically estimates the $E_g[E_s, P_0]$ curve as illustrated in Fig. 2.1a where for a given generation and load time series, the energy flow of storage and hence the state of charge as a function of time is simulated for a list of chosen storage capacities to find the GSE for each storage capacity. The proposed analysis derives an equation for $E_g[E_s, P_0]$ which is defined by a set of constants, called the critical capacities (CC), and an algorithm is developed to find these critical capacities as illustrated in Fig. 2.1b. This algorithm analyses the generation and load time series using either: i) a heuristics rules-based method or ii) an adaption of an existing algorithm primarily used for material fatigue analysis called the rainflow algorithm [41].

2.1 Conventional Simulation Analysis

The conventional approach calculates the GSE for a set of storage capacities, illustrated by Fig 2.2c, by simulating the time series of the state of charge (SoC) for each storage capacity in the set, illustrated by Fig. 2.2b. The SoC simulation uses the net generation time series which is the difference between the PV generation-power time series and the load-power time series illustrated in Fig. 2.2a. In the net generation time series, negative values represent energy required to be supplied from either the

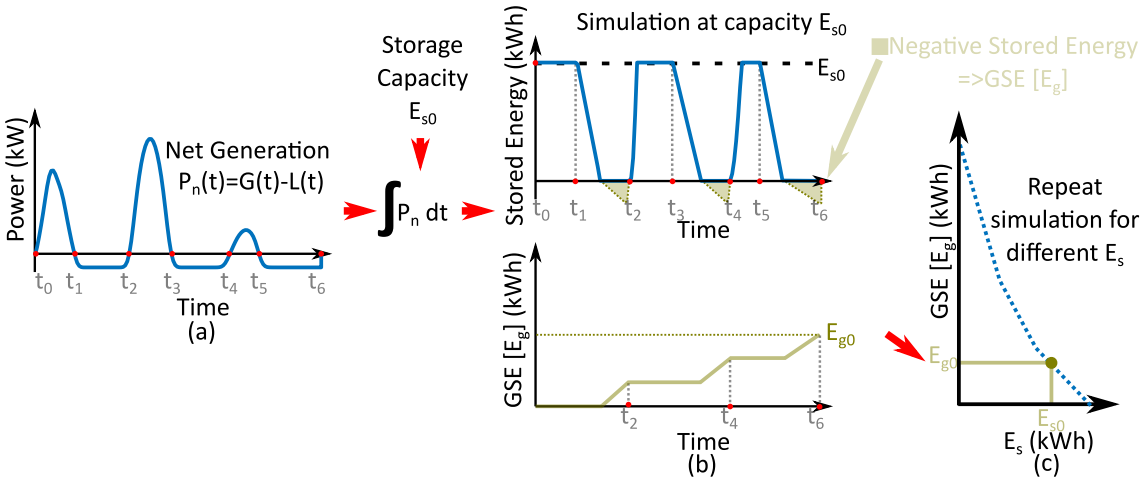

Figure 2.2: Summary of the conventional analysis to find the trade-off curve: (a) net generation-power time series, (b) simulating the SoC, (c) the GSE versus storage capacity trade-off

grid or storage and positive values represent energy which is either stored or sold as GFI.

The SoC simulation for a given storage capacity is described in [4, 13, 22, 52] by the mathematical expressions in (2.2) to (2.5). The limits on stored energy used in this expression has maximum $S_{max} = E_s$, where E_s is the selected storage capacity, and minimum $S_{min} = 0$, i.e. the minimum stored energy is an empty storage. Note the SoC, $S(t)$ can be normalised by the storage capacity.

$$S'(t) = S(t-1) + (G(t) - L(t))\Delta t \tag{2.2}$$

$$S(t) = \begin{cases} S_{min}, & \text{for } S'(t) \leq S_{min} \\ S'(t), & \text{for } 0 \leq S'(t) \leq S_{max} \\ S_{max}, & \text{for } S'(t) \geq S_{max} \end{cases} \tag{2.3}$$

$$E_g(t) = \begin{cases} S_{min} - S'(t), & \text{for } S'(t) \leq S_{min} \\ 0, & \text{for } S'(t) \geq S_{min} \end{cases} \tag{2.4}$$

$$E_f(t) = \begin{cases} 0, & \text{for } S'(t) \leq S_{max} \\ S'(t) - S_{max}, & \text{for } S'(t) \geq S_{max} \end{cases} \tag{2.5}$$

The SoC is simulated using a time-stepping method where the current SoC is updated based on the past SoC and the maximum/minimum storage limit. The term $S'(t)$ in (2.2) is the SoC for the current time-step (t) without applying either the maximum/minimum storage limits and is found by summing the energy previously stored $(S(t-1))$ at time $(t-1)$ with the energy transferred into storage $((G(t) - L(t))\Delta t)$ for the current time-step (t). By applying the storage limits to this non-limited SoC $(S'(t))$ as in (2.3) the SoC time series is found. If the non-limited SoC $(S'(t))$ is negative then the storage device is empty at time (t) and hence GSE occurs as shown in (2.4), note the annual GSE (E_g) is the sum of $E_g(t)$ across a given year.

If the non-limited SoC ($S'(t)$) is greater than the device's storage capacity then the storage device is full and hence GFI occurs as shown in (2.5). The annual GFI (E_f) is the sum of the $E_f(t)$ across a given year.

The simulation process in Fig. 2.2b is repeated for the entire set of storage capacities and the $E_g[E_s, P_0]$ curve is plotted for each combination of GSE and storage capacity in Fig. 2.2c. For example in Fig. 2.2b the storage capacity C_0 is simulated to produce the GSE value of GSE_0 and this combination is plotted in Fig. 2.2c. The $E_g[E_s, P_0]$ curve is generally linearly interpolated between each selected storage capacity and hence significant errors can occur if a small set of storage capacities is selected, leading to a trade-off between accuracy and computational time.

Note the conventional approach follows the assumptions discussed in Section 1.6 such that: i) storage is initially assumed full ($S(0) = S_{max}$), ii) the storage is assumed to be lossless (100% efficient), and iii) the power limits of the HES are ignored.

2.2 Proposed Critical Capacity Analysis Fundamentals

The proposed CCA method assumes that the $E_g[E_s, P_0]$ curve, for a given PV rating, has the features of a piece-wise linear (PWL) function and hence a closed-form solution can be derived using the canonical form of a PWL function. To summarise the definition of a PWL function from [39, 40], a curve of a single variable is PWL if it consists of both: i) a number of linear segments with various slopes, and ii) a number of breakpoints which describe the points of intersection between two linear segments and hence the points at which the slope changes. The CCA method shows that the linear segments of the $E_g[E_s, P_0]$ curve has a step change in slope of minus one (in the chosen per unit system) at each breakpoint. These breakpoints are called critical capacities as they characterize the $E_g[E_s, P_0]$ curve as illustrated in Fig. 2.3.

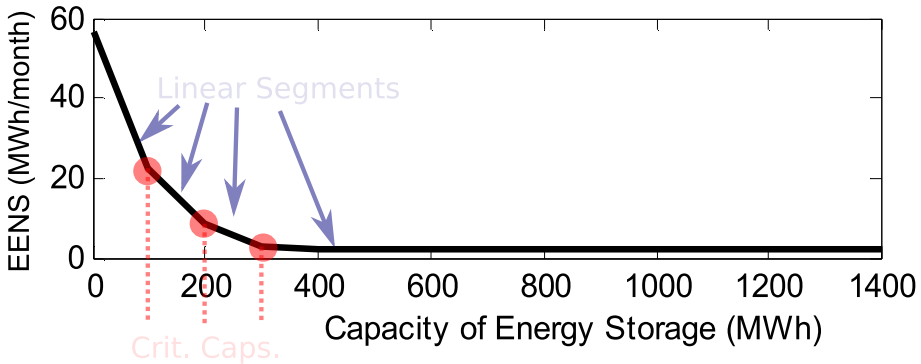

Figure 2.3: The $E_g[E_s, P_0]$ curve from [15], noting EESN is equivalent to GSE. The markup shows the linear segments (black) and breakpoints/critical capacities (red). The original image in [15] is copyright ©2010, IEEE.

A formal proof that the $E_g[E_s, P_0]$ curve is a PWL function has not been developed however the PWL nature of the curve can be seen in the literature, for example

in Fig. 2.3 a markup of the results from [15] are shown to contain linear segments. Note the literature has not commented on this PWL nature. The CCA method and its PWL-based equation is validated against the conventional simulation approach in Chapter 3 and both methods produce the same output which confirms the PWL nature of the $E_g[E_s, P_0]$ curve.

2.2.1 Deriving the $E_g[E_s, P_0]$ Equation in Canonical Piecewise Linear (PWL) Form

Equation (2.6) from [39,40], describes the canonical form of a one-dimensional PWL function with $(N+1)$ linear segments with $(N+1)$ slopes $(J_0, J_1, \cdots, J_N)$, and N breakpoints/critical capacities $(c_1, c_2, \cdots, c_N)$ as illustrated for the $E_g[E_s, P_0]$ curve in Fig. 2.4.

$$E_g[E_s, P_0] = a + bE_s + \sum_{i=1}^{N} \Delta J_i |c_i - E_s| \tag{2.6}$$

where:

$$a = E_g(0) - \sum_{i=1}^{N} \Delta J_i |c_i| \qquad b = \frac{J_0 + J_N}{2} \qquad \Delta J_i = \frac{J_i - J_{i-1}}{2}$$

Note (2.6) does not consider which linear segment contains the given E_s, i.e. the terms in the equation does not need to be evaluated between C_i to C_{i+1}, this is due to the nature of the equation which is discussed later in (2.8). Equation (2.6) depends on P_0 since the list of critical capacities are valid for the given P_0.

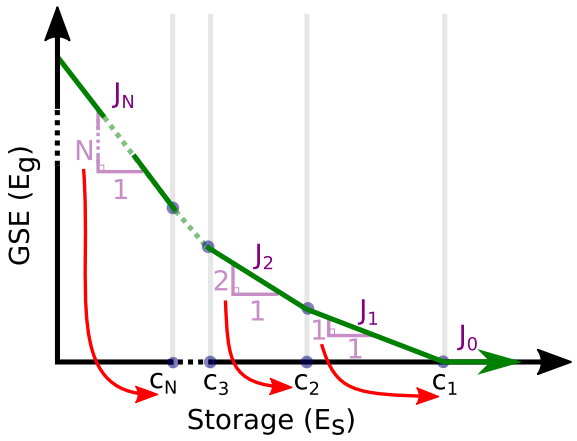

Figure 2.4: Illustrating the breakdown of the $E_g[E_s, P_0]$ curve into linear segments, where each segment is labeled by their slope J_0 to J_N and the critical capacities are labeled c_1 to c_N.

In Fig. 2.4 each linear segment is labeled in descending order, beginning at J_N and ending in J_0, and similarly the critical capacities are labeled in descending order.

The GSE in (2.6) is simplified by the following:

1. $\Delta J_i = \frac{1}{2}$ for all i as the change in slope is minus one at each critical capacity (for the chosen per unit system).

2. $b = -\frac{N}{2}$, since the linear segment J_0 has zero slope and linear segment J_N has $-N$ slope.

3. $a = E_g(0) - \frac{1}{2}\sum_{i=1}^{N} c_i$ since all critical capacities are positive then $|c_i| = c_i$.

$E_g(0)$ is the GSE required when no storage is installed at the given PV rating, i.e. given a HES with only PV generation (no storage) $E_g(0)$ describes the amount of load remaining after subtracting the energy supplied by the PV system (GEO_{PV} in Fig. 1.1). However $E_g(0)$ also describes, for a given PV rating, the amount of load energy which must be supplied through the combination of GSE and the stored energy (GEO_S in Fig. 1.1), for example if GSE is zero then storage supplies all of the remaining annual load and hence GEO_S equals $E_g(0)$.

$E_g(0)$ is found using the GSE at each critical capacity starting with zero GSE at c_1 and iterating up to find the GSE which occurs at zero storage capacity, such that:

$$
\begin{aligned}
E_g(c_1) &= 0 \\
\frac{E_g(c_2) - E_g(c_1)}{c_2 - c_1} = -1 &\implies E_g(c_2) = c_1 - c_2 \\
\frac{E_g(c_3) - E_g(c_2)}{c_3 - c_2} = -2 &\implies E_g(c_3) = c_1 + c_2 - 2c_3 \\
\frac{E_g(c_4) - E_g(c_3)}{c_4 - c_3} = -3 &\implies E_g(c_4) = c_1 + c_2 + c_3 - 3c_4 \\
&\vdots \\
E_g(c_N) &= \left(\sum_{i=1}^{N-1} c_i\right) - (N-1)c_N
\end{aligned}
$$

hence:

$$
\begin{aligned}
\frac{E_g(0) - E_g(c_N)}{0 - c_N} = -N \implies E_g(0) &= Nc_N + \left(\left(\sum_{i=1}^{N-1} c_i\right) - (N-1)c_N\right) \\
E_g(0) &= \left(\sum_{i=1}^{N-1} c_i\right) + c_N \\
E_g(0) &= \sum_{i=1}^{N} c_i \qquad (2.7)
\end{aligned}
$$

Equation (2.7) reveals that $E_g(0)$ is described by only the critical capacities for a given PV rating, which highlights the importance of critical capacities. By combining the equation for $E_g(0)$ with the piecewise-linear function for GSE in (2.6) a

closed-form equation for the GSE is derived for a fixed PV rating (P_0) as follows:

$$E_g(E_s, P_0) = a + bE_s + \sum_{i=1}^{N} \Delta J_i |c_i - E_s|$$

$$E_g(E_s, P_0) = \left(\sum_{i=1}^{N} c_i - \frac{1}{2} \sum_{i=1}^{N} c_i \right) - \frac{N}{2} E_s + \frac{1}{2} \sum_{i=1}^{N} |c_i - E_s|$$

$$E_g(E_s, P_0) = \sum_{i=1}^{N} \frac{1}{2} \Big((c_i - E_s) + |c_i - E_s| \Big) \tag{2.8}$$

The key component of (2.8) is the sum term $\frac{1}{2}((c_i - E_s) + |c_i - E_s|)$, which reveals that the GSE is a linear combination of the critical capacities. For a given storage capacity E_x all critical capacities less than E_x ($c_i < E_x$) do not contribute to the GSE as their sum term is zero and hence these critical capacities are said to be "inactive". All critical capacities greater than E_x ($c_i > E_x$) contributes ($c_i - E_x$) to the GSE and these critical capacities are said to be "active". The concept of active and inactive critical capacities is significant when discussing how to find critical capacities since active critical capacities indicate there are times within the year when a given storage capacity is unable to supply load and hence when GSE occurs.

An alternative expression for the GSE is derived by considering a variable index (n) where $(c_i - E_s) > 0$ for all critical capacities up to the index (c_n) hence:

$$E_g(E_s, P_0) = \sum_{i=1}^{n} (c_i - E_s) \quad \text{for } n \text{ such that } c_1 \geq \cdots \geq c_n \geq E_s \tag{2.9}$$

The outcome of (2.8) is a closed-form expression for the GSE in terms of storage capacity, for a specified PV rating, using only the list of critical capacities ($\boldsymbol{C} = \{c_1, \cdots, c_N\}$) and the CCA method provides an algorithm to find these critical capacities.

Note that critical capacities can share a common magnitude, for example $c_a = c_{a+1}$, and the resulting GSE for storage capacities less than the shared capacity (c_a) will have a slope of 2, or to describe this generally, if M storage capacities share a magnitude then the slope would change by M. For example consider in Fig. 2.4 if c_2 was shifted left until it equaled c_3 then the segment of the curve labeled with J_2 would have zero length and the curve would change from a slope of minus one to a slope of minus three at c_3. The GSE equation remains valid in this example as the GSE at c_2 equals the GSE at c_3 and the derivation of $E_g(0)$ would remain unchanged.

2.2.2 Finding Critical Capacities

Critical capacities define the $E_g[E_s, P_0]$ curve for a household at a given PV rating as observed in (2.8) and hence as illustrated by Fig. 2.5, critical capacities

are an attribute of a household with a given combination of: i) load time series, and ii) PV generation time series (for a given PV rating). Consider a household's net generation-power time series ($P_n(t)$) illustrated in Fig. 2.5a and the integral of $P_n(t)$ which describes the net generated-energy time series ($E_n(t)$) as illustrated by Fig. 2.5b.

The power time series plotted against the energy time series in Fig. 2.5c reveals loops resulting from the combination of: i) the availability of PV energy which could be stored (positive net power) describing the loop's upper-half (such as between t_2 and t_3), and ii) the requirement of load when no PV generation is available (negative net power) describing the loop's lower-half (such as between t_1 and t_2). The difference in the energy between the start and end of the loop's lower-half describes a critical capacity within that loop, as shown by the marked values c_1 to c_3 in Fig. 2.5c. These critical capacities are found by applying either a series of rules or applying the rainflow algorithm on the net generated-energy time series $E_n(t)$. The $E_g[E_s, P_0]$ curve is plotted in Fig. 2.5d using the identified critical capacities and the GSE equation (2.8).

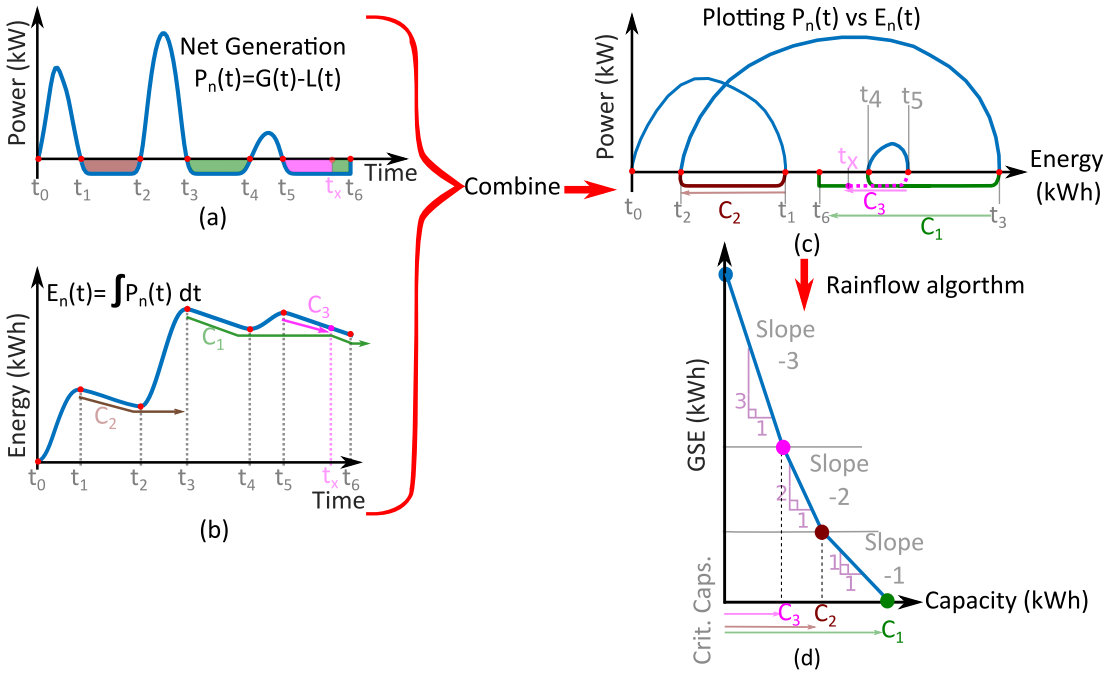

Figure 2.5: Summary of the proposed CCA method used to define the $E_g[E_s, P_0]$ curve. (a) net generation-power time series, (b) net generated-energy time series, (c) net generation-power versus net generated-energy, (d) the GSE versus storage capacity trade-off

The rules-based approach was developed by extending an existing technique of water-reservoir sizing in [53], as reservoir sizing shares many similarities to energy storage sizing. The reservoir sizing technique can find the majority of the critical capacities however some are missed, and these missing critical capacities can be found by defining and applying a set of rules to the output of the reservoir sizing technique. Applying these rules to the case study data identified all the critical

capacities however there is no proof that the existing set of developed rules will identify all the critical capacities for any arbitrary time series. For example there may exist special case rules which have not been identified from the case studies in this thesis. Hence an alternative method to identify critical capacities was developed using the rainflow algorithm which is a more generalised approach.

The purpose of the original rainflow algorithm was to identify mechanical stress cycles for fatigue analysis [41, 42] and it is also used for battery life analysis [54, 55]. The application of the rainflow algorithm to identify critical capacities was discovered in the development of the rules-based method when attempting to overlay a series of vectors representing the critical capacities on top of a plot of the net generation, similar to the arrows labeled c_1 to c_3 in Fig. 2.5b. The resulting overlaid plot had similar characteristics to the storage lifetime plots produced by the rainflow algorithm. The rainflow algorithm identifies cycles within the data, such as the loops in the power-energy plot seen in Fig 2.5c, and hence the rainflow algorithm identifies critical capacities within the net generated-energy time series (E_n).

Applying the original rainflow algorithm to the net generated-energy time series, $E_n(t)$ in Fig. 2.5b, would combine both the lower-halves and upper-halves of the loops in Fig. 2.5c to form a single cycle and hence the rainflow algorithm must be modified to distinguish between these lower (associated with the load critical capacities) and upper halves of the loops (associated with the generation critical capacities). Typically the load critical capacities and the generation critical capacities result in the same list of values and hence the term critical capacities is used. Generation critical capacities are only significant when storage is not assumed to initially be full and hence the GFI cannot be expressed in terms of GSE by (1.3b).

2.3 Illustrating the Critical Capacities in a Worked Example

Section 2.2 has highlighted the mathematical definitions for critical capacities and how they can be used to define the relationship of GSE to storage capacity. The following provides two example power time-series which can provides a step-by-step discussion to demonstrate:

1. How plotting power against energy (P-E plot) demonstrates the critical capacities as the difference in energy between two points in the plot.

2. The GSE is PWL with breakpoints (critical capacities) where the slope changes by -1.

These examples have assumed the power time-series is a square wave however the conclusions drawn from the P-E curve and the resulting GSE to storage characteristics do not depend on the shape. Rather these conclusions and characteristics

depend only on the energy consumed in each "discharge" cycle (when the net power is negative) and are irrespective of the form of $p(t)$ during the cycle.

These examples do not describe how the critical capacities are found but rather they are used to provide an intuitive understand of how critical capacities relate to both the time-series and to the GSE.

2.3.1 Worked Example 1

The first worked example considers a simple power time series in Fig. 2.6 with one period of negative net power, between points A and B, and one period of positive net power between points B and C. When the net power time series is negative, the period of time which it remains negative is called a discharge cycle and when the net power is positive it is called a charge cycle. The naming of charge/discharge cycles are based on whether energy is available to charge or discharge a potential storage capacity (irrespective of its state of charge). In Fig. 2.6 the zero crossing and end points of the curve are labeled with letters for easy referencing in the Energy and P-E plots.

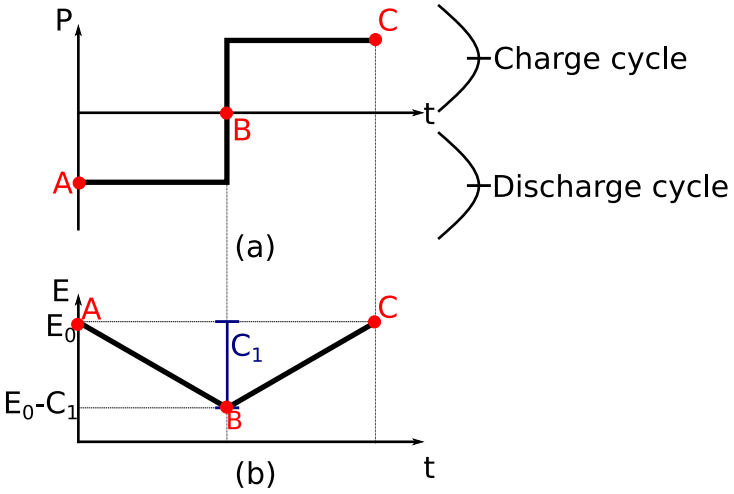

Figure 2.6: The power and energy time-series for Example 1. In the power time series, positive energy represents a charge cycle and negative energy represents a discharge cycle. The energy time-series is the integral of the power time-series with an initial energy $E(0)$ has a value of E_0

The net generated-energy time-series in Fig. 2.6 is the integral of the power time-series and the initial energy value (the constant of integration, E(0)) is set to an arbitrary value of E_0. Note the difference in energy between point A and point B is labeled as C_1 which is a critical capacity and is a key feature of this curve.

By plotting the power against the energy the resulting power-energy (P-E) plot is shown in Fig. 2.7. By traversing from point A to point B (a discharge cycle) requires the load to be supplied with C_1 units of energy. Traversing the curve from point B to point C shows that there is excess generation of C_1 units of energy which occurs since in this example the curve is symmetric (e.g. energy between A and B

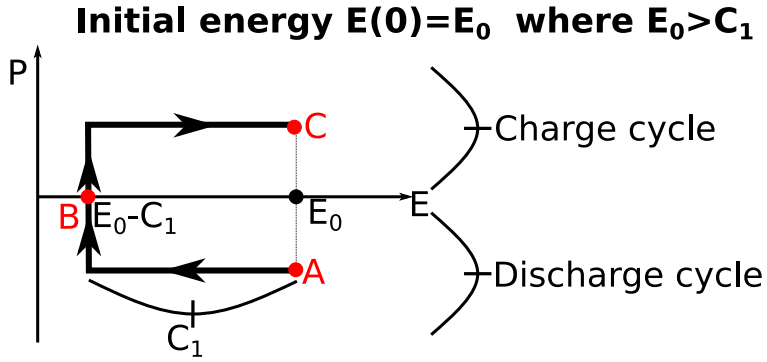

Figure 2.7: Combining the power and energy plots for Example 1 to form the P-E plot. The curve begins at A with initial energy E_0 and traverses clockwise as shown by the arrows. The critical capacity C_1 is the energy between A and B.

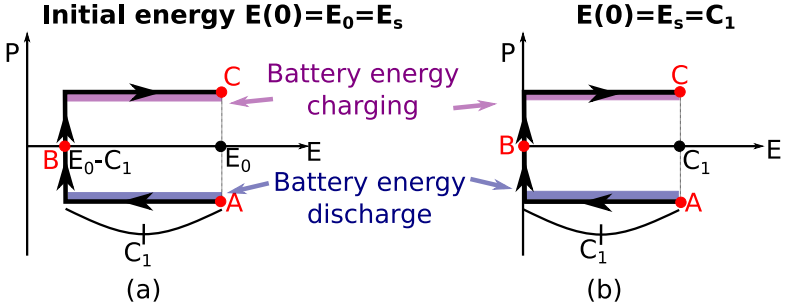

Figure 2.8: The power-energy plot if the initial energy $E(0)$ is equated to a battery capacity (E_S) of: a) E_0, and b) C_1. The energy between A and B now represents discharging storage and the energy between B and C represents charging the battery.

equals energy between B and C).

If a storage capacity is selected to be equal to the initial energy E_0, e.g. $E_s = E_0$, then the power energy curve provides information on the charging/discharging state of the battery. For example in Fig. 2.8a the storage discharges energy equal to C_1 between point A and point B and charges energy equal to C_1 between point B and point C. This charging and discharging behavior continues even when the storage capacity is reduced to $E_s = C_1$ which is shown in Fig. 2.8b.

When the storage capacity is selected below C_1, the resulting P-E plot in Fig. 2.9 demonstrates that storage is only able to supply a portion of the energy between A and B. The storage can supply its capacity E_1 to the load and the remaining load (energy E_x) must be supplied by GSE. Between points A and B the load requires energy equal to C_1 and since the storage has supplied an energy of E_1 then the GSE $E_x = C_1 - E_1$. Note since storage can only absorb energy of E_1 then between point B and C there is a point α where storage is full. The energy between B and α is used to charge the storage to full and the energy between α to C is exported to the grid.

If the storage capacity is decreased further from what is shown in Fig. 2.9 it is equivalent to shifting the power axis to the right and observing that the energy between A and B which is in the negative region of the energy axis is the GSE. The

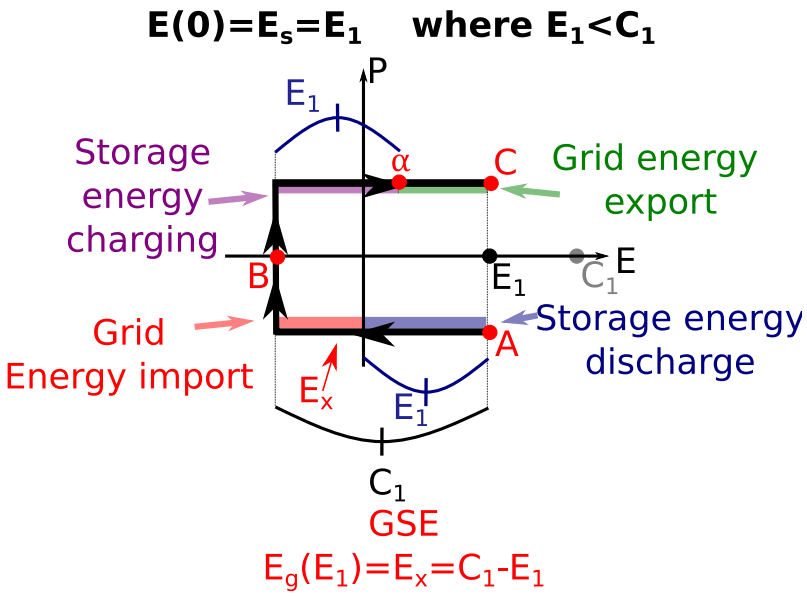

Figure 2.9: The power-energy plot if initial energy/storage capacity is equal to E_1 which is smaller than C_1. The key result is GSE E_x occurs between A and B and GFI occur between α and C.

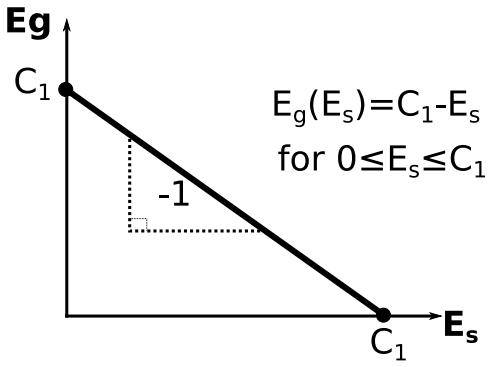

Figure 2.10: The resulting GSE to storage plot for Example 1. As observed in Fig. 2.9 the GSE is linearly related to storage

results from Fig. 2.9 can be generalized for any storage capacity E_s which is smaller than C_1. In this case the resulting GSE is $E_g(E_s) = C_1 - E_s$, and this is plotted in Fig. 2.10.

Note the initial energy $E(0)$ does not influence the critical capacities (e.g. C_1) and it only influences the resulting GSE if the first discharge cycle is negative, see Section 1.6 for details on how the initial storage capacity affects GSE.

2.3.2 Worked Example 2

The second worked example considers extending the time-series to consider two discharge cycles (A to B, C to D) and two charge cycles (B to C and D to E). The power time-series is shown in Fig. 2.11a and the energy time-series is shown in Fig. 2.11b. The energy time series in this example has two key points, C_1 the energy between A to B and C_2 the energy between C to D. The energy time series

also assumes an initial arbitrary energy amount $E(0) = E_0$.

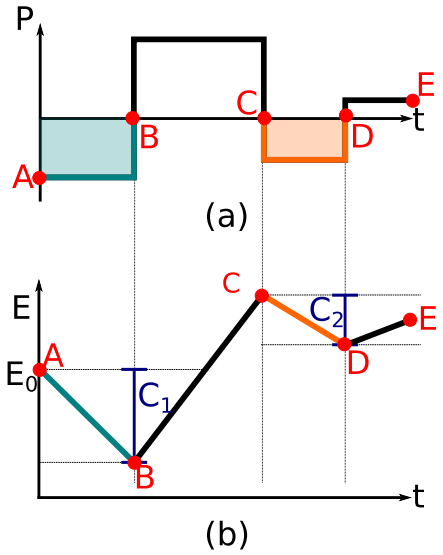

Figure 2.11: The power and energy time-series for Example 2. The energy plot has two critical capacities: i) C_1 the energy between A and B and ii) C_2 the energy between C and D.

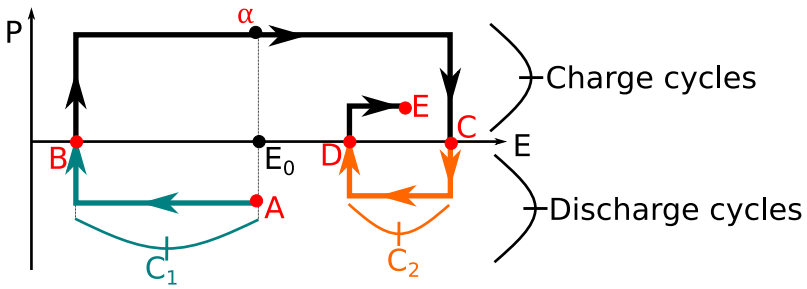

Figure 2.12: The P-E plot for example 2. The curve begins at A with initial energy E_0 and traverses clockwise as shown by the arrows. There are two critical capacities and their locations are also shown. Point α represents the position between C and D that would correspond to a full storage capacity, for storage capacity $E_s = E_0$.

The P-E plot for example 2 is Fig. 2.12 when the initial energy $E(0)$ is the value E_0. There are two critical capacities identified: i) C_1 between points A and B, and ii) C_2 between points C and D. This example is examined for two different storage capacities (E_s): a) between C_1 and C_2 in Fig. 2.13a, and b) less than C_2 in Fig 2.13b. The reason for considering these two storage capacities will be explained later in Fig 2.14. The power-energy plots in Fig. 2.13 are discussed in Table 2.1.

The $E_g[E_s, P_0]$ relationship in Fig. 2.14 highlights that there are two segments described by Fig. 2.13: i) segment A when storage is sized between C_1 and C_2, and ii) Segment B when storage is sized less than C_2. As shown in Fig. 2.13a and discussed in Table 2.1 when E_s is between C_1 and C_2 then the relationship between E_g and E_s has a slope of 1:1. When E_s is less than C_2 then the relationship between E_g and E_s has a slope of 2:1.

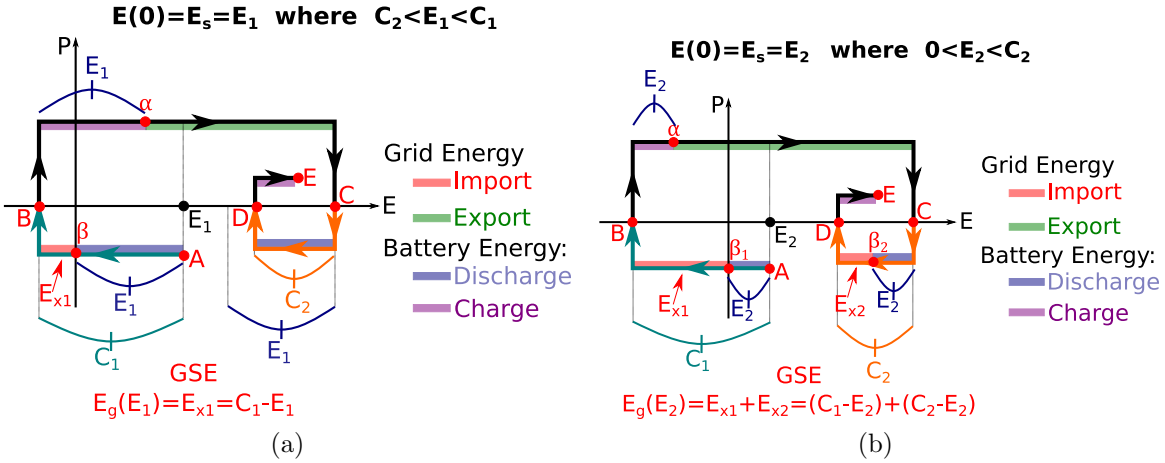

Figure 2.13: The power-energy plot for example two if storage capacity is: a) between C_1 and C_2, and b) less than C_2.

Table 2.1: Discussing the power-energy plots in Fig. 2.13 by examining the energy at each point, A to E, which highlights the relationship between grid sourced energy and storage

Fig. 2.13a, $C_1 < E_s < C_2$	Starting at point A, where storage is full, storage discharges until point β where storage is empty since $E_s < C_1$. Since storage is empty then grid energy (E_{x1}) must be imported to supply the load, note E_{x1} is the load energy between points β and B. Storage then charges between points B and α where it is then fully charged. Between points α and C the generated energy is sold to the grid. Storage discharges between points C and D, note there is no GSE since storage is: i) fully charged prior to point C, and ii) storage capacity E_s is larger than the energy between points C and D (i.e. is larger than C_2). Finally storage charges between points D and E. In this case the grid sourced energy E_g is the difference between C_1 and E_s and the relationship between E_g and E_s is 1:1.
Fig. 2.13b $E_s < C_2 < C_1$	The behavior of storage prior to point C is the same as above. However for this case, between points C and D there is an additional point β_2 where storage will become empty since $E_s < C_2$. This results in two instances where GSE occurs: i) between points A and B (the first critical capacity), and ii) between points C and D (the second critical capacity). In this case the grid sourced energy is the difference between both: i) C_1 and E_s, and ii) C_2 and E_s. Hence the relationship between E_g and E_s is 2:1, e.g. increasing E_s by 1 kWh causes E_g to increase by 2 kWh.

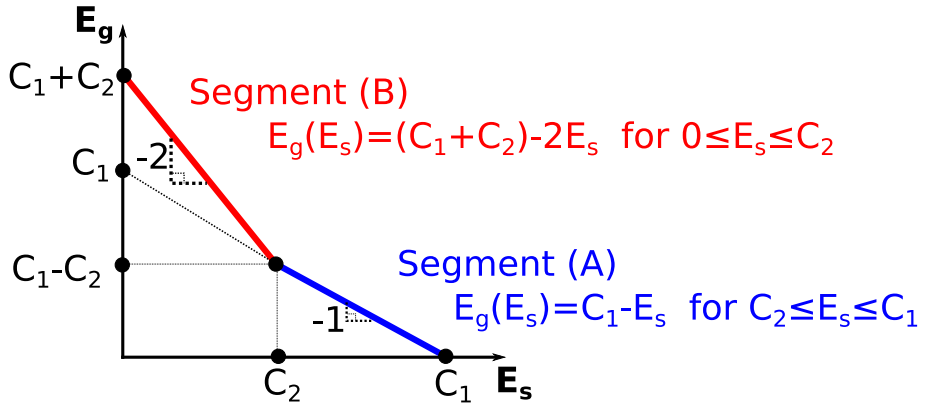

Figure 2.14: The GSE to storage capacity ($E_g[E_s, P_0]$) relationship for Example 2.

2.4 Techniques to Identify Critical Capacities

2.4.1 Rules-Based Identification

Fundamental Concept

The rules-based approach is based on water reservoir sizing techniques due to similarities between water reservoirs and energy storage shown by the comparison of terms in Table 2.2. For example water flow is equivalent to power and water volume is equivalent to energy.

Table 2.2: Equivalency between water storage terms and energy storage terms

Water Storage		Energy Storage	
Symbol	**Description**	**Symbol**	**Description**
Q	Water flow rate into reservoir	G	Power generation for a given PV rating
D	Water flow rate out of reservoir	L	Load power for a given household
$Q-D$	Net flow rate	$G-L$	Net generation power
$\sum(Q-D)$	Net cumulative volume	$\int(G-L)dt$	Net generated energy

Two common reservoir sizing techniques in [53] are the: i) Rippl method in Fig. 2.15(a) and ii) Sequent peak algorithm in Fig. 2.15(b). These two techniques find only the largest storage requirement (i.e. the largest critical capacity) and have not been developed to consider the trade-off between the reservoir size (storage capacity) and the amount of unsatisfied water demand (GSE).

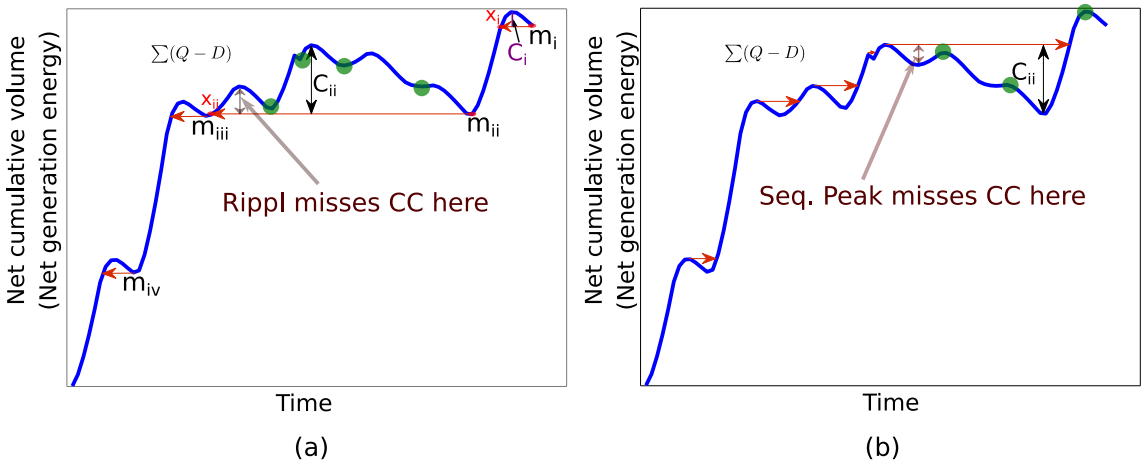

Figure 2.15: Example of a) Rippl method and b) Sequent peak analysis. Adapted from [53]. Q is analogous to generation, D is analogous to load and, the C_j values represent critical capacities

The Rippl method identifies the largest critical capacity through the following algorithm:

1. Beginning at the end of the net generated-energy time-series, identify the local minimum, m_i.
2. A horizontal line is drawn beginning at point m_i, moving backwards in time and ends when the line intersects the curve which occurs at point x_i.
3. The difference of energy between the horizontal line and the largest local maxima within the period between m_i and x_i describes a critical capacity C_i.
4. The next local minimum occurring earlier in time than point x_i is considered, i.e. m_{ii}.
5. Repeat steps 2 to 4 for the new local minimum until the beginning of the time series is reached.
6. The largest critical capacity is then the largest of $\{C_i, \cdots, C_{iv}\}$

The sequent peak algorithm in Fig. 2.15(b) operates similarly to the Rippl method except it begins at the start of the time series, identifies local maxima and each critical capacity is between the horizontal line (from step 2) and the smallest local minima within the period (from step 3).

In step 2, the start (m_i) and end time (x_i) of each horizontal line describes a period of time, called a zero net flow (energy) period, where the total inflow (generated energy) equals the total outflow (load's energy demand) and hence if generation is shifted (through sufficiently sized storage) to coincide with times of load then no supplementary supply (GSE) is required.

The Rippl method identifies a subset of the critical capacities and the missing critical capacities are shown by the four green circles in Fig. 2.15(a). The remaining critical capacities are identified by applying a series of rules to the periods of zero net energy identified by the Rippl method.

Rules Summary

The following summarises the rules developed to identify the critical capacities missed by the Rippl method and the development of these rules are detailed in Appendix A. To illustrate the rules an ideal net generation-power time series is constructed in Fig. 2.16a where positive net power represents power flows into either storage or to the grid and negative net power represents power flows to the load from either storage or the grid.

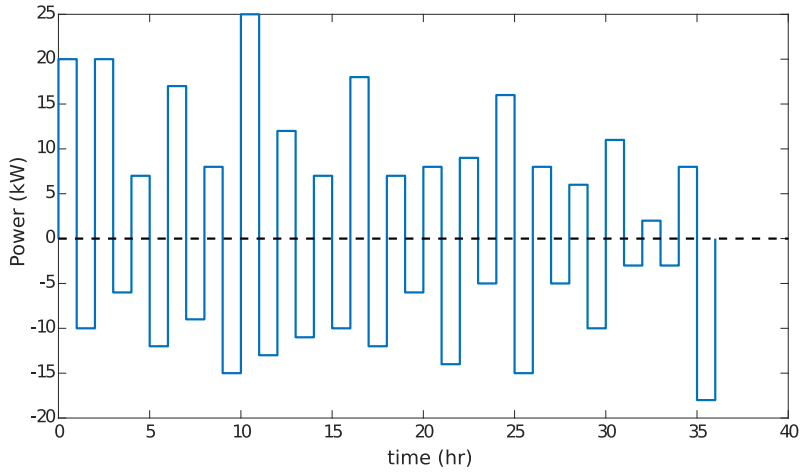

(a)

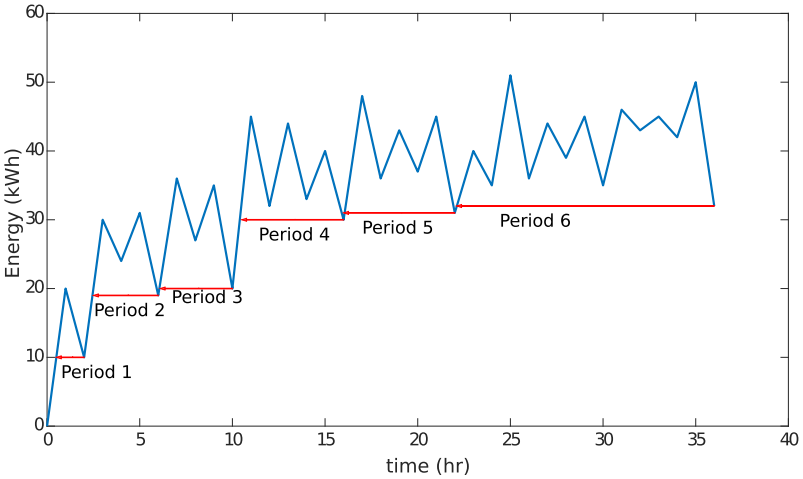

(b)

Figure 2.16: The constructed time series which demonstrates the rules developed to identify critical capacities: a) net generation power time series, b) net generated energy time series

Note the scale of both the power and energy time series in Fig. 2.16 have been selected to exaggerate the features of a typical net generation curve to more easily

observe the rules. The range of power values (-20 kW to 25 kW) is not representative of a typical household usage which would be significantly smaller and the time frame of the constructed time series is shorter than the more typical time frame where the net generation changes from positive to negative across multiple hours as opposed to one hour in the example. However the features of this constructed time series are similar to the features observed in the case study time series.

The net generated-energy time series is shown in Fig. 2.16b and the Rippl method identifies six periods of net zero-energy. A period of net zero-energy occurs when for a given period the total energy generated at an earlier time equals the total energy consumed and hence the load in a period of net zero-energy can be supplied by shifting only the energy generated during that period. For example supplying the load within Period 4 does not require any of the energy generated within Period 3. Since each of these periods have net zero-energy then, for a given storage capacity, the GSE within a given period is independent of all other periods and hence the total GSE is the sum of the GSE occurring within each period. Each period of net zero-energy contains at least one critical capacity and, as will be explained in Section 3.2, the number of critical capacities within a period is related to the number of times the net generation-power becomes negative.

Conceptually the rules used in the rules-based method are based on the discharging and charging behavior of storage and how this behavior causes GSE to occur. Hence there are two major rules which are used to identify critical capacities:

Rule (1): The discharging rule which is associated with the GSE that would occur when all of the stored energy has been consumed during a time of negative net generation and,

Rule (2): the charging rule which is associated with the GSE that would occur when the storage device is full during a time of positive net generation and hence some of the generated energy cannot be shifted to the load at a later time.

When applying the rules to a given net zero-energy period, at least one critical capacity will be found however the period may also contain additional critical capacities and hence depending on the features of the given period it may be separated into a smaller sub-period which is a subdivision of the original period. There are a number of sub-rules for these two major rules and which rule/sub-rule is applied depends on the time-series, i.e. the rules/sub-rules apply when a period (or sub-period) contains a specific set of features.

The application of the rules and the time series features which are used to indicate which rule should be used are seen in Fig. 2.17 which also demonstrates: i) the critical capacities' locations and ii) the sub-periods created by each rule. Note only Rule 1b.1, Rule 1b.2 and Rule 2b create sub-periods and the rules must be applied to these sub-periods to find additional critical capacities. In Fig. 2.17, row (1) is the

base case for the emptying rule (Rule 1a) and row (4) is the base case for the filling rule (Rule 2a). Algorithm 3 in Appendix A details the development of the rules.

Applying the rules in Fig. 2.17 to the constructed time series in Fig. 2.16 identifies the critical capacities shown in Table 2.3 where NG is the hourly net generated energy and CC are the critical capacities in kWh. The critical capacities are colour coded by shading based on whether they are identified via rule 1 (blue) or by rule 2 (green). This colour coding is important since it highlights the start and end point of the critical capacity (called the critical capacity duration) which is discussed later in Section 3.2. Table 2.3 is used to compare the results of the rules-based method and the rainflow method to confirm that both methods find the same critical capacity magnitudes and corresponding periods.

Table 2.3: The critical capacity magnitudes and time-step locations for each period in the time series from Fig. 2.16. The critical capacities identified by Rule 1 have blue shading and those identified by Rule 2 have green shading.

Time (hr)	1	2	3	4	5	6	7	8	9	10
Period No.	**Period 1**		**Period 2**				**Period 3**			
NG (kW)	20	-10	20	-6	7	-12	17	-9	8	-15
CC (kWh)	10				12		16			
			6						8	

Time (hr)	11	12	13	14	15	16	17	18	19	20	21	22
Period No.	**Period 4**						**Period 5**					
NG (kW)	25	-13	12	-11	7	-10	18	-12	7	-6	8	-14
CC (kWh)	15						17					
			12						9			
					7				6			

Time (hr)	23	24	25	26	27	28	29	30	31	32	33	34	35	36
Period No.	**Period 6**													
NG (kW)	9	-5	16	-15	8	-5	6	-10	11	-3	2	-3	8	-18
CC (kWh)			19											
	5				9									
					5				15					
									4					
											2			

The critical capacities from Table 2.3 are sorted in descending order and listed in Table 2.4. The critical capacities in this list are labeled as C_1 to C_{18} and the GSE at each critical capacity is found using (2.9). This table is then used to plot the $E_g[E_s, P_0]$ curve as shown later in Fig. 2.21.

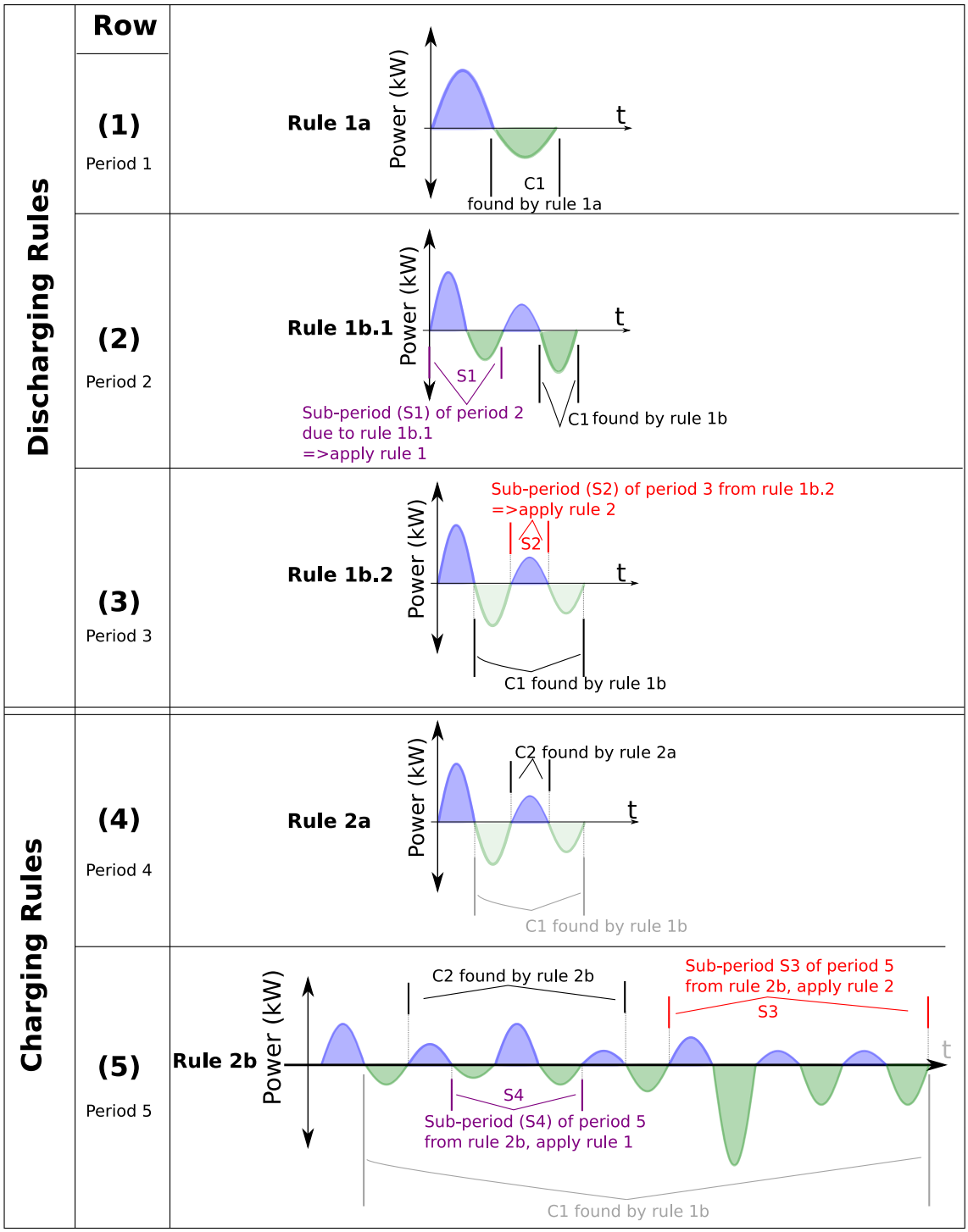

Figure 2.17: The various rules are illustrated using different time series, highlighting the location of each load critical capacity and where each sub-period is created. The full details on how these rules operate is in Appendix A.

Table 2.4: The critical capacities from Table 2.3 sorted in descending order and labeled C_1 to C_{18}. The GSE for a storage capacity sized at each critical capacity is also listed ($E_g[C_i]$ where C_i refers to the labeled critical capacity).

Label	C_1	C_2	C_3	C_4	C_5	C_6	C_7	C_8	C_9	C_{10}	C_{11}
Crit. Cap. (kWh)	19	17	16	15	15	12	12	10	9	9	8
$E_g[C_i]$ (kWh)	0	2	4	7	7	22	22	36	44	44	54
Label	C_{12}	C_{13}	C_{14}	C_{15}	C_{16}	C_{17}	C_{18}				
Crit. Cap. (kWh)	7	6	6	5	5	4	2				
$E_g[C_i]$ (kWh)	65	77	77	91	91	107	141				

2.4.2 Rainflow-Based Identification

The rainflow algorithm identifies all critical capacities with greater confidence than the rules-based approach since the rainflow algorithm is an established algorithm in the field of material fatigue analysis while the proposed rules were developed based on experience and observation of a limited set of net generation time series. Throughout the development of the rules-based method, exceptions to the developing rule-set would occur which required the creation of additional rules. Thus it is unclear if the proposed rule-set is sufficiently general to handle all time-series.

The output of the original rainflow algorithm is a list of values which contains a combination of critical capacities and other non-critical capacity values and hence the algorithm is modified to only provide the critical capacities.

A step-by-step guide to performing the rainflow algorithm, described by [43], is shown in Fig. 2.18 and an implementation of the algorithm, modified to provide only critical capacities, is presented in Appendix B. The rainflow algorithm begins by identifying the peaks/troughs or local maxima/minima of the net generation-energy time series which are marked by the red dots in Fig. 2.18a. The energy time series is then rotated clockwise 90 degrees and it is imagined that a raindrop is placed on the left-hand side of each peak which then falls along the curve (forward in time). The raindrop's path ends when any of the three following conditions are met:

End Condition 1:	The raindrop has reached the end of the time series.
End Condition 2:	The raindrop is opposite a future peak which has greater energy than the energy at the raindrop's starting time.
End Condition 3:	The raindrop has reached the path of an earlier raindrop, i.e. a raindrop starting at an earlier time.

The CCA method proposes that each raindrop represents a critical capacity with a magnitude described by the difference between the energy at the start of the raindrop's path and the energy at the point where the raindrop last leaves the curve before the end of the raindrop's path.

The time series in Fig. 2.18a contains 3 peaks which occur at: i) time t_1, ii) time t_3 and iii) time t_5. The critical capacities in this time series are found by placing a raindrop on the left-hand side of each of these peaks.

Beginning with Fig. 2.18b, the raindrop at the first peak starts at time t_1 and falls along the time series. The raindrop falls until it reaches the time marked t_3 where the raindrop's path ends since the energy peak at time t_3 is greater than the energy peak at time t_1 and this demonstrates the second end condition. The critical capacity labeled C_2 is found by taking the difference between the energy

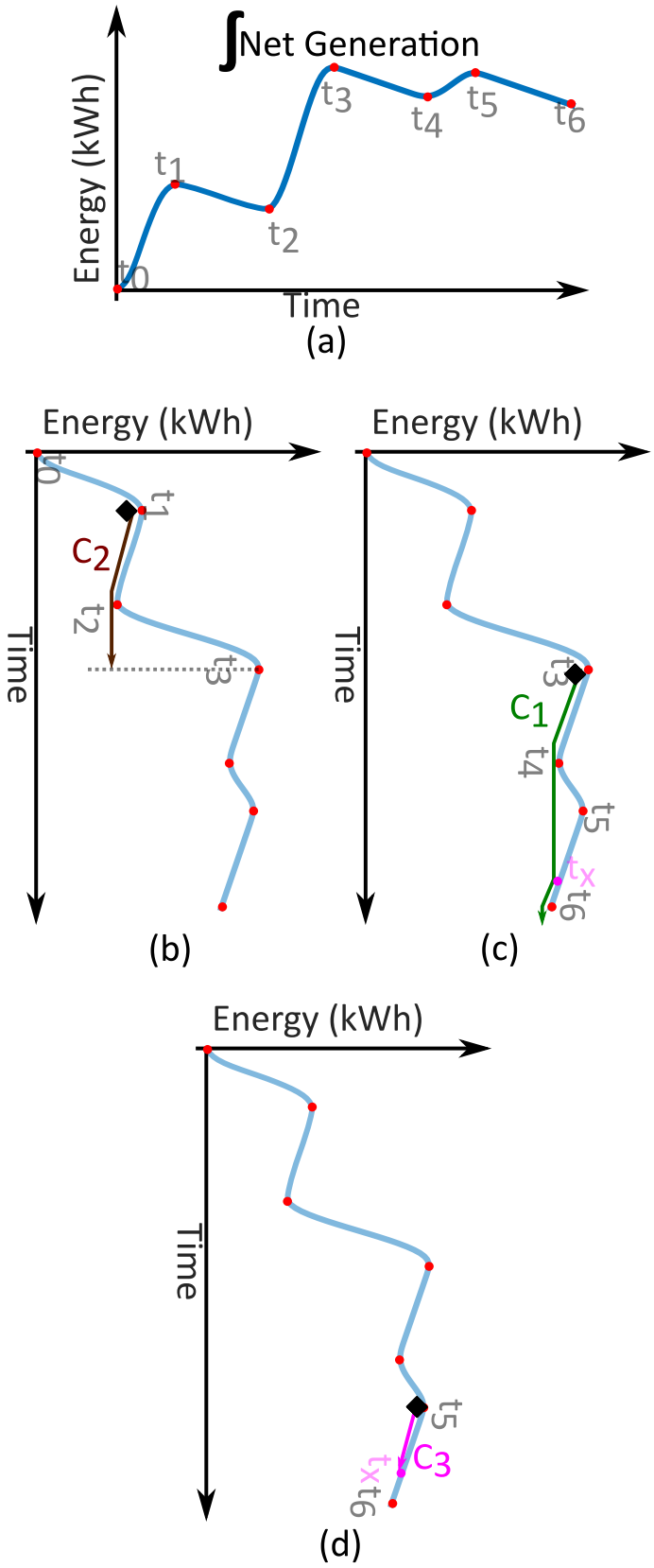

Figure 2.18: Rainflow algorithm operations, a) Example net generated-energy time series with peaks/troughs identified, b) demonstrating end condition 2, c) demonstrating end condition 1, d) demonstrating end condition 3.

value at time t_1 and the energy value at time t_2, since time t_2 is the instant before the raindrop "falls off the curve".

The second peak's raindrop in Fig. 2.18c starts at the time t_3 and travels along the curve until time t_4 where it falls off the curve. Note that the energy at time t_5 is less than the energy at time t_3 hence this is not an end condition. The raindrop continues to fall until it lands on the curve at time t_x and travels along the curve until time t_6. At time t_6 the raindrop is at the end of the time series and this demonstrates the first end condition. The critical capacity labeled C_1 is the difference between the energy at time t_3 and the energy at time t_6.

The final peak's raindrop in Fig. 2.18d starts at time t_5 and travels along the curve until time t_x where it reaches the path of an earlier raindrop and this demonstrates end condition 3. The critical capacity labeled C_3 is the difference between the energy at time t_5 and the energy at time t_x.

Note that the critical capacities were numbered in decreasing order of size. In practice, all critical capacities are found first and then are sorted afterwards.

The standard rainflow algorithm would repeat the above process by placing a raindrop on the right-hand side of each trough and the difference in the energy values found for these trough raindrops are added to the list obtained for the peaks. The list of values found by the trough raindrops are called generation critical capacities and the list of values found by the peak raindrops are called load critical capacities. Typically the list of both generation critical capacities and load critical capacities only differ by at most two values depending on whether storage is initially assumed full or empty. As storage is assumed full initially, the generation critical capacities list contains one additional value compared to the load critical capacities list however this value occurs at a significantly large storage capacity where GSE is zero and hence typically does not influence the maximum benefit analysis. As mentioned in Section 2.2.2 typically only load critical capacities are necessary to be found.

The analogy of raindrops falling along the curve is useful to explain the general principles of the rainflow algorithm however the typical implementation of the algorithm, such as [56], processes the time series without considering whether a given raindrop begins at a peak or at a trough. Hence the algorithm in [56] can be modified to find only the raindrops starting at peaks and hence identify the (load) critical capacities for a given time series.

The rainflow algorithm is applied in Fig. 2.19 to the example time-series from Fig. 2.16. In Section 2.4.1, the rules-based approach identified the critical capacities for the constructed time series shown in Fig. 2.16. Now applying the rainflow algorithm to the same constructed time series is found to produce the same results as the rules-based approach - which is seen by comparing the rainflow results in Fig. 2.19 to the rules-based results in Table 2.3.

For example in Period 1 the rules-based approach found a load critical capacity of 10kWh and the rainflow analysis also identifies the same 10kWh critical capacity.

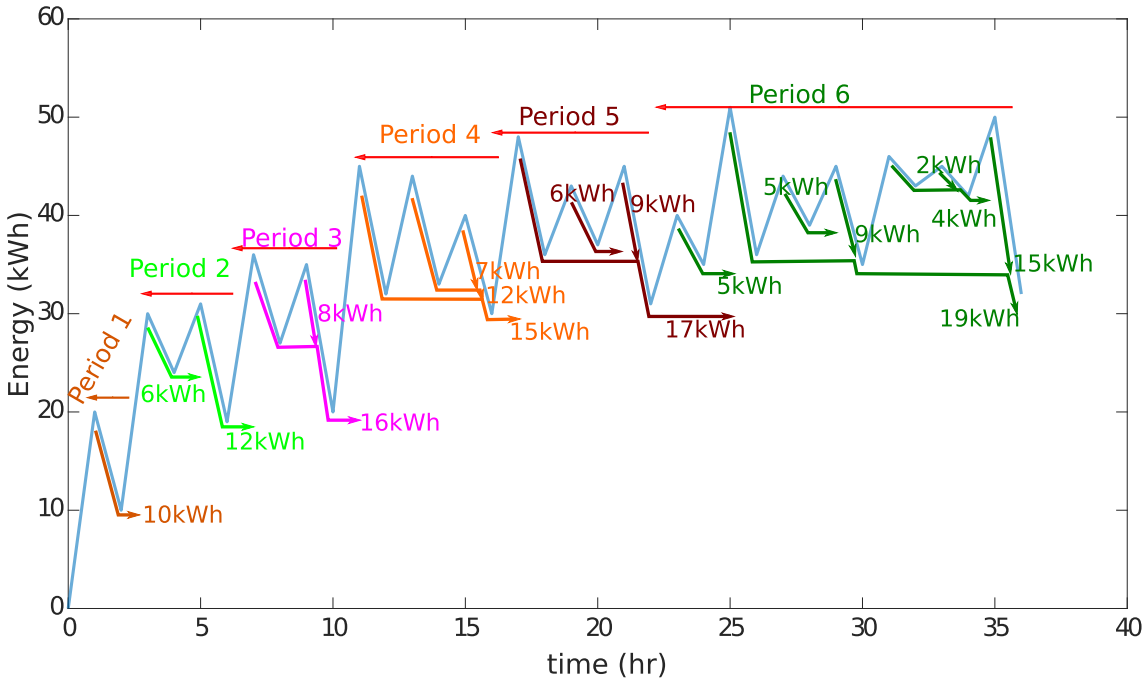

Figure 2.19: The energy time series used to discuss the rules-based approach (Fig. 2.16b) examined using the rainflow raindrop analogy. The critical capacities found in each period corresponds to the same capacities identified by the rules-based method in Table 2.3.

In Period 3 the rules-based approach had found two critical capacities : i) 16kWh occurring between the time-steps of hour 7 to hour 10 and ii) 8kWh occurring between the time-step of hour 9 and hour 10, the rainflow method found the same critical capacities within the same time-steps.

2.5 Relationship between Critical Capacities and Storage Capacity

The CCA method is validated against the conventional approach using the constructed time series from Fig. 2.16. The validation of the CCA method using an actual household's data is provided in Chapter 3.

The GSE to storage capacity curve ($E_g[E_s, P_0]$) for the constructed data is shown in Fig. 2.20a. The conventional approach selects a range of storage capacities. For example this may be chosen between 0 kWh and 19 kWh with a step size of 1.3 kWh. Then the GSE, shown by the circles in Fig. 2.20a, is found by simulating the state of charge (SoC) at each selected storage capacity. The range of E_s in the simulation was selected to provide a sufficient number of E_g and E_s points to capture the general shape of the curve. The CCA rainflow method finds the critical capacities shown by the crosses in Fig. 2.20a and the GSE at each critical capacity is found using the GSE equation (2.8) to produce the solid line in Fig. 2.20a. The result shows that the CCA method produces the same $E_g[E_s, P_0]$ results as the

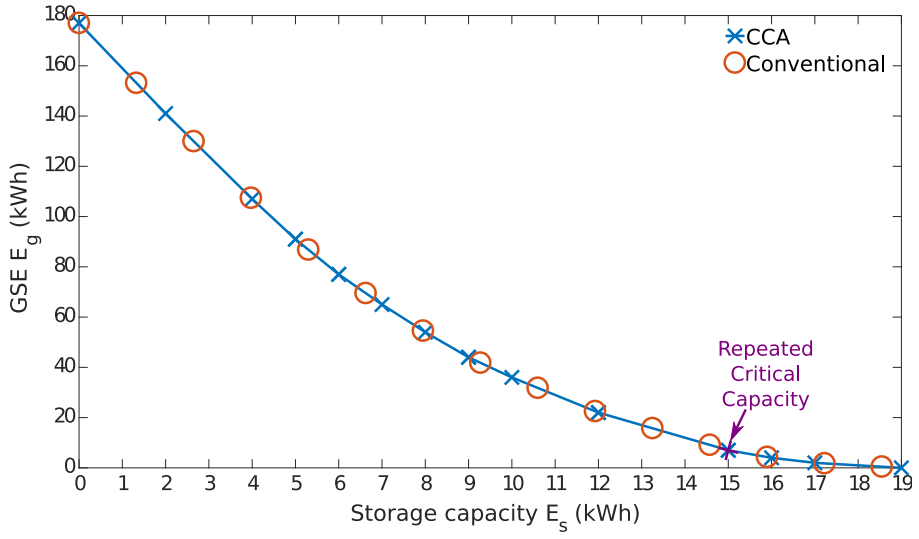

(a)

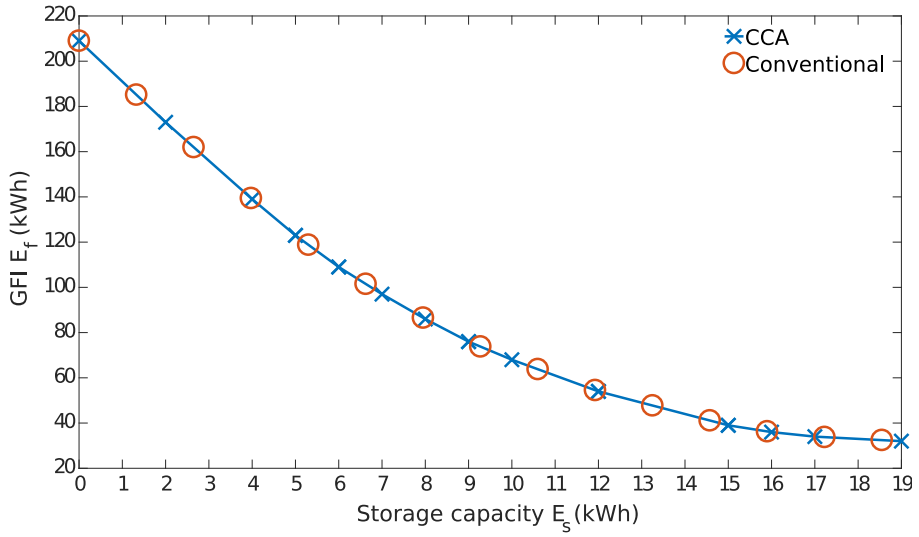

(b)

Figure 2.20: Validating the GSE and GFI equations for a given PV rating (P_0) by comparing the results of the conventional time-stepping simulation approach to the CCA method using the example time series from Fig. 2.16. a) $E_g[E_s, P_0]$ curve, and b) $E_f[E_s, P_0]$ curve

conventional simulation approach for this example.

The GFI is validated in Fig. 2.20b where the circles represent the simulated points and the solid curve was found using the equation for GFI in terms of GSE in (1.3b). It is shown that the CCA method produces the same $E_f[E_s, P_0]$, where E_f is feed-in energy, results as the conventional approach under the assumption that storage is initially full.

Note Fig. 2.19 shows there is a repeated critical capacity of 15kWh seen in both Period 4 and Period 6 and hence in Fig. 2.20 the slope for storage capacities less than 15kWh has the ratio of GSE (kWh) to storage capacity (kWh) of 1:5 as opposed to 1:4 which would occur if the critical capacity was not repeated.

2.6 Relationship between Critical Capacity and PV Rating

The CCA method provides a closed-form equation for the GSE in terms of storage capacity for a specific combination of: i) load time series, and ii) generation time series, for a given PV rating. While the CCA method can not find a closed-form equation for GSE in terms of PV rating, the critical capacities from CCA can be used to provide an estimate of the relationship between GSE and PV rating under a given set of assumptions. To understand the estimate of the GSE to PV rating relationship and the assumptions of this estimate, the impact of PV rating variation on critical capacities is discussed in this section.

A change in PV rating causes the critical capacities to change such that there is: i) a change in the number of critical capacities (Critical Capacity Property 1), and ii) a change in the magnitude of each critical capacity (Critical Capacity Property 2). As the PV rating increases, the critical capacity magnitudes will approach their minimum values and this defines an upper limit on the effect which PV rating can have on critical capacities. To discuss the critical capacity variation with storage capacity, first the critical capacity magnitude asymptotes due to increasing PV rating is discussed and then the reason why critical capacities change due to PV rating is discussed.

2.6.1 Minimum Critical Capacity Asymptotes for Increasing PV Rating

Fig. 2.21 demonstrates a given constant load power time series and two generation time series for different PV ratings, where PV rating 2 is larger than PV rating 1. Plotting the net generation for both PV ratings shows that PV rating 2 has lower GSE since it supplies the load shown by the shaded blue area in Fig. 2.21 and hence the critical capacity magnitudes for this rating are smaller.

The critical capacity asymptote is then deduced by introducing a PV rating, PV_L, between PV rating 1 and PV rating 2 such that $PV_1 < PV_L < PV_2$ as shown

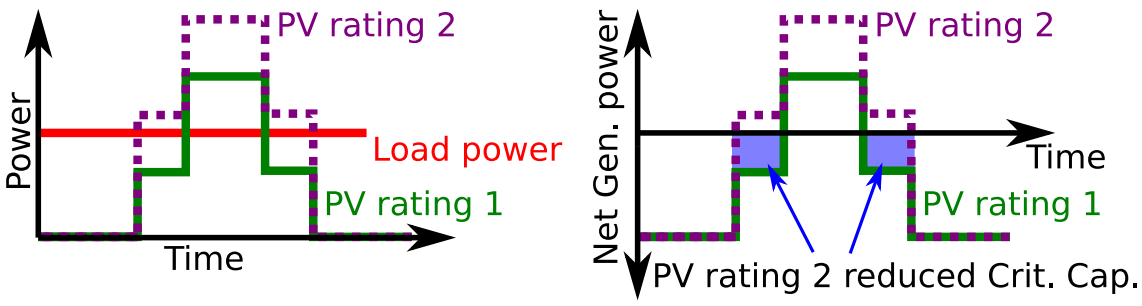

Figure 2.21: Illustrating the effect of PV rating on GSE and the critical capacities using a simplified example net generation-power time series.

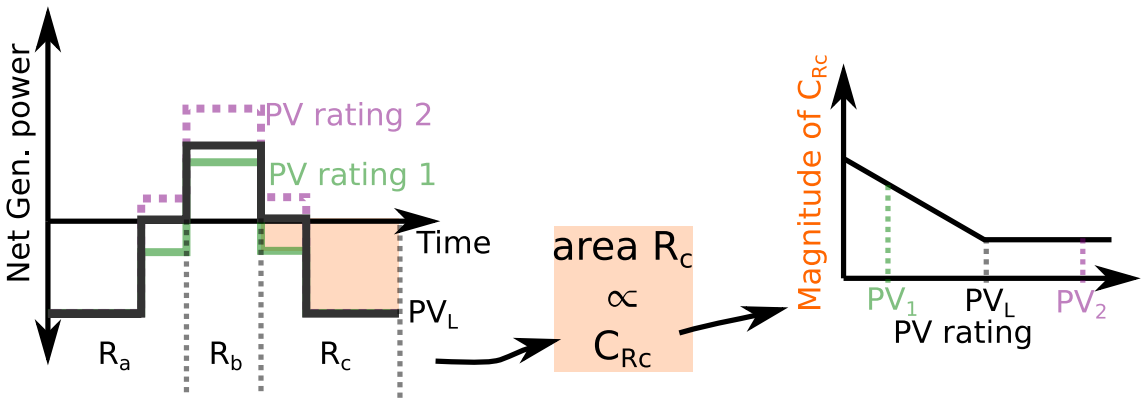

Figure 2.22: Illustrating the minimum critical capacity asymptote as PV ratings increases, using the time series from Figure 2.21.

in Fig. 2.22. Then three periods are defined within the net generation power time series labeled R_a, R_b and R_c where in the periods R_a and R_c the net generation can be both positive and negative and in period R_b the net generation is always positive. Note there exist two critical capacities in this example, one in period R_a and one in period R_c.

The area between the curves and the time axis within period R_c is proportional to its corresponding critical capacity (C_{Rc}) magnitude. As the PV rating increases from PV_1 towards PV_L the magnitude of C_{Rc} decreases. For further increase in PV ratings greater than the PV_L, such as PV_2, the magnitude of R_c does not change from the magnitude recorded at PV_L. Note in this simple case the value of PV_L is finite since the time series is discrete however in practical cases with smooth curves then PV_L would be infinite. Hence the critical capacity magnitudes will approach their respective minimum values when the PV rating approaches infinity.

The impact of PV rating on the critical capacities and the $E_g[E_s, P_0]$ curve is observed in Fig. 2.23 which is produced using the case study data in Chapter 3. Fig. 2.23 shows the region containing all valid $E_g[E_s, P_0]$ curves for different PV ratings where the GSE has an upper limit of 365 days where all load is supplied by GSE, and a lower limit defined by the curve labeled PV_L, the PV rating corresponding to minimum critical capacity magnitudes. As PV rating increases, the $E_g[E_s, P_0]$ curves moves from the 0 pu point in the top right-hand corner towards the curve for PV_L.

The assumption in Section 3.1.2 is that storage is initially full and hence there is no unavoidable GSE which means the curves in Fig. 2.23 reach the x-axis for sufficiently large values of storage. It is also assumed that the analysis begins at the start of the year, 1st of January at midnight, which is also discussed in Section 3.1.2.

2.6.2 Effect of PV Rating on Critical Capacities

The variation in PV rating causes three changes in the critical capacities:

1. Increasing PV rating typically reduces the duration of each critical capacity

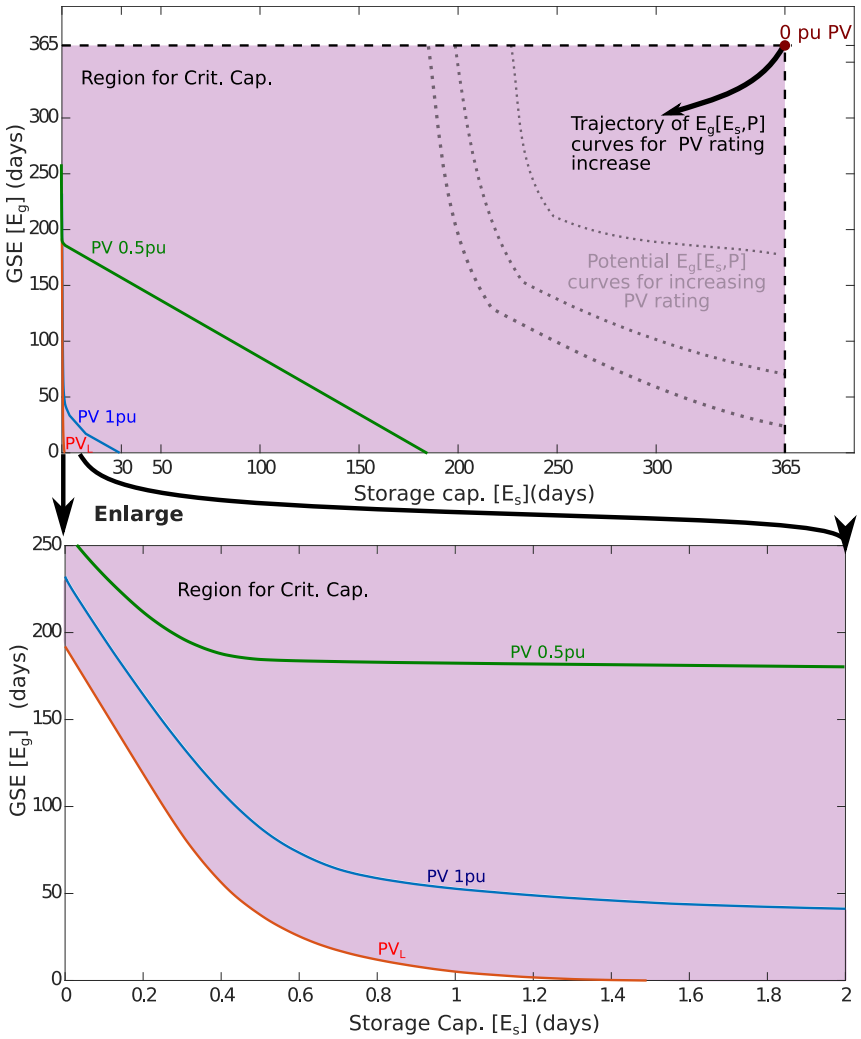

Figure 2.23: Demonstrating the potential area for load critical capacities between zero PV rating and the PV_L PV rating. Beyond PV_L the $E_g[E_s, P]$ curve does not change. Note since this curve uses the discrete case study data then PV_L is not infinite.

(duration refers to Critical Capacity Property 2).

2. Increasing PV rating generally reduces the magnitudes of each critical capacity as illustrated by Fig. 2.21.

3. Increasing PV rating changes the number of critical capacities since changing the PV rating changes the number of negative net generation periods (Critical Capacity Property 1).

The first change is observed by examining the net generation energy time series and plotting the time interval at which the critical capacities occurs, as shown in Fig. 2.24 where the first five largest critical capacities are plotted for three PV ratings of 0 pu, 1 pu and 2 pu. As a reminder, 1 pu PV rating means the PV panel will produce the same annual energy as the load demand. Thus at the end of the year, a PV rating of 0 pu has a negative net generation equal to a year's worth of generation and a PV rating of 2 pu would have an excess of a year's worth of generation. In

Fig. 2.24 the length of each of the boxes labeled C_1 to C_5 represents the time interval of each critical capacity for their respective PV ratings (blue for 1 pu PV, red for 2 pu PV) and the height of the box represents their relative magnitude to each other.

In Fig. 2.24, consider comparing the first critical capacity for PV ratings of 1 pu and 2 pu. The first critical capacity for a PV rating of 1 pu begins in late autumn and continues until about halfway through spring while the first critical capacity for a PV rating of 2 pu occurs over a much smaller interval of time during only winter. A similar observation can be made for the time intervals of the other four critical capacities. Note for the 0 pu PV case there is only one critical capacity.

The second change, reduction in the critical capacity magnitudes, is observed in Fig. 2.25 by comparing the first ten critical capacities for the selected set of PV ratings which includes the PV_L from Fig. 2.23. As shown, by increasing the PV rating the magnitude of each critical capacity reduces and by comparing PV ratings 0.5 pu to 4 pu it appears that the increase in PV rating reduces the extreme cases such that the magnitudes of the first ten critical capacities are closer together.

The third change, the change in the critical capacity list length, is observed in Fig. 2.26 which plots the critical capacity list length against the PV rating. For small PV ratings, an increase in PV rating results in a rapid increase in list length until a threshold is reached, in this example at about 0.25 pu, beyond which increases in PV rating causes a reduction in the number of critical capacities. Further increasing PV rating reduces the number of critical capacities until the PV rating PV_L is reached at which point the number of critical capacities no longer changes.

The reason why the critical capacity magnitudes and number of critical capacities change (second and third change) can be explained by examining how the net generation power time series changes due to changes in PV rating. The two effects are: i) Generation smothering, and ii) Generation splitting. These effects are named based on their effect on the shape of the net-generation time series.

Net Generation Smothering

The smothering effect is shown in Fig. 2.27 for an example generation and load time series where for small PV ratings the load is larger than the PV output during the generating period (when PV generation is non-zero) and the load is said to "smother" the generation since the net generation is always negative during the generating period. As a result for small PV ratings there will only be one period of negative net generation within the time series and hence there is only one critical capacity. With the larger PV rating of PV_L shown, then the net generation is always zero during the generating period and hence the net generation is un-smothered. For the un-smothered case the time series has two negative net generating periods, one on either side of the generating period, which means the number of critical capacities in this interval of time has increased. The elimination of the smothering

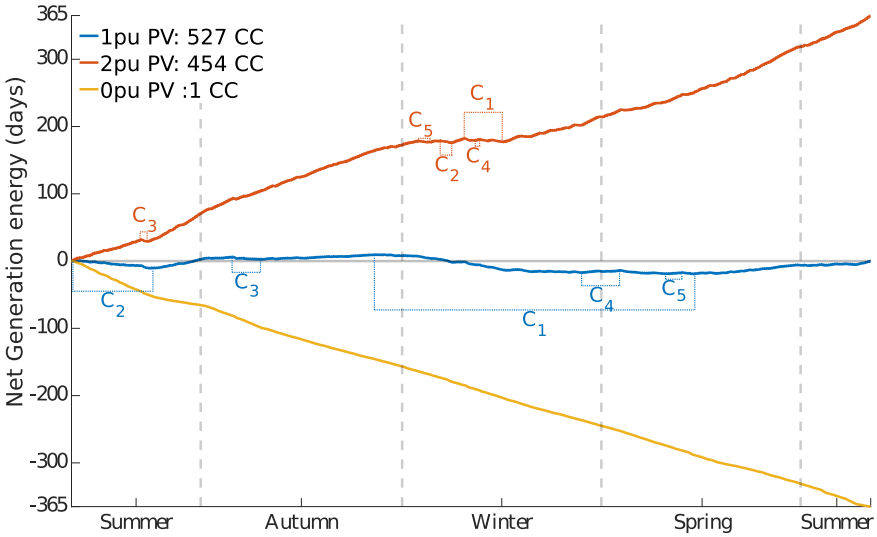

Figure 2.24: The net-generated energy for 0pu, 1pu and 2pu PV ratings demonstrating the first change, the reduced duration of the critical capacities as PV rating increase. The number (list length) of critical capacities is also shown in the legend.

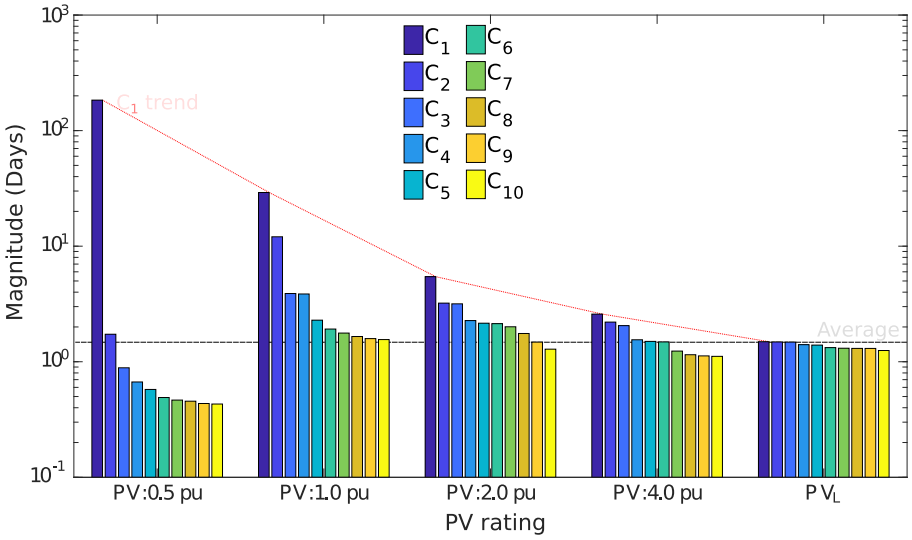

Figure 2.25: The magnitudes of the ten largest critical capacities for a number of PV ratings demonstrating the second change, a general reduction in critical capacity magnitudes as PV rating increases. Note the magnitude has a log scale.

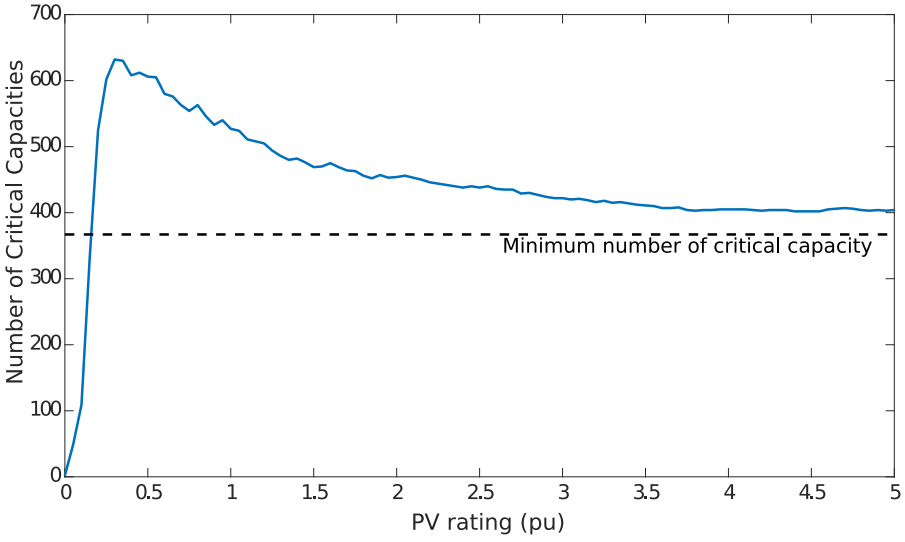

Figure 2.26: The relationship between PV rating and critical capacity list length demonstrating the third change, the critical capacity list length changes as PV rating increases. Note the dashed line shows the critical capacity list length for PV_L.

effect increases the number of critical capacities and reduces the magnitude of the critical capacities and this is observed in Fig. 2.26 for PV ratings between 0 pu and 0.5 pu.

Net Generation Splitting

The splitting effect is shown in Fig. 2.28 for an example generation and load time series. For small PV ratings the net generation during the generating period is "split" into multiple periods of positive and negative net generation. There are four negative net generating periods and hence four critical capacities.

When the PV rating is increased to PV_L there is sufficient generation to supply all load during the generating period and hence the net-generation is un-split resulting in only two periods of negative net generation as seen in Fig. 2.28. The avoidance of splitting of the net generation time-series reduces the number of critical capacities which is seen in Fig. 2.26 for PV ratings above 0.5 pu. Avoiding splitting the net generation also reduces the critical capacity magnitudes as the PV rating increases.

Combination of Generation Splitting and Smothering

The smothering and splitting effects can both occur during the same period of time. For example when a generating period becomes un-smothered there is an increase in the number of negative periods, until a given threshold PV rating is reached. With further increases in PV rating the reduction in splitting then reduces the number of negative periods, which is shown in Fig. 2.26. The result is that as the PV rating is increased from a low small PV rating the un-smothering effect is initially dominant and hence the overall number of critical capacity increases. For higher PV ratings a further increase in PV rating tends to reduce splitting and hence the number of critical capacity will tend to decrease as the PV rating approaches PV_L.

While one effect may be dominant it is possible for both splitting and smothering to occur simultaneously. For example in Fig. 2.26 at around 1.5 pu PV rating where the splitting effect is dominant, there is also a slight increase in the critical capacity list length which is a result of the un-smothering effect.

2.6.3 Constructing the GSE and PV Rating Equation

Currently no closed-form equation has been derived for the relationship between the GSE and PV rating. However the GSE equation (2.9) can be modified and decomposed into three key terms which can be used to analytically estimate the optimal HES size in Chapter 4. The objective of this decomposition is to develop a simple equation for GSE that is differentiable in terms of PV rating and is suitable for the MBI estimation in Chapter 4.

Equation (2.9) from Section 2.2.1 has considered the GSE in terms of a variable storage capacity (E_s) with a fixed PV rating (P_0). If this equation is instead

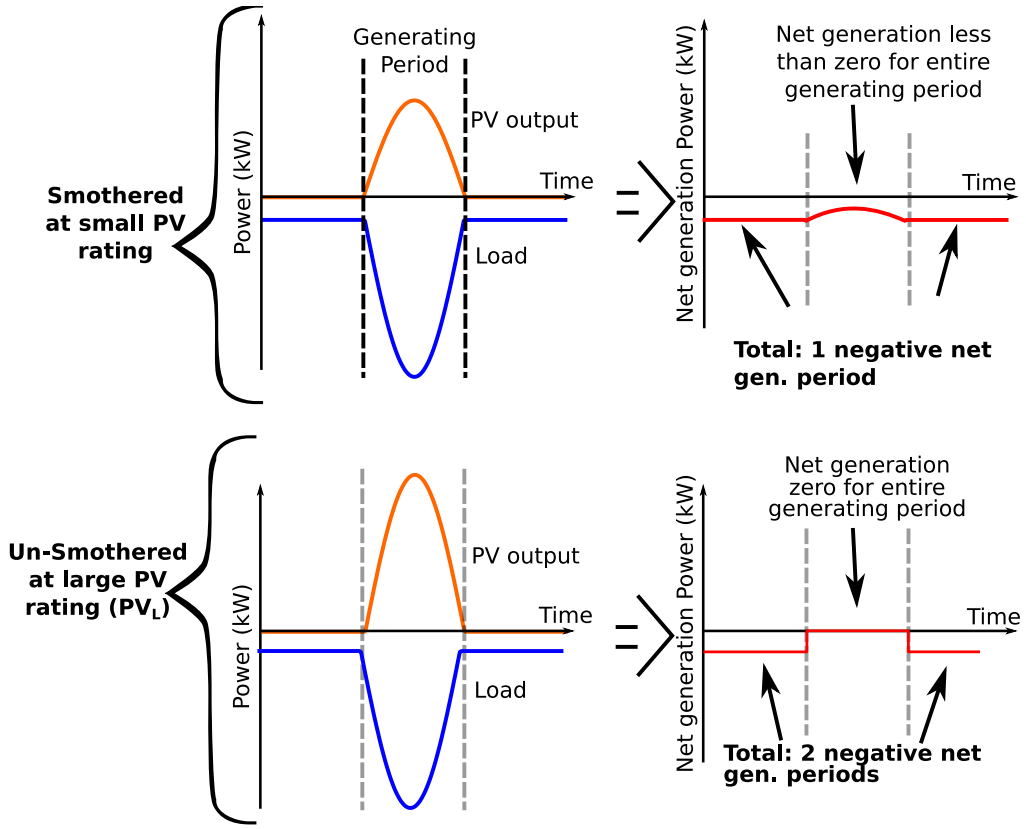

Figure 2.27: Illustration of smothering effect. For the low PV ratings the net generation is smothered and for the large PV rating (PV_L) the net generation is un-smothered.

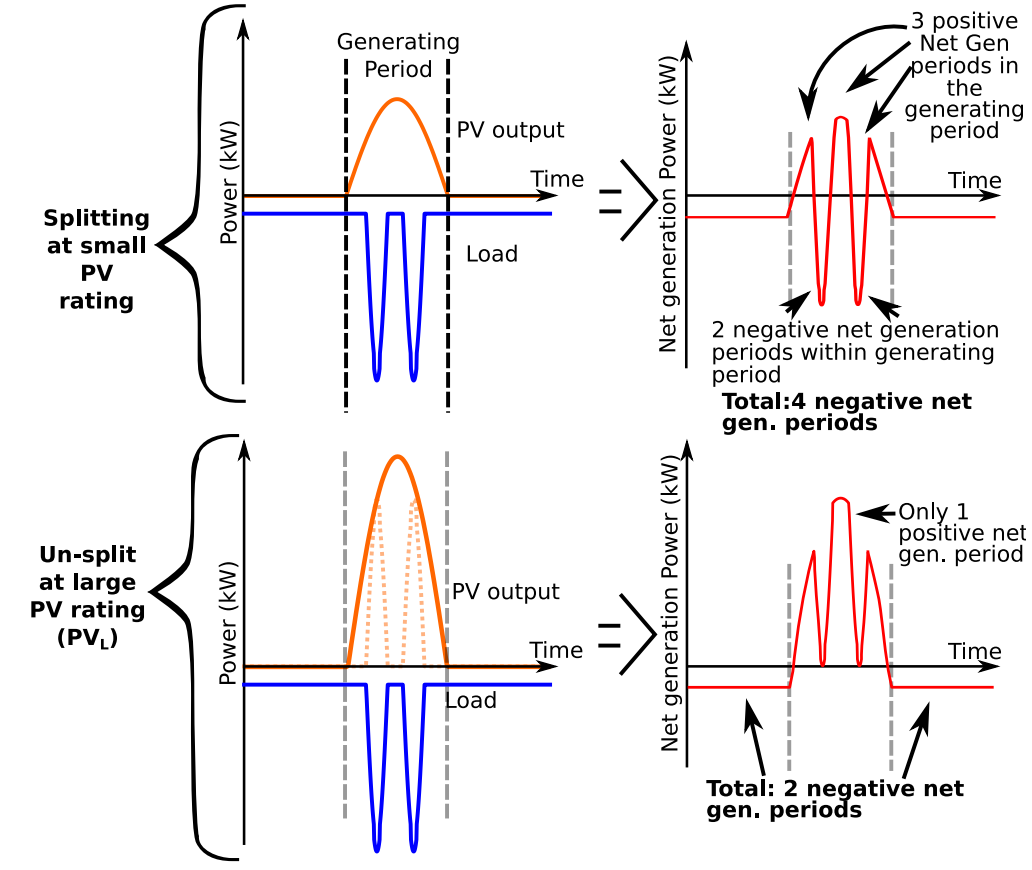

Figure 2.28: Illustration of splitting effect. For the low PV ratings the net generation is split but for the large PV rating (PV_L) the net generation is un-split

written in terms of a variable PV rating (P) and a fixed storage (E_{s0}) then the resulting equation is as shown in equation (2.10). Note that the critical capacity list ($\boldsymbol{C}[\boldsymbol{P}] = \{C_1, \cdots, C_N\}$) depends on PV rating, P, and the number of critical capacities $n[E_{s0}, P]$ in (2.10) depends on both the PV rating and the chosen storage capacity E_{s0}.

$$E_g(E_s, P_0) = \sum_{i=1}^{n}(c_i - E_s) \qquad \text{(2.9 Repeated)}$$

$$E_g(E_{s0}, P) = \sum_{i=1}^{n[E_{s0},P]} (c_i[P] - E_{s0})$$

$$E_g(E_{s0}, P) = \left(\sum_{i=1}^{n[E_{s0},P]} c_i[P]\right) - \left(\sum_{i=1}^{n[E_{s0},P]} E_{s0}\right)$$

$$E_g(E_{s0}, P) = \left(\sum_{i=1}^{n[E_{s0},P]} c_i[P]\right) - n[E_{s0}, P] \times E_{s0} \qquad (2.10)$$

$$\text{for } n[E_{s0}, P] \text{ such that } c_1 \geq \cdots \geq c_n \geq E_{s0} \geq c_{n+1} \geq \cdots > c_N$$

Consider that the first n critical capacities can be written as follows, note the $c_i[P]$ is written as simply c_i since each part of the following has the same PV rating:

$$\sum_{i=1}^{N[P]} c_i = \left(\sum_{i=1}^{n[E_{s0},P]} c_i\right) + \left(\sum_{i=n[E_{s0},P]+1}^{N[P]} c_i\right)$$

$$\sum_{i=1}^{n[E_{s0},P]} c_i = \left(\sum_{i=1}^{N[P]} c_i\right) - \left(\sum_{i=n[E_{s0},P]+1}^{N[P]} c_i\right)$$

$$\text{Let: } E_{g0}[P] = E_g[0, P] = \left(\sum_{i=1}^{N[P]} c_i\right) \quad \text{and} \quad E_L[P] = \left(\sum_{i=n[E_{s0},P]+1}^{N[P]} c_i\right)$$

$$\text{hence} \sum_{i=1}^{n[E_{s0},P]} c_i = E_{g0}[P] - E_L[E_{s0}, P]$$

where $E_{g0}[P]$ is the GSE for the PV rating of P with zero storage capacity and $E_L[E_{s0}, P]$ is the load energy supplied by all critical capacities smaller than the given storage capacity. Note that $E_{g0}[P]$ depends on only the PV rating while $E_L[E_{s0}, P]$ depends on both the PV rating and the given storage capacity E_{s0}. $E_L[E_{s0}, P]$ is the sum of the critical capacity magnitudes smaller than E_s.

Hence the GSE in terms of PV rating from (2.10) can be written as:

$$E_g(E_{s0}, P) = E_{g0}[P] - E_L[E_{s0}, P] - n[E_{s0}, P] \times E_{s0}$$

$$E_g(E_{s0}, P) = E_{g0}[P] - (E_L[E_{s0}, P] + E_U[E_{s0}, P]) \tag{2.11}$$

where:

$$E_{g0}[P] = \left(\sum_{i=1}^{N[P]} c_i[P] \right), \; E_U[E_{s1}, P] = n[E_{s1}, P] \times E_{s1},$$

$$E_L[E_{s1}, P] = \left(\sum_{i=n[E_{s1},P]+1}^{N[P]} c_i[P] \right)$$

where $E_U[E_{s0}, P]$ is the load energy supplied by the n critical capacities which are larger than the given storage capacity, i.e. for these critical capacities the given storage capacity would supply E_{s0} of energy per critical capacity. The physical meaning of E_U and E_L is as followed:

1. E_U is the total energy that storage supplies to the load each time it is fully discharged and,

2. E_L is the total energy that storage supplies to the load each time it is partially discharged.

The critical capacities can be used to determine how many times storage is fully discharge and the amount of energy storage supplied when it is partially discharged. If storage is greater than a critical capacity, then it is partially discharged and hence supplies energy equal to the critical capacity's magnitude to the load (which forms E_L). If storage is less than a given critical capacity, then it represents a full discharge and hence storage fully supplies its capacity to the load (which forms E_U).

Both the full and partial discharge cases of storage is shown in an example in Fig. 2.29 for two critical capacities and two fixed storage capacities. Fig. 2.29a presents the example with two critical capacities, $C_1 = 10$ kWh and $C_2 = 5$ kWh, and a fixed storage capacity of 8 kWh. The shaded blue area represents energy in storage and the unshaded area (white) represents energy consumed. This storage capacity is placed next to each critical capacity in Fig. 2.29b which demonstrates how much energy the given storage capacity will provide to the load for each critical capacity.

To summarise the two cases:

1. For $E_{s0} = 8$ kWh (Fig. 2.29b): for C_1, storage is fully discharged and provides 8 kWh of energy to the load. For C_2, storage is partially discharged and provides 5 kWh. In this case $E_U = 8$ kWh and $E_L = 5$ kWh.

2. For $E_{s0} = 4$ kWh (Fig. 2.29c): for C_1, storage is fully discharged and provides 4 kWh of energy to the load. For C_2, storage is also fully discharged and provides 4 kWh to the load. Thus the energy storage provides is $E_U = 8$ kWh.

Hence there are two key terms in (2.11) which are:

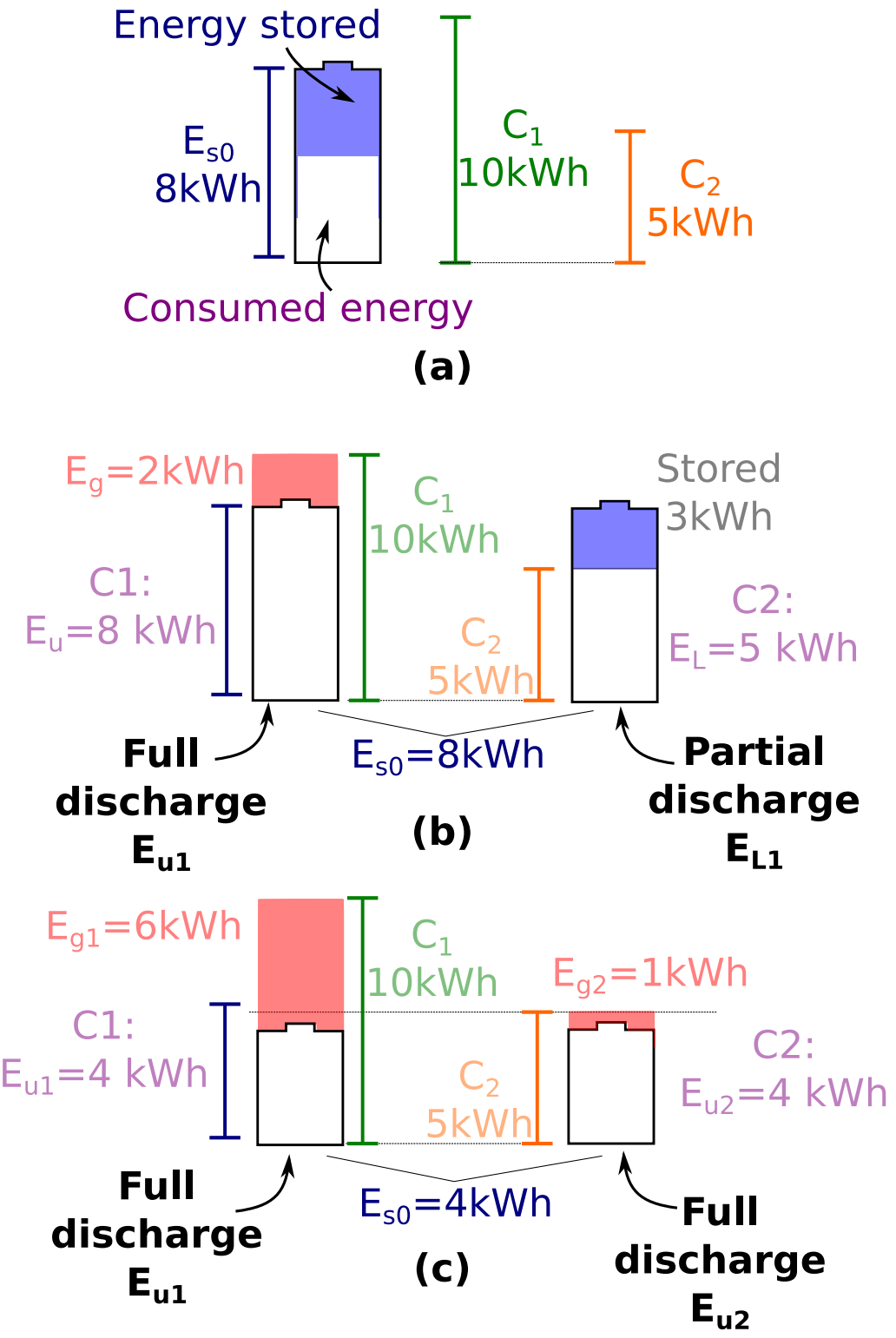

Figure 2.29: An example to illustrate the definitions of E_L and E_U:' a) The example of two critical capacities, $C_1 > C_2$ and a storage capacity of 8 kWh, b) the energy flows when storage is 8 kWh, c) the energy flows when storage is reduced to 4 kWh.

1. $E_{g0}[P]$ is the GSE with no storage capacity for PV rating P. This is equivalent to the annual load minus the PV's grid energy offset (GEO), i.e. the portion of PV generation directly supplied to the load which offsets GSE. This term depends on only the PV rating.

2. $(E_L[E_{s0}, P] + E_U[E_{s0}, P])$ is the amount of annual load supplied by storage. This is also known as the GEO of storage. This term depends on both the PV rating and the storage capacity E_{s0}.

An example of (2.11) is shown in Fig. 2.30 using the baseline case study data for a number of different storage capacities. Note the GSE is found for each storage capacity curve using (2.11) for a range of PV ratings. Note that it is assumed that the storage device is initially full which means for the case with 50 days of storage capacity there are 50 days of GSE which can be supplied without any PV generation.

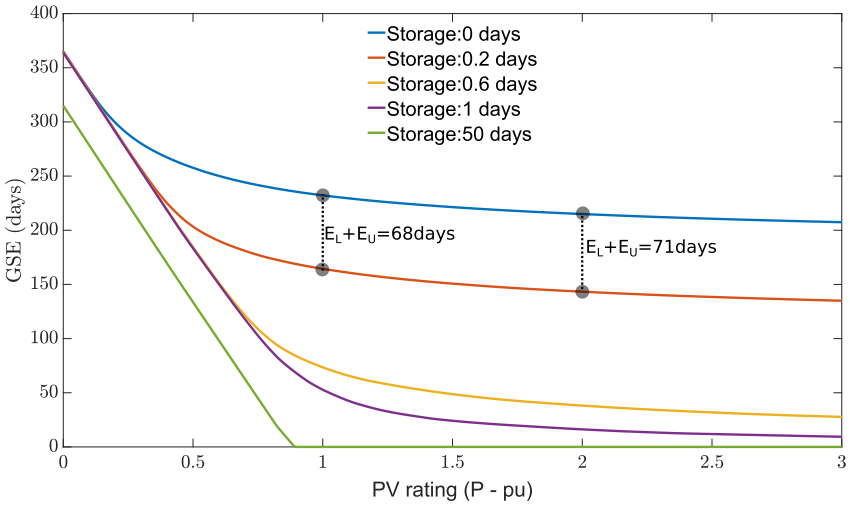

Figure 2.30: An example of GSE to PV rating curves for the case study where each curve demonstrates a given storage capacity

The storage capacity curves in Fig. 2.30 are considered for small (< 0.25 pu) and large PV ratings (> 0.25 pu). For small PV ratings and small storage capacities (< 1 day) the GSE curve is approximately equal to the curve for no storage capacity $E_{g0}[P]$ shown in blue. For larger PV ratings the curves of various storage capacities are approximately a shifted version of the zero storage curve, for example Fig. 2.30 shows that the GSE difference between 0.2 days of storage and no storage at both 1 pu PV rating and 2 pu PV rating is approximately equal.

The disadvantages of (2.11) is that the critical capacities must be found for a range of PV ratings, however the advantages are that:

1. The GSE equation is separated into two terms, where: i) one which depends only the PV rating, and ii) one which depends on both the PV rating and the storage capacity.

2. By separating these terms, it is simpler to define an equation which estimates the sensitivity of GSE with respect to variation in PV rating, which is essential for estimating the optimal HES size in Chapter 4.

It is assumed in Chapter 4 that the sensitivity of GSE to PV rating is dominated by the E_{g0} term and is not greatly impacted by the amount of energy provided by storage $(E_L + E_U)$. This assumption is used since finding the sensitivity of $(E_L + E_U)$ with respect to PV rating is difficult to derive since both terms depend on n which is difficult to obtain in a closed form. Hence for a discrete set of PV ratings, the sensitivity of GSE to PV rating depends only on the list of critical capacities for those PV ratings, assuming the difference between those PV ratings is small.

Chapter 3

Critical Capacity Analysis: Discussion and Validation

In this chapter the following aspects of the critical capacity analysis (CCA) method are discussed:

1. The assumptions made by CCA and their effect on the GSE to storage capacity ($E_g[E_s, P_0]$) curves.
2. The key properties of the CCA which provide analytical insight.
3. The advantages of CCA over the conventional (simulation) method.

Finally this chapter validates the CCA method using a case study. This case study compares the CCA method to the conventional (simulation) method by comparing their respective: i) GSE to storage capacity ($E_g[E_s, P_0]$) curves, and ii) GSE to PV rating ($E_g[E_{s0}, P]$) curves. This comparison shows a strong agreement between the curves obtained by CCA and through the simulation method. Hence the CCA method will be used in Chapter 4 to derive an estimation of the household's maximum benefit for a given investment.

3.1 Assumptions of CCA

The list of assumptions in Section 1.6 is discussed in detail in the following.

3.1.1 Assumed storage power limits

The consequence of the power limit assumption is illustrated in Fig. 3.1(a) where the ideal (no limit) transfer of power into and out of storage is shown in red and the power limited transfer is shown in purple. The limited power transfer cannot be above or below the storage power limits described by +Plim (charge) and -Plim (discharge). Note the generation convention is used.

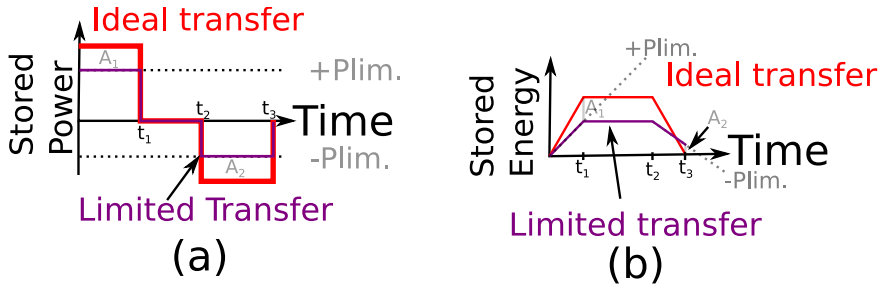

Figure 3.1: Demonstrating the issues with the power limit assumptions: a) example power time transfer to/from storage (net generation), b) State of charge of storage capacity

The differences between the power limited case and the no limit case is the energy areas labeled A_1 and A_2 in Fig. 3.1(a). For the power limited case the energy contained within these areas cannot be transferred into and out of storage and hence there is a fixed amount of GFI (A_1) and GSE (A_2) which would occur regardless of

the energy storage capacity. These fixed amounts of GFI and GSE do not occur for the ideal transfer case where power limits are ignored and hence the proposed CCA method would underestimate both the GSE and the GFI.

Fig. 3.1(b) shows the state of charge for the ideal transfer and the limited transfer. At the time t_1 the limited transfer curve is A_1 energy units below the ideal transfer curve, meaning A_1 energy units were not transferred into storage and hence there is a GFI of A_1. Similarly at time t_2 the limited transfer curve would transfer A_2 energy units less than the ideal transfer amount and hence there is a GSE of A_2 due to the limited storage discharge rate.

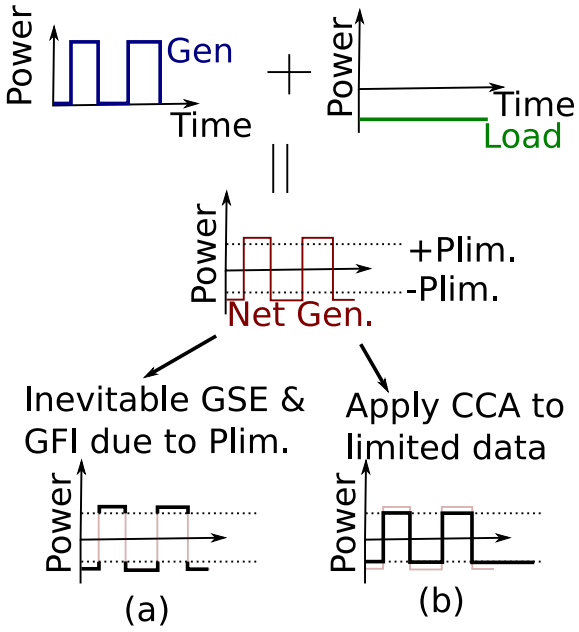

Figure 3.2: Potential solution to include power limits in CCA

While not implemented in this thesis, a potential solution to modifying the CCA to include power limits is presented in Fig. 3.2. The net generation time series is separated into two time series where one of the time series would be used to find any GSE and GFI due to storage power limits and the second time series would contain the critical capacities for a power limited storage device. The separation is shown in Fig. 3.2 where (a) shows the time series considering only power values above the limit and (b) shows the separate time series used for CCA for a power limited storage device.

3.1.2 Initial SoC

If the HES storage device is assumed to be initially full then there is an additional source of energy being added into the HES analysis. To highlight the effect of the initial SoC assumption two extremes are considered: i) storage is initially full, and ii) storage is initially empty. The difference between these two extremes is demonstrated in Fig. 3.3.

The time series shown in Fig. 3.3(a) shows that if the net power time series is initially negative, e.g. the time series starts at midnight at the start of the year, then there is a fixed amount of energy labeled A_1 which is supplied by either storage or GSE depending on whether the storage is initially full or empty respectively.

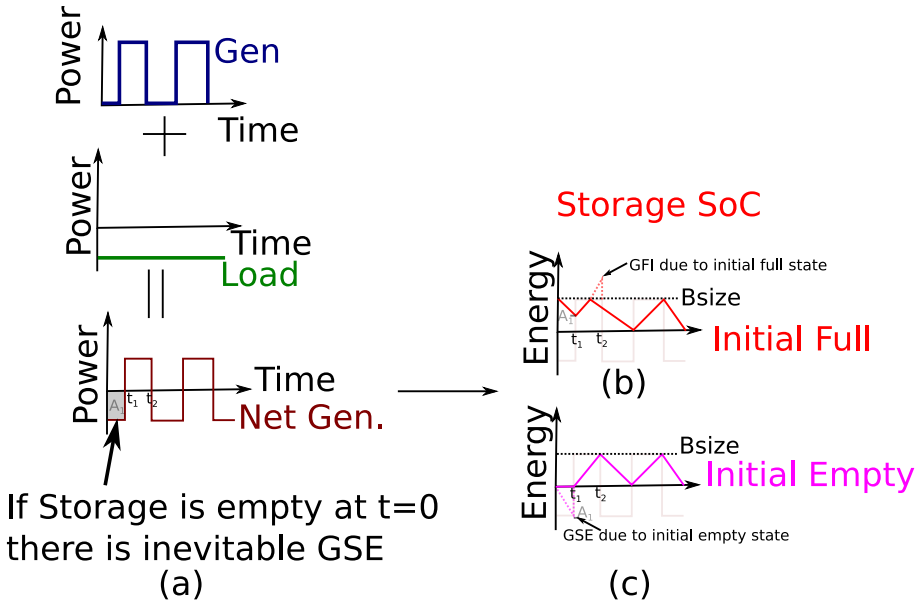

Figure 3.3: Demonstrating the assumption of initial SoC: a) the example net generation time series, b) storage is initially full, c) storage is initially empty

If storage is initially full, shown in Fig. 3.3b, then storage can supply the initial energy A_1 however the storage device will become full when generation occurs between times t_1 and t_2 and hence GFI occurs. If storage is initially empty, shown in Fig. 3.3c, then the initial energy amount A_1 must be supplied by GSE and there is no GFI between t_1 and t_2.

The effect of initial SoC can vary depending on the rating of storage capacity but can have an impact on the accuracy of the GSE and GFI curves and hence on the optimal HES size. For small storage capacities the initial SoC has minimal impact on the overall GSE and GFI relationship to storage capacity however for larger storage capacities, e.g. capacities required for off-grid application, the initial SoC

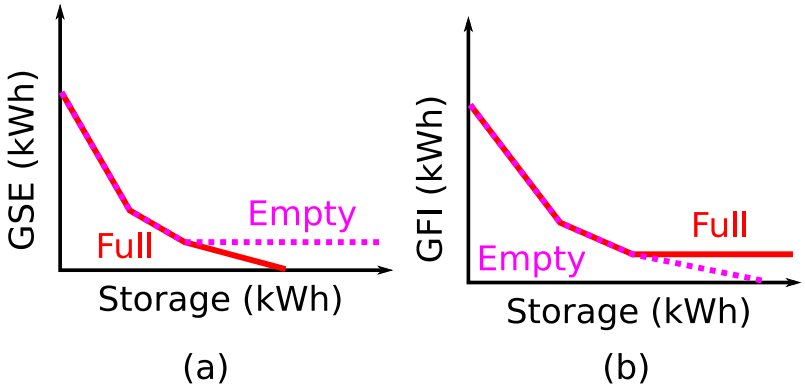

Figure 3.4: Demonstrating the effect of full and empty initial SoC on the GSE and GFI to storage capacity trade off: a) GSE trade off, b) GFI trade off.

significantly affects the resulting GSE and GFI curves. When storage is assumed to be initially full there is a storage capacity which ensures zero GSE and the GFI curve has a fixed amount of GFI for large storage capacities as shown in Fig. 3.4. When storage is assumed to be initially empty there is a fixed amount of GSE which must supply the first negative time interval and the GFI has a storage capacity which results in zero GFI shown in Fig. 3.4.

3.1.3 Assumed Efficiency of Storage Device

The proposed CCA method assumes that the transfer of energy into and out of storage has no loss which reduces the accuracy of the GSE and GFI to storage capacity trade off curves. The illustration in Fig. 3.5 highlights the issue by comparing a 100% efficient storage device to a 80% efficient storage device. The 80% efficient device has energy lost during the discharge period between i) t_0 and t_1 and ii) t_2 and t_3, resulting in GSE during these periods while the 100% efficient case has no GSE.

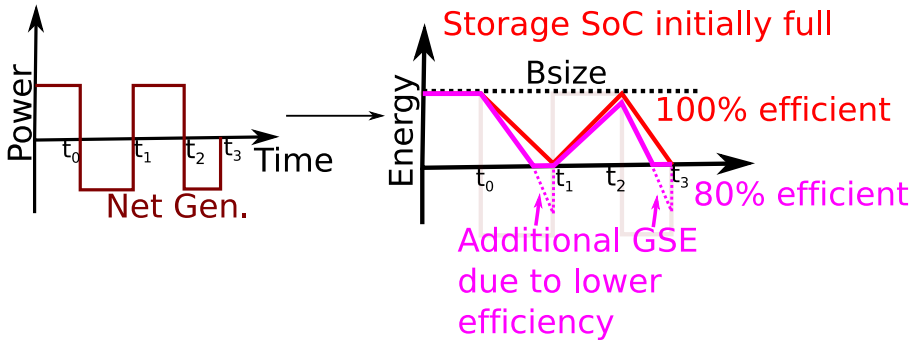

Figure 3.5: The difference between storage time-series due to storage devices with 100% and 80% efficient storage devices. The device with 80% efficiency incurs additional GSE.

The effect of non-ideal efficiency on the optimization of the HES is to add some errors to the GSE and GFI which is found using the CCA method. The effect of losses is sensitive to the number of charging and discharging periods within the year.

3.1.4 State of Charge Limits

This thesis assumes the SoC will vary as needed to supply the given load between 0% and 100%. There are cases where it is desired to limit the SoC between a given maximum and minimum value. For example for a HES to provide backup power the SoC must be limited to a minimum value to ensure sufficient reserves are available to supply the household for a given number of hours.

The effect of SoC limits on the optimization of the HES is that the GSE would be inaccurate if a minimum or maximum SoC is required.

3.2 Key Properties of Critical Capacities

The methods used to identify critical capacities has revealed two important properties of critical capacities. There are:

1. The critical capacity list length N which describes the number of critical capacities for a given time-series. For example a time-series will have N critical capacities listed as $\boldsymbol{C} = \{c_1, c_2, \cdots, c_N\}$.

2. A given critical capacity has both a magnitude and a time duration.

The first property of the critical capacity list length N can be described by the following:

Critical Capacity Property 1: Number of Critical Capacities

For a given PV rating (P_0), there is a list of critical capacities which describes the $E_g[E_s, P_0]$ curve for a given load time-series. This list contains as many entries as the number of troughs (local minima) in the energy time series and hence is equal to the number of times the net generation-power time series becomes negative. The length of this list is called the number of critical capacities for a given PV rating.

This property is demonstrated using the raindrop analogy in Fig. 2.19 which contains both 18 raindrop paths shown by the arrows below the curve and 18 critical capacities shown by the kWh listed below the arrow. For a given raindrop's path to exist there must be a peak which is followed by a trough otherwise the raindrop does not travel along the curve. Hence the time series shown in Fig. 2.19 contains 18 troughs which equals the number of critical capacities in this time series. This energy time-series was originally from the power time-series in Fig. 2.16a which can be seen to have 18 periods of negative power.

Peaks in the energy time series occur when the net generation-power is ideally positive which occurs during daylight hours when the PV system is generating and troughs in the energy time series occur when the net generation-power is negative which typically occurs at night when the PV system cannot generate. Hence a typical year has ideally 365 critical capacities as the net generation-power is positive for 365 periods and is negative for 365 periods. However an actual year, such as in the case study, may have more than this since the net generation-power time series may be negative more than once per day, for example if there is high cloud cover during the middle of a given day such that the PV output drops below the demand then there would be an additional period of negative net generation occurring during that day.

The second property that a given critical capacity has both a magnitude and a duration is described by the following:

Critical Capacity Property 2: Magnitude and Duration

For a given PV rating (P_0), there is a list of critical capacities which describes the $E_g[E_s, P_0]$ curve for a given load time-series.
For each critical capcity in this list, the magnitude of a given critical capacity is simply the kWh capacity which describes its breakpoint on the $E_g[E_s, P_0]$ curve, as discussed in Section 2.2.1.
The duration of a given critical capacity refers to a time interval (of the power or energy time-series) during across which the critical capacity is found, i.e. in the rainflow analogy the start and end time of the raindrop defines this interval.

The magnitude and duration property is demonstrated for the energy time-series in Fig. 2.19 for the 18 raindrops (critical capacities) demonstrated by the arrows below the curve. The magnitude is the kWh value next to each arrow. The duration is represented by the start and end point of each arrow, noting each arrow ends at a negative period. The duration is examined in detail for five of the critical capacities in Fig 3.6 and these critical capacities are labeled C_A to C_E.

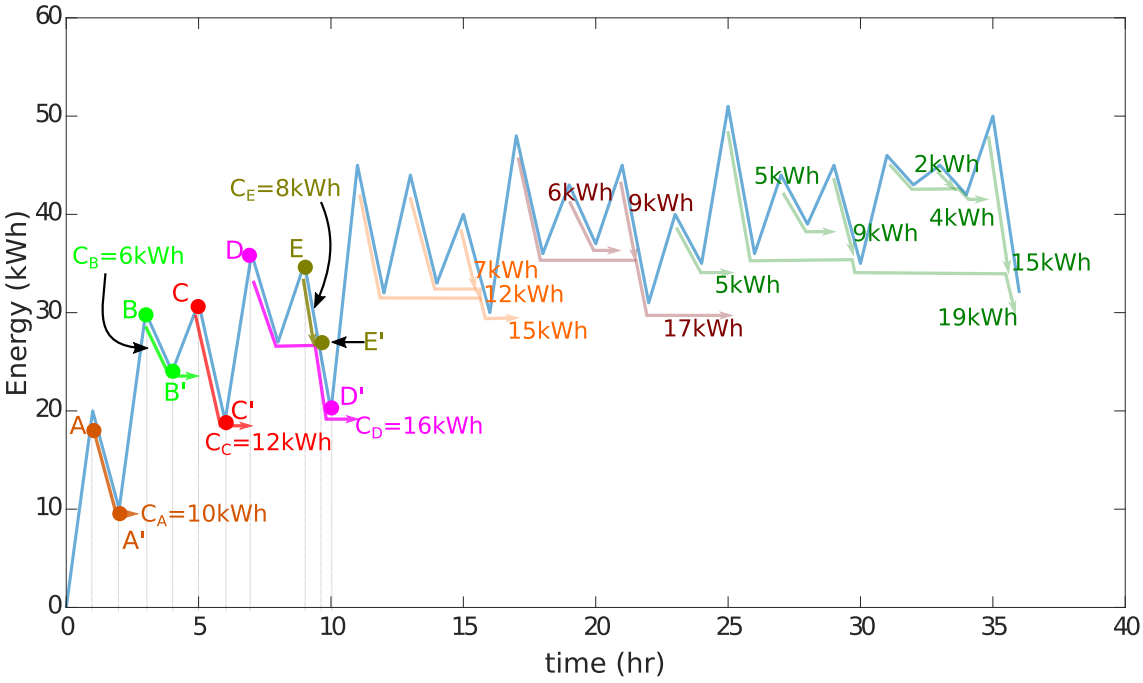

Figure 3.6: The rainflow raindrop analogy from Fig. 2.19, highlighting the duration of 5 critical capacities labeled C_A to C_E which were arbitrarily chosen to demonstrate their duration.

The critical capacity labeled C_A has a magnitude of 10 kWh and its duration starts at point A and ends at A′. Similarly the critical capacity labeled C_B has a magnitude of 12 kWh and a duration between points B and B′. A similar statement can be made for the critical capacities labeled C_D to C_E. Note the rainflow algorithm finds both the magnitude and the labeled time points (e.g. A and A′).

The importance of the critical capacity duration is that it describes when the GSE occurs. For example if storage is sized at 8 kWh then the GSE between the critical capacities labeled C_A to C_E will be:

1. Between A and A′ there will be $10 - 8 = 2$ kWh of GSE.
2. Between B and B′ there is no GSE (as $C_B < 8$ kWh).
3. Between C and C′ there will be $12 - 8 = 4$ kWh of GSE.
4. Between D and D′ there will be $16 - 8 = 8$ kWh of GSE.
5. Between E and E′ there will be no GSE (as $C_E < 8$ kWh).

Thus the total GSE for a storage capacity of 8 kWh associated with these five critical capacities is 14 kWh.

There are two key advantages of knowing a critical capacity's duration. The first, as seen above, is being able to determine where the GSE occurs across the time series for any given storage capacity without needing to simulate the state of charge.

The second advantages is based on understanding the magnitude of critical capacities. By listing critical capacities in order of descending magnitude then the duration of each critical capacity will determine what period of the year caused a given magnitude. While not conducted in this work, this could be used to provide insight into whether time-factors such as seasonal generation variation or weekday/weekend load variation have the largest impact on each critical capacity's magnitude.

3.3 Advantages of CCA

CCA produces the same GSE to storage capacity ($E_g[E_s, P_0]$) curve as the conventional simulation method; however, CCA has two advantages: i) a closed-form equation for GSE in terms of storage capacity resulting in greater physical insights and ii) improved computational speed.

The improved computational speed refers to the actual time (runtime) taken to calculate either: i) the GSE and GFI for a number of HES sizes or ii) the required HES size to achieve maximum benefit at a given investment. This aspect is more important when simulations involving high-resolution generation and load data over long periods of time needs to be analysed

3.3.1 Closed-form GSE Equation

The key benefit of the CCA method is the closed-form equations for both: i) GSE in terms of storage capacity in (2.8) and ii) the decomposition of terms for the GSE

to PV rating relationship in (2.11). These two equations are used to develop the MBI estimation equation in Chapter 4.

The closed-form advantage of CCA over the simulation technique is illustrated by Fig. 3.7 where a rectangular grid is drawn on the axes of PV rating and storage capacity such that the grid intersections represent a given HES size. The simulation approach simulates each HES size while the CCA method finds the critical capacities for each PV rating and uses an equation to describe the GSE at any point along the horizontal PV line.

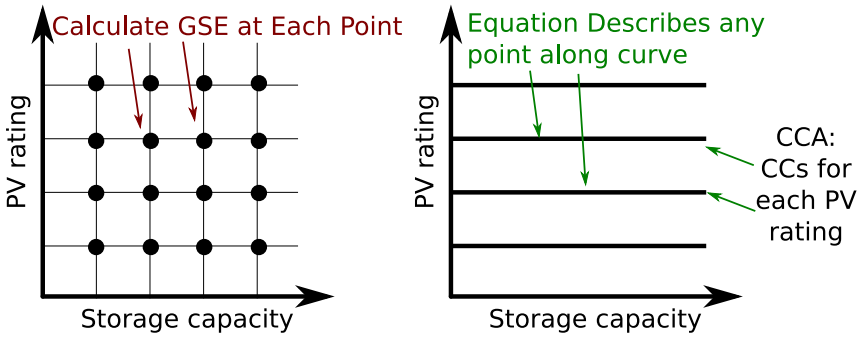

Figure 3.7: A comparison between CCA and the simulation method for finding GSE in the PV versus storage plane to demonstrate the advantage of CCA. Note the above mentioned equation for the CCA method calculates the GSE for any storage capacity at the given PV rating

3.3.2 Computational Speed

The CCA method is computationally faster than the simulation method when a high accuracy $E_g[E_s, P_0]$ curve is required; however, if the E_g at a single E_s is required then the simulation method is faster. The runtime of both methods can be compared using their respective pseudocodes, where algorithm 1 describes the simulation method and algorithm 2 describes the CCA method. Both algorithms share a common set of input parameters which are: i) the number of time steps in both the generation and load time-series data (T), ii) the selected set of PV ratings (P) and iii) the selected range of storage capacities (B). These parameters have the largest impact on the runtime of both methods.

The following examines both algorithms to compare their expected runtime. The result will describe how the runtime is affected by the values of the inputs into the algorithm (P, B, and T). For example if the runtime is proportional to T this would mean it is proportional to the number of time-steps. If the runtime is proportional to BT then it is proportional to the product of: i) the number of storage capacities (B), and ii) the number of time steps (T).

The simulation method in Algorithm 1 has a three-level nested loop with loops for each: i) PV rating, ii) storage capacity, and iii) time step. Hence the runtime of the simulation method is expected to be proportional to PBT.

Algorithm 1 Pseudocode for simulation method

Notation: T is the number of time points in the generation/load data. B is the number of storage capacities simulated. P is the number of PV ratings simulated.

```
for p = 1 to P do
    for b = 1 to B do
        for t = 1 to T do
            Find the storage state at each time step t
            Record any GSE and GFI
        end for
    end for
end for
```

Algorithm 2 Pseudocode for CCA approach.

Notation: T is the number of time steps in the generation/load time series. P is the PV rating list length. B is the storage capacities list length. M is the local min/max list length where $M \leq T$. R is the residues list length where $R \leq M \leq T$.

```
for p = 1 to P do
    for t = 1 to T do
        Find all of the M local minima/maxima.
    end for
    for m = 1 to M do
        Identify the critical capacities based on the 3 point rainflow criteria.
        Any points which do not fit the criteria are residues.
    end for
    for r = 1 to R do
        Process residues to find remaining critical capacities.
    end for
    for b = 1 to B do
        Apply the GSE equation (2.8) and GFI equation (1.3b) for each b capacity
    end for
end for
```

The CCA method in algorithm 2 has a two-level nested loop where the first level is a loop for each PV rating and the second level contains four individual loops: i) a loop for each time step, ii) a loop for each local minima and maxima, iii) a loop for each residue R, and iv) a loop for each storage capacity. Hence the runtime of the CCA method is expected to be proportional to $(PT + PM + PR + PB)$. Note the worst-case runtime condition for the CCA method occurs when both: i) the number of local minima and maxima are equal to the number of time steps, and ii) each local minima and maxima are also a residue. Hence the worst-case occus when $T = M = R$ and the runtime is proportional to $(3PT + PB)$.

To summarise, the runtime derived from the algorithms of CCA and simulation are:

1. Simulation runtime is proportional to (PBT) and

2. CCA runtime is proportional to $(PB + 3PT)$.

The runtime of both methods is proportional to the same PB component hence as the number of PV ratings (P) and storage capacities (B) increases, to much greater values than the time-steps T, then both methods would have similar runtimes. However typically the number of PV ratings and the number of storage capacities are much less than the number of time-steps.

Fig. 3.8 plots the actual runtime (in seconds) for both methods when they are used to find the GSE and GFI for a square list of HES sizes (i.e. $P = B = N$). Using the summary of the derived runtimes: i) the simulation runtime is proportional to N^2T and ii) CCA's runtime is proportional to $(N^2 + 3NT)$.

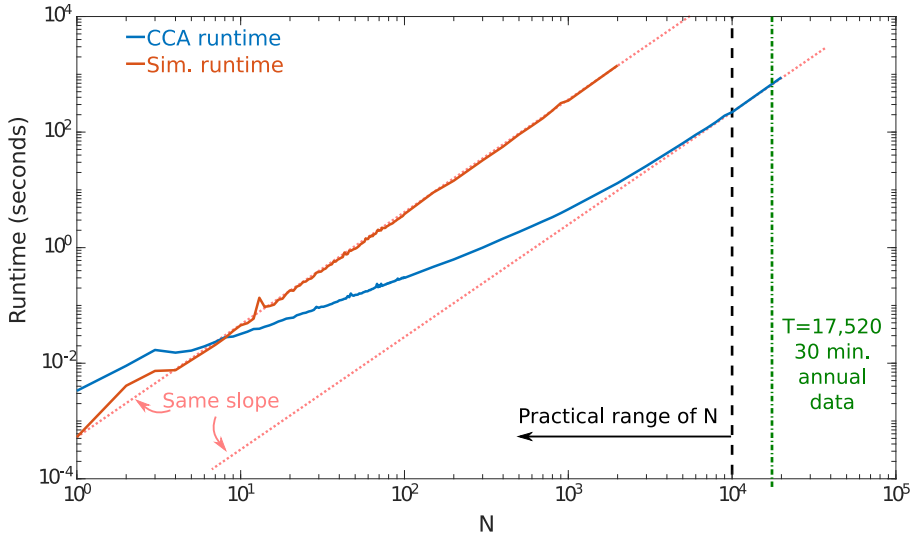

Figure 3.8: Estimating the time complexity of both the simulation method and CCA method using an input of N HES sizes. Note both curves have similar runtime when N approaches the case study's time-step (T) of half hourly annual data.

For small N (< 10), the result in Fig. 3.8 shows CCA is slower then simulation, which matches the derived runtime since for small N $(N^2T < N^2 + 3NT)$. As N increases it can be seen that CCA becomes much faster than simulation since for large N, $(N^2T > N^2 + 3NT)$. As N approaches the number of time-steps T, shown by the vertical line in Fig. 3.8, the simulation and CCA method runtime both increase at the same rate. This is observed in Fig. 3.8 where both the CCA and simulation runtime appear to increase with a slope of N^2. As previous mentioned, the practical range of N is typically larger than 10 and smaller than the number of time-steps T since a value of N in this range is usually sufficient to accurately produce the $E_g[E_s, P_0]$ curve and the MBI plot shown in Chapter 4.

Table 3.1 shows a breakdown of the runtime for both methods for five sets of PV sizes (P) and storage capacities (B). The table shows the CCA method is faster when the GSE is required for more than 10 storage capacities which is common when an accurate $E_g[E_s, P_0]$ curve is required.

Table 3.1: Runtime comparison for simulation and CCA to find the GSE and GFI for a range of PV ratings (P), a range of storage capacities (B) and number of time steps in both the generation/load data (T)

Case	$\boldsymbol{P}$	$\boldsymbol{B}$	$\boldsymbol{T}$	**Simulation**	**CCA**	**Runtime ratio (Sim:CCA)**
(1)	1	1	8,760	0.49 ms	3.0 ms	0.17:1
(2)	1	10	8,760	4.7 ms	3.2 ms	1.47:1
(3)	1	100	8,760	46 ms	4 ms	11.5:1
(4)	100	100	8,760	4.5 s	0.42 s	10.7:1
(5)	100	100	87,600	60 s	4.6 s	13:1

The following compares the cases in Table 3.1 to highlight key differences in the runtime of both methods.

When comparing case 1 to case 3:

1. The CCA method has minimal difference in runtime since once the critical capacities have been identified for a given PV rating, the runtime only depends on the number of storage capacities and using the GSE equation (2.8).

2. The simulation method has a linear increase in runtime relative to the increase in storage capacity values, e.g. when the storage values increase 10 times then the runtime increases 10 times.

Comparing case 4 to case 3:

1. For CCA, when 100 PV ratings are added (to case 3) then the runtime is increased by approximately 100 times (from 4 ms to 400 ms).

2. For simulation when 100 PV rating are added (to case 3) then the runtime increases by approximately 100 times (from 46 ms to 4.5 s)

For case 5 when the number of time steps is increased by 10, the runtime of both methods also increases by approximately 10 times.

To summarise, the simulation method runtime in Table 3.1 is linearly related to both: i) the range of PV ratings, and ii) the range of storage capacities. The CCA method runtime is approximately constant for different ranges of storage capacities and is linearly related to the range of PV ratings. Both methods are linearly related to the number of time steps T.

3.4 Validation of CCA using a Case Study

The validation of CCA consists of comparing CCA to the simulation method using their: i) GSE to storage capacity ($E_g[E_s, P_0]$) curves, and ii) GSE to PV rating ($E_g[E_{s0}, P]$) curves.

The CCA method has derived two equations in Chapter 2 which are:

1. A closed-form equation, (2.8), for a fixed PV rating (P_0) which finds the GSE (E_g) in terms of storage capacity (E_s), defining the $E_g[E_s, P_0]$ curve.

2. A decomposition of the GSE to storage relationship, (2.11), which finds, for a fixed storage capacity (E_{s0}), the GSE in terms of a discrete range of PV ratings (P), defining the $E_g[E_{s0}, P]$ curve.

The CCA method uses these two equations to produce the $E_g[E_s, P_0]$ and the $E_g[E_{s0}, P]$ curves and an equivalent set of curves can be produced using the simulation method. The simulation method would produces these curves by simulating the storage capacity state of charge for the sets of different PV ratings and storage capacities.

Two sets of analysis, using the case study data from Section 1.7, is performed:

1. The base case Section 1.7.2 considers a given household (H1) and a given year of solar irradiation (2005).

2. A set of sensitivity studies considering:

   (a) The 5 households described in Section 1.7.3.

   (b) The 5 years of solar irradiation data in Section 1.7.4.

For each of these cases the $E_g[E_s, P_0]$ curve and the $E_g[E_{s0}, P]$ curve show strong agreement between simulation and CCA. Note it is not necessary to compare the grid feed-in (GFI) since, as seen in equation (1.3b), if the GSE is known then the GFI is known so the following section only provides curves of GSE.

3.4.1 Validation of GSE to Storage Equation for a Fixed PV Rating

In Chapter 2, CCA defines the closed-form equation for the GSE (E_g) as a function of storage capacity (E_s) at a fixed PV rating (P_0) as follows:

$$E_g[E_s, P_0] = \sum_{i=1}^{N} \frac{1}{2}\Big((c_i - E_s) + |c_i - E_s|\Big) \qquad \text{(2.8 Repeated)}$$

where c_i are the critical capacities at the fixed PV rating P_0 for the given household. This equation is validated for the base case household in Fig. 3.9a which shows very close agreement between the CCA results (solid line) and the conventional simulation approach (dots) for the six evenly spaced PV ratings between 0.5pu and 3pu.

The $E_g[E_s, P_0]$ curve is affected by: i) the annual load time series (the household's load data) and ii) the annual solar irradiation (used to calculate generation data). Hence the results of the GSE equation are examined for different household

load profiles and for different years of solar irradiation data. The GSE equation is validated against the conventional method for the six different household load profiles (H1 to H6), with a PV rating of 1 pu in Fig. 3.9b and for six different years of generation data in Fig. 3.9c. These two figures demonstrate very close agreement between the closed-form GSE equation and the conventional simulation approach and shows the robustness of the GSE equation and CCA method.

3.4.2 Validation of the GSE to PV Rating Equation Decomposition

As described in Chapter 2, the CCA method does not yield a closed-form relationship between GSE and the PV rating for a fixed storage capacity ($E_g[E_{s0}, P]$). However it does demonstrate that the GSE ($E_g[E_{s0}, P]$) for a discrete set of PV ratings and fixed storage capacity can be calculated using the three separate terms in (2.11). These three terms, described in Section 2.6.3, are: i) $E_{g0}[P]$ the GSE with no storage capacity, ii)$E_L[E_{s0}, P]$ the energy that storage supplies to critical capacities less than the fixed storage capacity E_{s0} and iii) $E_U[E_{s0}, P]$ the energy that storage supplies to critical capacities greater than E_{s0}.

Separating the GSE equation into these three terms are important in Chapter 4 since only E_{g0} is necessary to estimate the sensitivity of GSE to variations in PV ratings and hence derive an equation for the maximum benefit for a given investment. The following will demonstrate that: i) each of these three terms are independent from each other, ii) each term can be calculated using both the list of critical capacities and the given storage capacity, and iii) the GSE calculated from these terms matches the GSE found using the conventional simulation method.

As a reminder (2.11) is as follows:

$$E_g(E_{s0}, P) = E_{g0}[P] - (E_L[E_{s0}, P] + E_U[E_{s0}, P]) \qquad \text{(2.11 repeated)}$$

where:

$$E_{g0}[P] = \left(\sum_{i=1}^{N[P]} c_i[P] \right), \; E_U[E_{s0}, P] = n[E_{s0}, P] \times E_{s0}$$

$$E_L[E_{s0}, P] = \left(\sum_{i=n[E_{s0},P]+1}^{N[P]} c_i[P] \right)$$

where $c_i[P]$ is the list of critical capacities for PV rating P, E_{g0} is the GSE at zero storage capacity and the combination $(E_L + E_U)$ describes the total energy supplied by storage. Note the GSE at zero storage capacity (E_{g0}) describes the load energy remaining after removing PV self-consumption, hence (2.11) describes the remaining load energy less then the energy supplied by storage ($E_L + E_U$).

The separation of the GSE into the three terms is demonstrated in Fig. 3.10 for

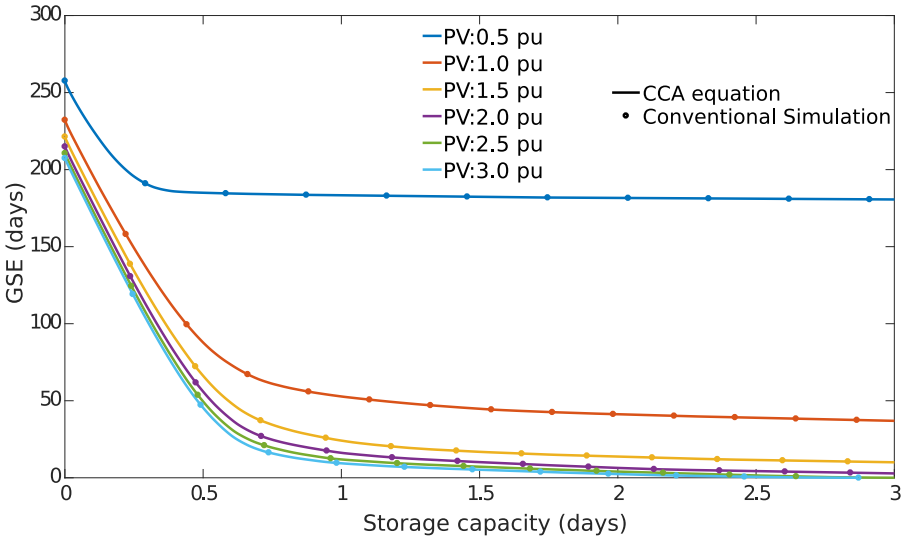

(a)

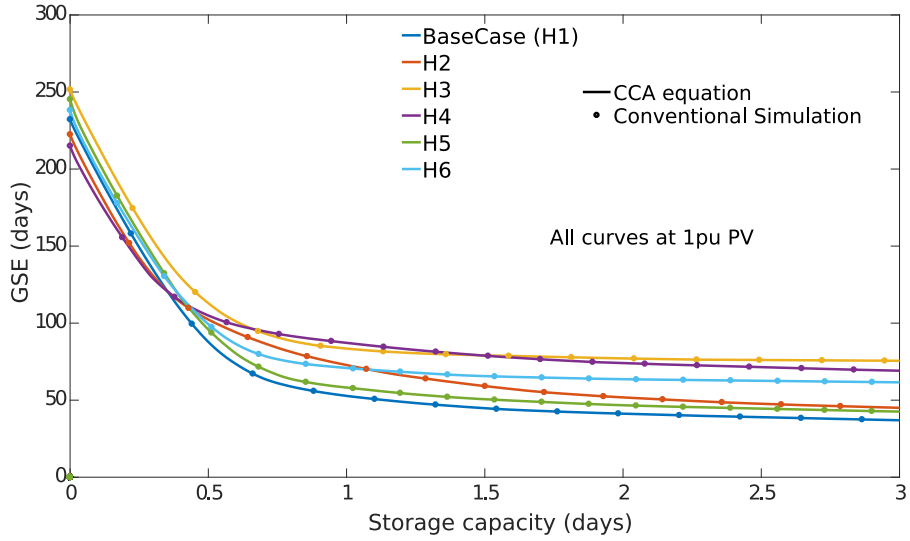

(b)

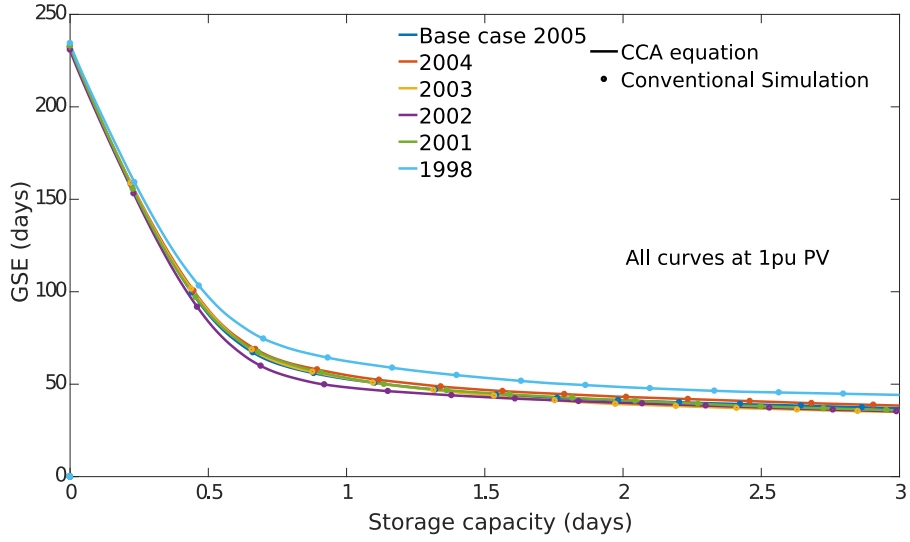

(c)

Figure 3.9: The $E_g[E_s, P_0]$ curves using the closed-form equation (solid lines) compared to conventional simulation (circles) for: a) base case for a range of PV ratings, b) a selection of different household loads for a PV rating of 1 pu, c) a range of generation data years for a PV rating of 1 pu

four fixed storage capacities: i) 0.2 days, ii) 0.6 days, iii) 1 day, iv) 50 days. The total GSE is shown by the dashed line, the GSE at zero storage capacity (E_{g0}) is shown by the solid line and the energy supplied by storage is shown by the two shaded regions (E_L and E_U). Each term is calculated using their respective definition in (2.11) while the total GSE shown is found using the conventional simulation approach. Hence Fig. 3.10 demonstrates that the GSE can be accurately found from these three terms.

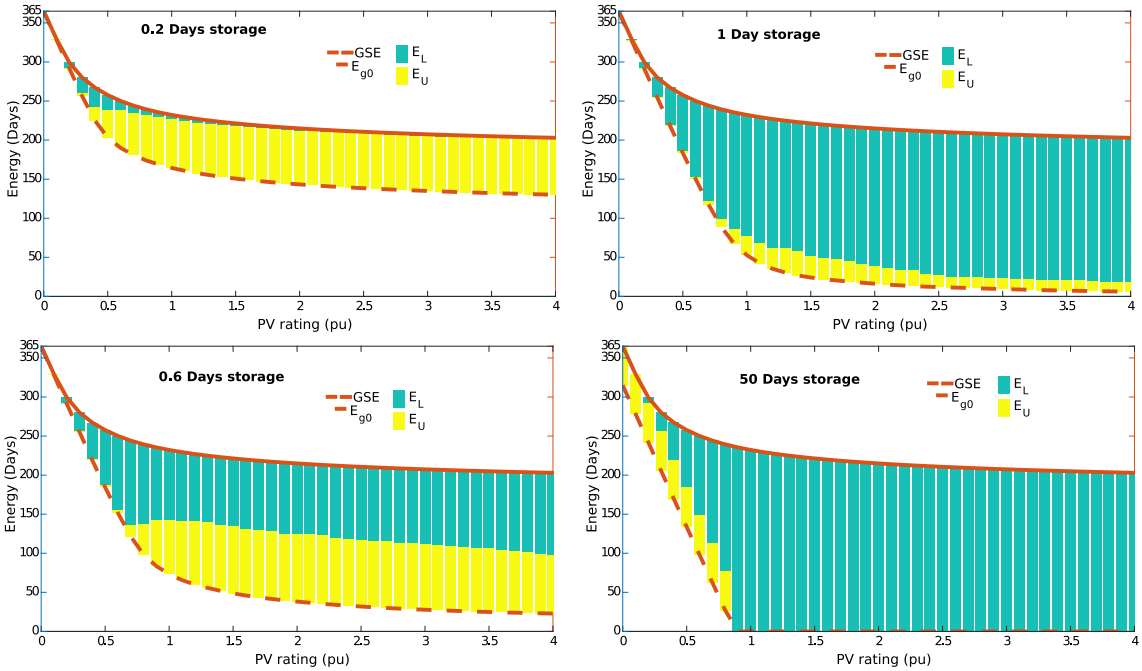

Figure 3.10: Demonstrating the separation of $(E_g[E_{s0}, P])$ into the three terms: i) $E_{g0}[P]$, ii)$E_L[E_s0, P]$ and iii)$E_U[E_{s0}, P]$). The solid line representing the GSE with zero storage capacity (E_{g0}) and the GSE curve represents the GSE with the respective storage capacity of 0.2 days, 0.6 days, 1 day and 50 days. The two shaded regions represent the energy supplied by storage E_L and E_U.

Note in Fig. 3.10 for larger than 1 pu PV rating the ratio between E_U and the E_L is expected to be different for different storage capacities. For small storage capacities the E_U term should dominate as storage supplies a small amount of energy to each critical capacity larger than itself. With approximately half a day of storage the supplied stored energy is equally split between E_U and E_L since, for this case study, the average critical capacity magnitude is approximately half a day. At large storage capacities, the E_L term should dominate as the majority of stored energy is supplied to critical capacities smaller than the storage capacity. The 1 pu PV rating is important here since this ensures there is sufficient annual generated energy to be stored to supply the load.

Fig. 3.10 demonstrates that the GSE can be accurately found from the three terms in (2.11) thus in Chapter 4 these three terms will be used to estimate the MBI. The estimation in Chapter 4 shows that the sensitivity of GSE to variations in PV ratings depends mainly on the first term E_{g0} as the other two terms (E_L and

E_U) do not vary significantly for PV ratings at which installing storage would be considered sensible (1 pu PV rating or greater).

Chapter 4

Household Maximum Benefit for a Given Investment

This chapter provides a definition of the maximum benefit per investment (MBI) and discusses two techniques used to find the household MBI. These two techniques are: i) the numerical search method, and ii) the n-estimation method. The n-estimation method derives an equation to estimate the MBI by using the two equations (GSE to storage capacity in (2.8) and GSE to PV rating in (2.11)) from Chapter 2. These equations are used to produce a simpler method to examine the MBI's sensitivity to changes in the household's capital costs and grid tariffs. The analysis presented in this chapter will consider a single-rate energy tariff which is presently used for most households in South Australia. The household's capital costs and grid tariffs are summarised in the assumptions in Section 1.6, Table 1.3.

Note this chapter contains a number of functions with bold symbols, e.g. $B[\mathbf{E_h}, \mathbf{E_f}]$, which represents when a function's term is itself a function of the variables E_S and P.

4.1 Chapter Structure

This chapter is separated into three main parts:

1. The definition of the problem (Section 4.2 and Section 4.3)
2. The derivation of the n-estimation method (Section 4.5)
3. The validation of the n-estimation method (Section 4.6)

4.2 Definition of a Household's Maximum Benefit for a Given Investment (MBI)

A household's annual benefit ($B[E_h, E_f]$), described in Section 1.2, is derived by offsetting grid supplied energy (GEO, E_h) purchased at the grid energy supply tariff (c_g) and by supplying energy to the grid (GFI, E_f) at the feed-in tariff price (c_f). The benefit equation is:

$$B\big[\mathbf{E_h}[\mathbf{E_s}, \mathbf{P}], \mathbf{E_f}[\mathbf{E_s}, \mathbf{P}]\big] = \mathbf{E_h}[\mathbf{E_s}, \mathbf{P}] \times c_g + \mathbf{E_f}[\mathbf{E_s}, \mathbf{P}] \times c_f \qquad \text{(1.4 repeated)}$$

where the GEO and the GFI depend on the HES capacity ($[E_s, P]$) in which the storage capacity is E_s and the PV rating is P. Note the benefit equation in this form is a function of two multi-variable functions.

The benefit can be simplified in terms of only a single multi-variable function by using the relationship between GEO, GFI and GSE (grid-sourced energy, E_g). The benefit is simplified in terms of only the GSE in Section 1.2 as shown by (2.1)

and is rearranged in equation (4.1) to highlight the dependence on both: i) the GSE $E_g[E_s, P]$ and ii) the PV rating P.

$$B\big[\mathbf{E_g}[\mathbf{E_s}, \mathbf{P}]\big] = (L - \mathbf{E_g}[\mathbf{E_s}, \mathbf{P}])c_g + (G_1 \times \mathbf{P} - L + \mathbf{E_g}[\mathbf{E_s}, \mathbf{P}])c_f \quad \text{(2.1 repeated)}$$

$$B\big[\mathbf{E_g}[\mathbf{E_s}, \mathbf{P}]\big] = \mathbf{P} \times G_1 c_f - \mathbf{E_g}[\mathbf{E_s}, \mathbf{P}](c_g - c_f) + L(c_g - c_f) \quad (4.1)$$

where L is the annual load (kWh) and G_1 is the annual generation (kWh/kW$_{pk}$). Note with both zero storage capacity ($E_s = 0$) and zero PV rating ($P = 0$) then the all load within the year must be supplied from the grid ($E_g = L$) and (4.1) has zero benefit $B = 0$.

The capital investment is $I[E_s, P]$ for a HES with storage capacity E_s and PV rating P which is defined by equation (1.1) and hence for each HES size there is: i) a single PV rating, ii) a single storage capacity, iii) a calculated investment value and iv) a calculated benefit. Note C_P refers to the price per kW$_p$ of PV and C_E refers to the price per kWh of storage.

$$I[E_s, P] = P \times C_P + E_s \times C_E \quad \text{(1.1 repeated)}$$

A range of HES sizes can share a common benefit as shown in the example case in Fig. 4.1a where contours of constant benefit are plotted on the axes of PV rating and storage capacity. These contours are plotted using CCA by finding the GSE, hence benefit, at each critical capacity for each PV rating. Note in Fig.4.1, both the benefit and investment are normalised to the household's annual energy cost when no HES is installed, i.e. $[E_s = 0, P = 0]$ which has annual cost $L \times c_g$.

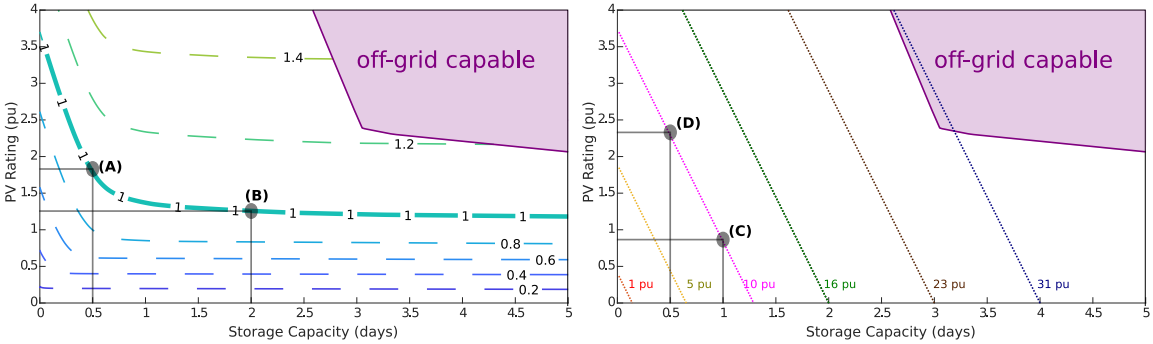

(a) (b)

Figure 4.1: Contours of benefit and investment on the axes of PV rating and storage capacity, a) contours of constant benefit, b) contours of constant investment

An example of two HES sizes is shown in Fig. 4.1a which share a common benefit of 1 pu are: i) point A with $E_s = 0.5$ days, $P = 1.8$ pu, and ii) point B with $E_s = 2$ days, $P = 1.25$ pu. Note that a benefit of 1 pu means a zero annual energy cost, which occurs when either all load is supplied by GEO or, more generally, that the income from GFI equals the cost of purchasing GSE. The energy storage

is normalised against the average daily energy consumption and the PV rating is normalised against the rating required to supply annual energy equivalent to the household's annual energy consumption.

For a given investment (I_x), shown by the lines in Fig. 4.1b, there is a range of HES sizes that satisfy equation (1.1), for example an investment of 10 pu can purchase the HES sizes marked by the two points: i) C with $E_s = 1$ day, $P = 0.8$ pu, or ii) D with $E_s = 0.5$ days, $P = 2.3$ pu. Note to achieve off-grid operation, the case study household requires a high investment of about 31 pu (that is 31 times the baseline annual energy cost) and would achieve only 1 pu benefit since energy could not be sold to the grid in this situation. This emphasises that off-grid operation is generally uneconomical at the current price of capital (PV and storage). The off-grid contour is found by finding the largest critical capacities for a range of PV ratings since storage capacity with size equal to the largest critical capacity has no annual GSE.

If the contours of benefit are overlaid with the contours of investment, as shown in Fig. 4.2, then it can be seen that for any given investment there exists a maximum benefit which can be obtained, called the maximum benefit per investment (MBI). The MBI in Fig 4.2 was found using the search method described in Section 4.4. The MBI occurs when the investment line is a tangent to a given benefit contour or alternatively the tangent of a benefit contour is coincident with the investment line. For example in Fig. 4.2 for 5 pu capital investment the MBI is at point (A) and the investment line is a tangent to the benefit contour of 0.7 pu. Similarly when the investment is 8.66 pu the MBI is at point (B) such that the investment line is tangent to the benefit contour of 1 pu at this point. For these two capital investment amounts, moving away from the marked points (A) and (B) along their respective investment lines results in decreasing benefit.

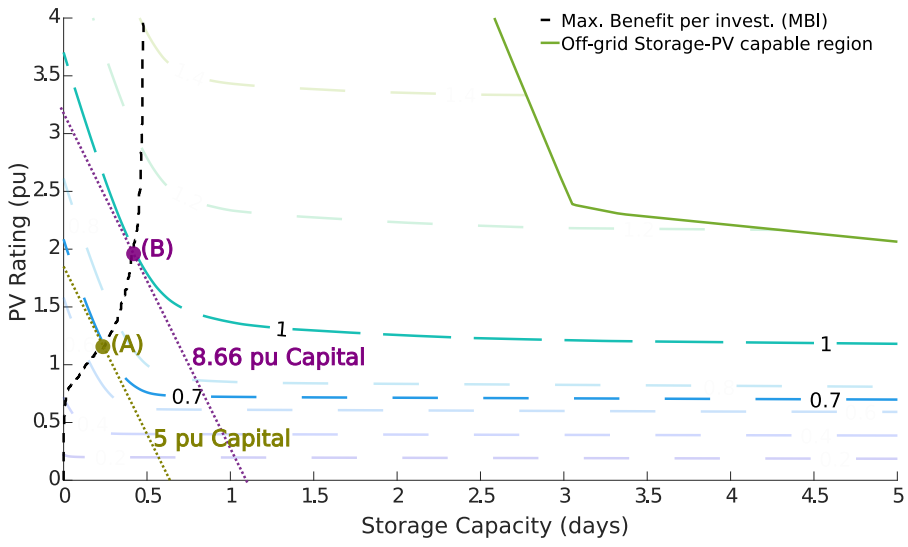

Figure 4.2: Demonstrating the optimal HES sizes which define the maximum benefit per investment (MBI) trajectory, shown as the black dashed line

Two simplifying assumptions made in the MBI analysis are: i) the cost of PV rating and storage capacity is linearly proportional to their respective rating/capacity, and ii) units are available in any desired rating/capacity. In practice the capital cost per unit rating/capacity is generally lower for larger units and the options of size for commercial units are typically in discrete increments, e.g. a supplier may sell a 1 kW and 2 kW PV system but may not sell a 1.2 kW PV system. These assumptions would affect the MBI by changing the shape of the investment contours and hence would reduce the accuracy of the proposed MBI estimation method. However the goal of this chapter is to provide a fast and simple method to estimate the MBI which also provides an intuitive understanding of the MBI's sensitivities and thus these assumptions are considered acceptable for the initial MBI estimation.

4.3 The MBI Expressed as an Optimsation Problem

Finding the maximum benefit per investment (MBI) can be formulated as an optimization problem where the maximum benefit is found by searching all of the HES sizes which share a given investment (I_0). Formally this can be written as:

$$\begin{aligned} \underset{E_s,P}{\text{maximise}} \quad & B\big[E_g[E_s,P]\big] \\ \text{subject to} \quad & I[E_s,P] = I_0 \end{aligned} \tag{4.2}$$

where $B[E_g[E_s,P]]$ is described by the benefit equation in (4.1) and $I[E_s,P]$ is described by the investment in (1.1).

Finding the MBI is a concave problem[1] which is easier to solve compared to non-concave problems. The MBI is shown to be a concave problem by considering either: i) the benefit against storage capacity (Fig. 4.3a) with constant investment contours and ii) the benefit against PV (Fig. 4.3b) with constant investment contours. For the two plots in Fig. 4.3 the maximum benefit at each investment contour is shown by the points marked (A) to (E). To provide a common point of reference for the two plots in Fig. 4.3 consider the benefit for installing only PV and no storage, i.e. the y-axis from Fig. 4.2. In Fig. 4.3a the benefit for only PV is shown by a vertical line along the y-axis. Traveling from the y-axis along a given investment contour causes the PV rating to decrease while the storage capacity increases such that the investment is constant. In Fig. 4.3b the benefit of investing in only PV is shown by the dashed line labeled "No storage" and traveling from this line along an investment contour line towards the origin also causes an increase in storage capacity and corresponding decrease in PV rating such that the investment is constant.

The MBI shown in Fig. 4.2 is a concave problem due to three key factors:

[1] An optimsation problem is concave when a concave function (benefit) is maximised over a concave set (investment).

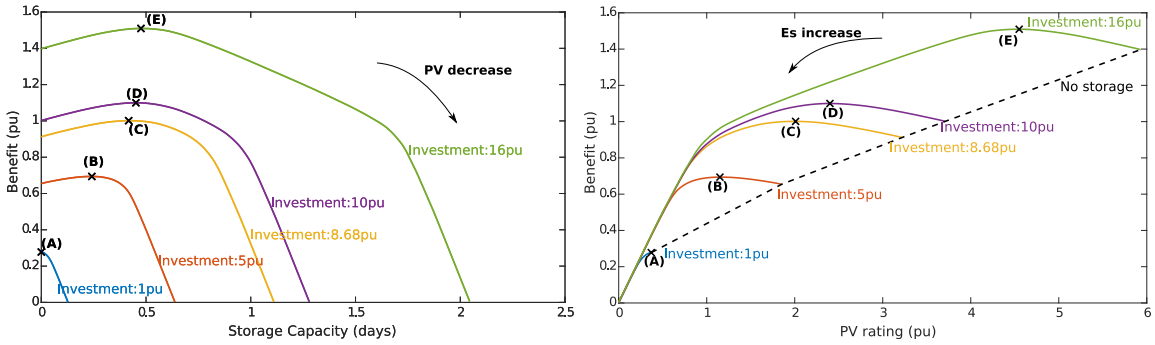

(a) (b)

Figure 4.3: Contours of constant investment on the axes of: (a) benefit and storage capacity, (b) benefit and PV rating. Both plots shows the benefit along each investment contour is concave

1. The assumption of a single-rate energy tariff (Section 1.6) means the benefit is linearly related to the annual GSE scaled by the energy tariff.

2. The piecewise-linear (PWL) relationship between GSE and storage capacity for a given PV rating shown by $E_g[E_s, P_0]$ in (2.8).

3. The linear relationship between GSE and PV rating for a given storage capacity shown by $E_g[E_{s0}, P]$ in (2.11).

Since the benefit linearly changes with GSE and the GSE never decreases when the PV rating and storage capacity increases, the benefit along a diagonal line in Fig. 4.2 is concave. For different types of energy tariffs, such as energy costs which depend on the time of use or if there is an additional charge depending on the maximum demand, the problem may not be concave.

4.4 Comparing Methods to Solve the MBI Optimisation

Two methods of finding the MBI are:

1. The search-based method, which is simple to implement but computationally expensive.

2. The proposed novel approach, called the n-estimation method, which uses analytical techniques to provide an estimate for the MBI.

A summary comparing these two methods is shown in Fig. 4.4.

The search method in Fig. 4.4a begins by selecting a range of capital investment values and then selecting a range of HES sizes along each investment line. For a given capital investment the maximum benefit is found by comparing the benefit of each HES size along that investment line, which is found using either the CCA or

the simulation method. The accuracy of the results depends on both: i) the number of investment lines, and ii) the number of HES sizes.

Note the search-based approach has many aspects which can be optimized, for example if in Fig. 4.4a for a given investment if the benefit is found for an initial storage capacity of zero then the maximum benefit can be found by slowly incrementing the storage capacity until the resulting benefit no longer increases. This is an improvement since fewer storage capacities would be tested however the outcome is still sensitive to both: i) the selected increment in storage capacity, and ii) the tolerance of the benefit change, i.e. at what difference in benefit does the search converge to the maximum benefit.

The proposed n-estimation method analytically solves the MBI as an optimisation problem and for the list of critical capacities for a given PV rating the method derives an equation for the index (n) of the critical capacity which would result in maximum benefit. Note the index (n) can be a non-integer as discussed in Section 4.5.4 and the optimal solution is found using interpolation. By repeating this approach for different PV ratings the MBI trajectory is found. The n-estimation method is shown in Fig. 4.4b where firstly the list of critical capacities is found for a range of PV ratings and then the n-index equation is used to find the index (and hence optimal storage capacity) for each PV rating.

The derivation of the n-estimation equation and its validation is the focus of the remainder of this chapter.

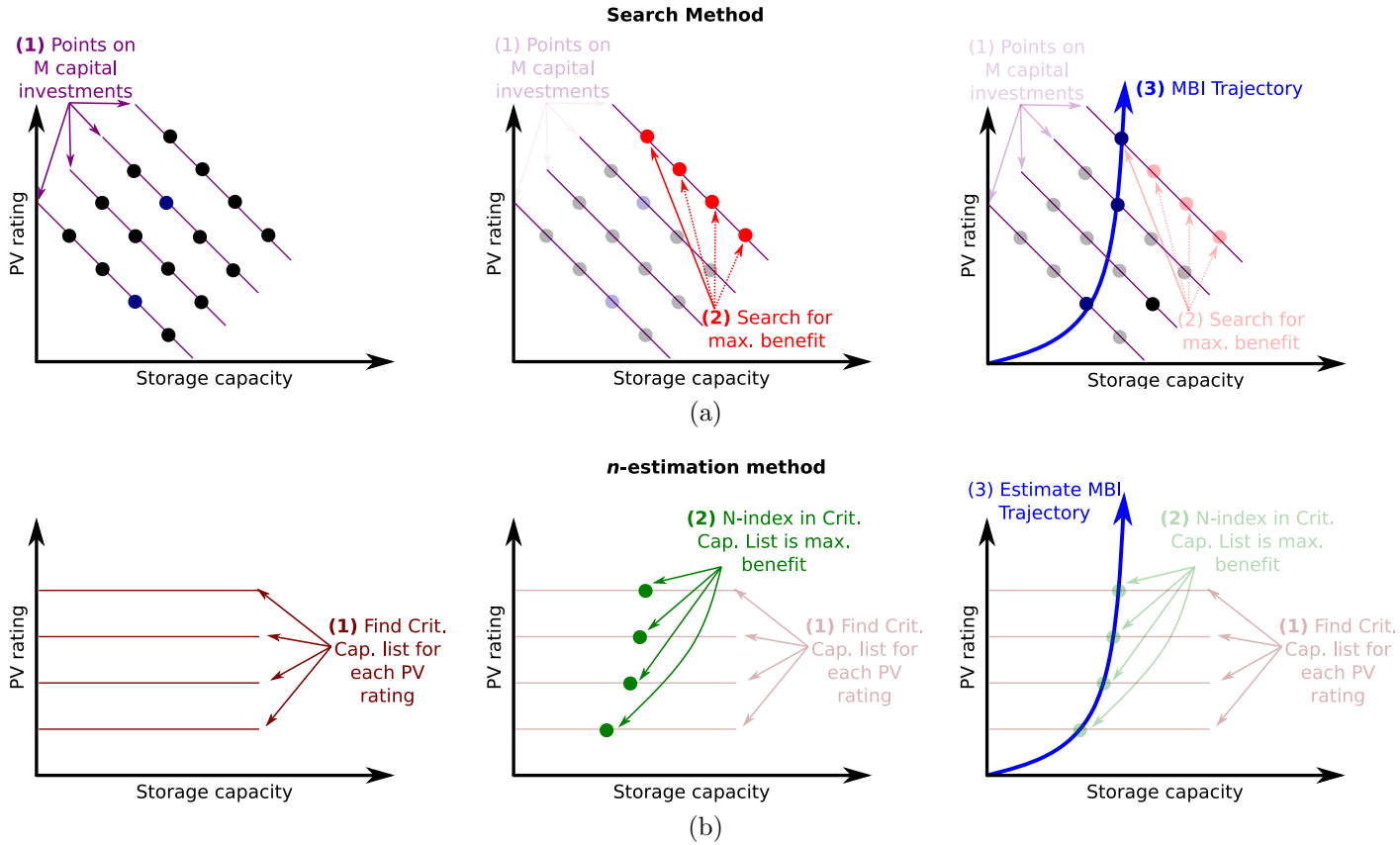

Figure 4.4: An overview of the two methods for solving the optimisation problem. a) Search method, b) n-estimation method. Both methods consist of three steps.

4.5 Developing the n-Estimation Method

The n-estimation method analytically solves the MBI optimisation problem, which is described in (4.2), by using the method of Lagrange multipliers. The Lagrange method can be explained using the relationship between the benefit, a given investment and a given HES size. This relationship is shown in Fig. 4.5 by plotting a number of constant benefit contours (B_{-1}, B_0, B_1), a line of constant investment I_0 and the given HES size (P_0, E_{s0}) which has capital investment of I_0.

In Fig. 4.5 the line labeled I_0 represents all possible combinations of HES sizes which have a capital investment of I_0. The benefit contours are labeled B_{-1}, B_0 and B_1 in the order of increasing benefit, that is $B_{-1} < B_0 < B_1$. By comparing the investment line I_0 to each of the benefit contours it is shown that the maximum benefit along I_0 occurs when I_0 is a tangent to the benefit contour of B_0 which occurs at the optimal HES size of $[E_{s0}, P_0]$. The observation that the maximum benefit occurs when investment lines are tangents to benefit contours is a key component to the Lagrange method.

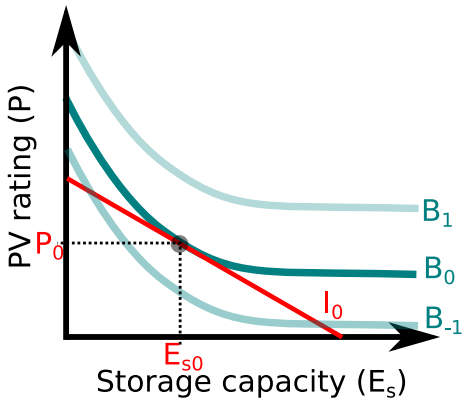

Figure 4.5: Demonstrating the relationship between benefit, investment and a given HES size. The benefit contours are B_{-1}, B_0 and B_1, the investment is I_0 and the optimal HES size along I_0 is the point $[P_0, E_{s0}]$.

The Lagrange method states that the function being optimised (benefit) will be maximum when both the function and the constraint (investment) share a tangent. Two curves share a tangent at a given point if: i) at the given point the tangents of both curves have the same slope, and ii) the tangents of both curves intersect at that given point.

For the first condition, two curves have the same slope when their gradient vectors differ by only a scalar and this scalar difference is called the Lagrange multiplier. Hence when the benefit gradient vector is a scalar multiple of the investment gradient vector then the two curves have the same slope.

For the second condition, it is trivial to determine the point at which the benefit's tangent and investment's tangent intersect since the investment is a straight line and the tangent of a straight line is itself. Hence the investment equation can be used to determine if the two tangents intersect at a given point.

To formally describe these two conditions, the MBI will occur at the point $[E_{s0}, P_0]$ for a given investment I_0 when both the following conditions are satisfied:

1. $\nabla B[E_{s0}, P_0] = \lambda_0 \nabla I[E_{s0}, P_0]$ for the gradient of the benefit ∇B, the gradient of the investment ∇I and the Lagrange multiplier (λ_0).

2. $I[E_{s0}, P_0] = I_0$, for the point $[E_{s0}, P_0]$ in the gradient vector.

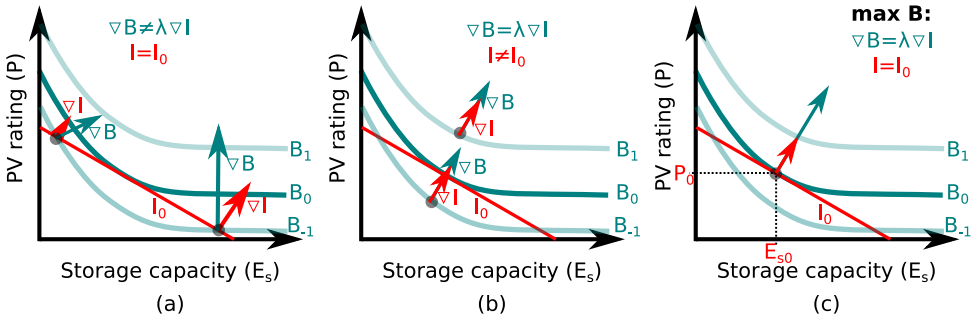

Figure 4.6: Illustration of the concept of Lagrange multipliers, where the gradient of B is a scalar multiple of the gradient of I and the constraint $I = I_0$

These two conditions are demonstrated in Fig. 4.6, where the gradient of the benefit and the gradient of the investment are both right angles to, and point away from their respective curves. Three cases are demonstrated in Fig. 4.6 where the maximum benefit is required for investment I_0: a) two points where the benefit and investment intersect at the given HES size but their gradient vectors are in different directions, b) two points where both gradient vectors are in the same direction but the point at which this occurs is not on investment I_0, and c) when both gradient vectors are in the same direction at a point on the investment I_0, hence the MBI occurs at this point. Using these two conditions, the Lagrange method allows the MBI optimization problem to be written as a set of linear equations which can be solved analytically. Hence the MBI is expressed with the following set of equations, where the maximum benefit for the investment (I_0) will occur at the optimal HES size of ($[E_{s0}, P_0]$) such that:

$$\nabla B[E_{s0}, P_0] = \lambda_0 \nabla I[E_{s0}, P_0] \tag{4.3a}$$

$$\begin{bmatrix} \frac{\partial B}{\partial E_s}\Big|_P [E_{s0}, P_0] \\ \frac{\partial B}{\partial P}\Big|_{E_s} [E_{s0}, P_0] \end{bmatrix} = \lambda_0 \begin{bmatrix} \frac{\partial I}{\partial E_s}\Big|_P [E_{s0}, P_0] \\ \frac{\partial I}{\partial P}\Big|_{E_s} [E_{s0}, P_0] \end{bmatrix} \tag{4.3b}$$

$$I_0 = P_0 \times C_P + E_{s0} \times C_E \tag{4.4}$$

where (4.3a) is expanded as (4.3b) such that:

1. $\frac{\partial}{\partial E_s}\Big|_P [E_{s0}, P_0]$ represents the sensitivity (of benefit B or investment I) to variations in storage capacity (assuming constant PV rating, P) and this sensitivity is evaluated at the point $[E_{s0}, P_0]$,

2. $\frac{\partial}{\partial P}\Big|_{E_s}[E_{s0}, P_0]$ represents the sensitivity (of benefit B or investment I) to variations in PV rating (assuming constant storage capacity, E_s) and this sensitivity is evaluated at the point $[E_{s0}, P_0]$.

In (4.3) there are three equations, three unknowns variables (λ_0 and $[E_{s0}, P_0]$) and one known variable (I_0) and these equations are separated in (4.5).

$$\frac{\partial B}{\partial E_s}\Big|_P[E_{s0}, P_0] = \lambda_0 \frac{\partial I}{\partial E_s}\Big|_P[E_{s0}, P_0] \tag{4.5a}$$

$$\frac{\partial B}{\partial P}\Big|_{E_s}[E_{s0}, P_0] = \lambda_0 \frac{\partial I}{\partial P}\Big|_{E_s}[E_{s0}, P_0] \tag{4.5b}$$

$$I_0 = P_0 \times C_P + E_{s0} \times C_E \tag{4.5c}$$

These equations can be simplified by eliminating the Lagrange multiplier λ_0 using (4.5a) and (4.5b). Note the following sensitivities are evaluated at the point $[E_{s0}, P_0]$:

$$\lambda_0 = \frac{\partial B}{\partial E_s}\Big|_P \frac{1}{\frac{\partial I}{\partial E_s}|_P}$$

$$\lambda_0 = \frac{\partial B}{\partial P}\Big|_{E_s} \frac{1}{\frac{\partial I}{\partial P}|_{E_s}}$$

$$\frac{\partial B}{\partial E_s}\Big|_P \frac{1}{\frac{\partial I}{\partial E_s}|_P} = \frac{\partial B}{\partial P}\Big|_{E_s} \frac{1}{\frac{\partial I}{\partial P}|_{E_s}} \tag{4.6}$$

The sensitivity of investment to variations in both storage capacity and PV in (4.6) is found by using the investment equation (1.1) as shown in the following:

$$I[E_s, P] = P \times C_P + E_s \times C_E \qquad \text{(1.1 Repeated)}$$

$$\frac{\partial I}{\partial E_s}\Big|_P[E_{s0}, P_0] = C_E \tag{4.7a}$$

$$\frac{\partial I}{\partial P}\Big|_{E_s}[E_{s0}, P_0] = C_P \tag{4.7b}$$

Hence the maximum benefit for a specified investment, I_0 can found by solving for the two unknowns (E_{s0}, P_0) in the two equations of (4.8).

$$\left(\frac{\partial B}{\partial E_s}\Big|_P[E_{s0}, P_0]\right)\frac{1}{C_E} = \left(\frac{\partial B}{\partial P}\Big|_{E_s}[E_{s0}, P_0]\right)\frac{1}{C_P} \tag{4.8a}$$

$$I_0 = P_0 \times C_P + E_{s0} \times C_E \tag{4.8b}$$

There is a choice in (4.8) between whether the investment I_0 or the PV rating P_0 is the specified parameter since both have a unique solution for the maximum benefit. Consider the MBI plot in Fig. 4.2 and note that a horizontal line (constant PV) or a diagonal line (constant investment) both intersect with the MBI trajectory

only once, which means either parameter has a unique solution to (4.8). Note that vertical lines (constant storage) can intersect the MBI trajectory multiple times. For example at zero storage capacity or around 0.5 pu storage capacity, and hence storage capacity can not be used as the specified variable in (4.8).

The derivation of the n-estimation equation solves (4.8) analytically by assuming that the PV rating P_0 is specified and the optimal storage capacity (E_{s0}) and investment (I_0) to be the unknown variables.

Terms used to derive the n-index equation

A brief description of all the parameters used in deriving the n-index equation is provided in Table 4.1.

Table 4.1: List of parameters used in deriving the n-index equation

Cost Parameters	**Description**
B	Annual Benefit ($)
c_g	Grid supply tariff ($/kWh)
c_f	Grid feed-in tariff ($/kWh)
C_E	Cost of energy storage ($/kWh)
C_P	Cost of PV ($/kW$_p$)
Energy Parameters	
P	PV rating (kW$_p$)
E_s	Storage capacity (kWh)
E_g	Annual grid supplied energy (GSE)
Household Parameters	
G_1	Annual generation (kWh) per kW$_p$ of PV
L_1	Annual load (kWh)
$E_{g0}[P]$	Annual GSE for a given HES size with PV rating P and no storage.
Optimal Parameters	
P_0	The optimal PV rating for a given investment I_0
E_{s0}	The optimal storage capacity for a given investment I_0
I_0	The given investment containing optimal HES size $[E_{s0}, P_0]$ at which maximum benefit occurs.

4.5.1 Sensitivity of Benefit to Variations in Storage Capacity

The sensitivity of the benefit to variations in storage capacity in (4.9) is derived from the simplified benefit equation in (4.1).

$$B\big[\mathbf{E_g}[\mathbf{E_s}, \mathbf{P}]\big] = \mathbf{P} \times G_1 c_f - \mathbf{E_g}[\mathbf{E_s}, \mathbf{P}](c_g - c_f) + L(c_g - c_f) \qquad \text{(4.1 Repeated)}$$

$$\frac{\partial B}{\partial E_s}\Big|_P = -\frac{\partial E_g}{\partial E_s}\Big|_P (c_g - c_f) \tag{4.9}$$

The sensitivity of benefit to variations in storage capacity is shown to be directly related to the sensitivity of GSE to storage capacity and hence can be derived from the closed-form equation between GSE and storage capacity. As shown in the following section the result of this derivative is:

$$\frac{\partial B}{\partial E_s}\Big|_P [E_{s0}, P_0] = n[P_0](c_g - c_f)$$

where $n[P_0]$ is the n^{th} critical capacity for the given (constant) PV rating P_0.

Sensitivity of GSE to variations in storage capacity

The relationship between GSE and storage capacity is described by (2.8) for a given storage capacity E_s, constant PV rating P_c and the critical capacities $\boldsymbol{C} = \{c_1, \cdots, c_N\}$.

$$E_g[E_s, P_c] = \sum_{i=1}^{N} \frac{1}{2}\Big((c_i - E_s) + |c_i - E_s|\Big) \tag{2.8 Repeated}$$

However finding the sensitivity of (2.8) to variations in storage capacity is complex due to its discontinuities. Hence the simplified version of the GSE equation in (2.9) is used to find the sensitivity of GSE to storage capacity. This simplified equation only considers the first n critical capacities which are greater than the given storage capacity, since these critical capacities are the only terms which contribute to the GSE.

$$E_g[E_s, P_c] = \sum_{i=1}^{n[P_c]} (c_i - E_s) \quad \text{for } n \text{ such that } c_1 \geq \cdots \geq c_n \geq E_s \tag{2.9 Repeated}$$

The sensitivity of GSE to variations in storage capacity is then:

$$\begin{aligned} \frac{\partial E_g[E_s, P_c]}{\partial E_s} &= \sum_{i=1}^{n[P_c]} \frac{\partial}{\partial E_s}(c_i - E_s) \\ \frac{\partial E_g[E_s, P_c]}{\partial E_s} &= \sum_{i=1}^{n[P_c]} (-1) \\ \frac{\partial E_g[E_s, P_c]}{\partial E_s} &= -n[P_c] \end{aligned} \tag{4.10}$$

where n is the slope of the GSE to storage capacity curve and also corresponds to an index in the list of critical capacities. This is shown in Fig. 4.7 which plots the GSE to storage capacity curve containing four critical capacities $\boldsymbol{C} = \{C_1, C_2, C_3, C_4\}$

such that $C_1 > C_2 > C_3 > C_4$ and the curve can be separated into three segments where each segment starts at critical capacity C_k and ends at critical capacity C_{k+1}. The slope of each segment is described by $\boldsymbol{M} = \{M_1, M_2, M_3\} = \{-1, -2, -3\}$ where M_k is the slope between critical capacities C_k and C_{k+1}.

Note in Fig. 4.7b the solid black circles shows that a given storage capacity value belongs to a given segment and an empty circle shows that a value is not included in the segment. For example the storage capacity at C_2 is included in segment 1 and not in segment 2, hence $\frac{\partial E_g}{\partial E_s} = -1$ at C_2.

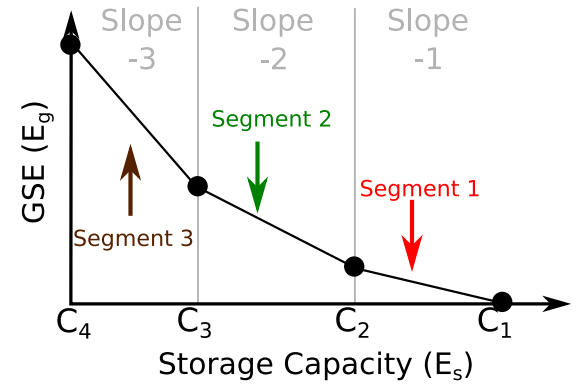

(a)

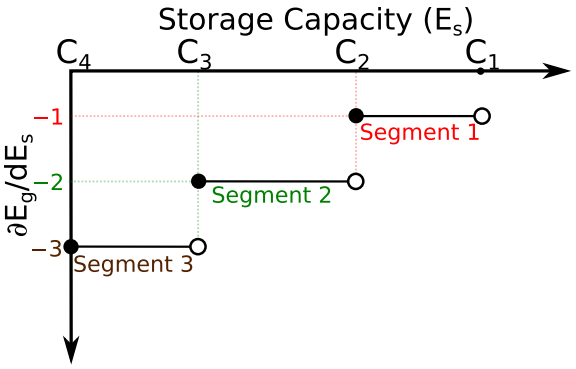

(b)

Figure 4.7: Demonstrating how the slope of the GSE to storage capacity depends on the critical capacities: a) GSE to storage capacity, b) sensitivity of GSE to variations in storage capacity

In Fig. 4.7a if the storage capacity is selected in segment 1 (e.g. $n = 1$) such that $C_2 \leq E_s < C_1$ then the slope is -1, which is shown in Fig. 4.7b. If the storage capacity is selected in segment 2 (e.g. $n = 2$) such that $C_3 \leq E_s < C_2$ then the slope is -2. Similarly for a storage capacity within segment 3 (e.g. $n = 3$) the slope is -3. This demonstrates the concept that the value of n in (4.10) defines both the slope and the index in the list of critical capacities. This concept of n being an index in the critical capacity list is a core concept to the n-estimation method. Note that n may not be an integer and hence Section 4.5.4 discusses how to handle this case.

By substituting for the sensitivity of GSE to storage capacity in (4.10) into (4.9) the sensitivity of benefit to variations in storage capacity is found as:

$$\frac{\partial B}{\partial E_s}\Big|_P = -\frac{\partial E_g}{\partial E_s}\Big|_P (c_g - c_f)$$
$$\frac{\partial B}{\partial E_s}\Big|_P = n[P](c_g - c_f) \tag{4.11}$$

and evaluating this at the point $[E_{s0}, P_0]$:

$$\frac{\partial B}{\partial E_s}\Big|_P [E_{s0}, P_0] = n[P_0](c_g - c_f) \tag{4.12}$$

where $n[P_0]$ describes the n^{th} critical capacity for the given PV rating P_0.

4.5.2 Sensitivity of Benefit to Variations in PV Rating

The sensitivity of the benefit to variations in PV rating is derived in equation (4.13) from the simplified benefit equation (4.1).

$$B\big[\mathbf{E_g}[\mathbf{E_s}, \mathbf{P}]\big] = \mathbf{P} \times G_1 c_f - \mathbf{E_g}[\mathbf{E_s}, \mathbf{P}](c_g - c_f) + L(c_g - c_f) \qquad \text{(4.1 Repeated)}$$
$$\frac{\partial B}{\partial P}\Big|_{E_s} = G_1 c_f - \frac{\partial E_g}{\partial P}\Big|_{E_s} (c_g - c_f) \tag{4.13}$$

Hence the sensitivity of benefit to variations in PV rating depends on the sensitivity of GSE to variations in PV rating.

A closed-form solution between GSE and PV rating has not been found however Chapter 2 decomposes the GSE equation (2.9) into three key components which define the relationship between GSE to PV rating for a range of PV ratings. The decomposed equation, in (2.11), is used to derive an estimate for the sensitivity of benefit to variations in PV rating for the assumptions described in the following section. As shown in the following section the result of deriving the sensitivity of benefit to variations in PV rating is:

$$\frac{\partial B}{\partial P}\Big|_{E_s} [E_{s0}, P_0] \approx G_1 c_f - \frac{\partial E_{g0}}{\partial P}\Big|_{E_s=0} (c_g - c_f)$$

where:

$$E_{g0} = E_g[0, P_0] \approx \left(\sum_{i=1}^{N} c_i[P_0] \right)$$

Note the term E_{g0} refers to the GSE with no storage capacity and while its sensitivity to PV rating may appear to be a source of complexity for the estimation method, this sensitivity is small. The value of E_{g0} depends on only the list of critical capacities for each PV rating and this list is required regardless of whether the search or n-estimation method is used to find the MBI.

The following describes how the sensitivity of GSE to PV rating is derived.

Sensitivity of GSE to variations in PV rating

In Chapter 2 the estimation of GSE for a given PV rating (P) with a fixed storage capacity (E_{s1}) is described by (2.11) and hence the sensitivity of GSE to variations in PV rating can be described by (4.14). Note that E_{g0} is, for zero storage capacity, the annual load remaining after removing the PV self-consumption, i.e. the portion of generated energy consumed by the household, hence each PV rating has a different E_{g0} which is independent of storage capacity. A plot of E_{g0} in terms of PV rating for the base case is shown in Fig. 3.10 with the curve labeled no storage capacity.

$$E_g(E_{s1}, P) = E_{g0}[P] - (E_L[E_{s1}, P] + E_U[E_{s1}, P]) \qquad \text{(2.11 Repeated)}$$

where:

$$E_{g0}[P] = \left(\sum_{i=1}^{N[P]} c_i[P] \right), \quad E_U[E_{s1}, P] = n[E_{s1}, P] \times E_{s1}$$

$$E_L[E_{s1}, P] = \left(\sum_{i=n[E_{s1},P]+1}^{N[P]} c_i[P] \right)$$

Hence:

$$\left.\frac{\partial E_g}{\partial P}\right|_{E_s} \approx \left.\frac{\partial E_{g0}}{\partial P}\right|_{E_s=0} \tag{4.14}$$

Assuming, as justified below, that:

$$\frac{\partial}{\partial P}|_{E_s}(E_L[E_{s1}, P] + E_U[E_{s1}, P]) \approx 0 \text{ for small } E_{s1} \text{ and for large PV ratings}$$

In (4.14) there is an assumption that the sensitivity of the energy supplied by storage ($E_L + E_U$) due to variations in PV ratings has minimal impact on the total sensitivity of GSE to variations in PV rating. This assumption is valid when either i) the storage capacity is small (less than 0.2 days), or ii) the PV rating is greater than 1pu.

To justify the validity of this assumption, consider the definition of E_L and E_U in (2.11) where it can be seen that their sensitivities to PV rating is approximately the sensitivity of the critical capacities to variations in PV rating. In Section 2.6.2 it is shown that the variations in the critical capacity magnitudes and the total number of critical capacities is small when the PV rating becomes large. Hence for larger PV ratings a small variation in critical capacities results in a small variation in (E_L+E_U) hence their sensitivity, for large PV rating, is small. When storage capacity is small, storage will only contribute a small amount of energy when compared to E_{g0} hence

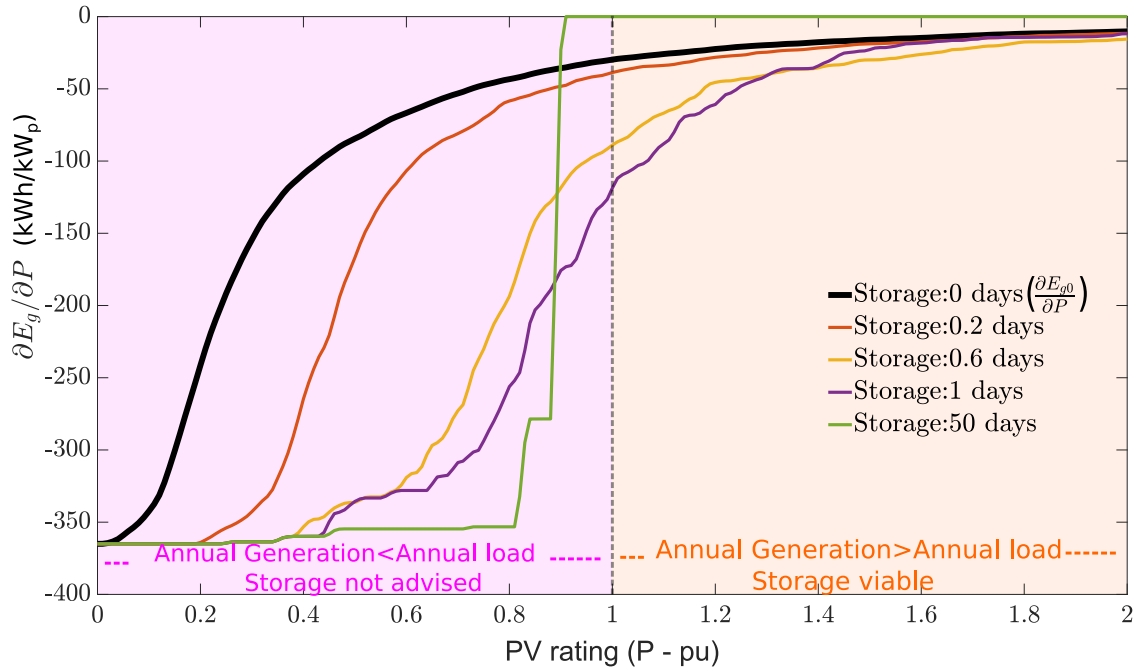

(a)

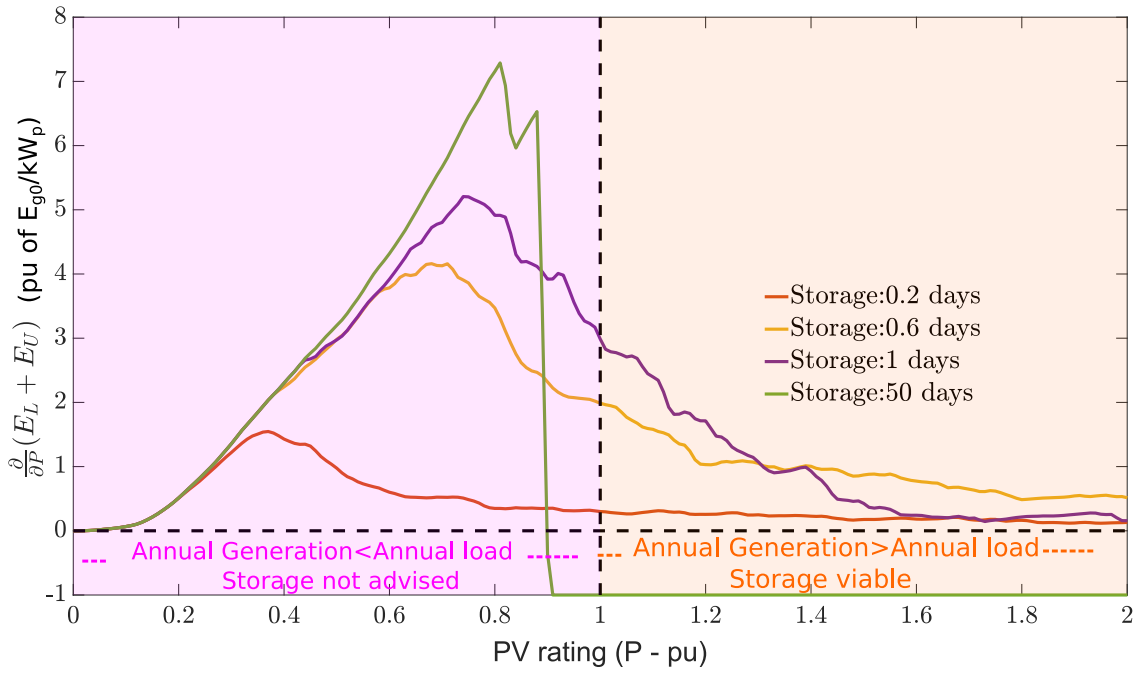

(b)

Figure 4.8: Examples of (4.14), which plots: a) the sensitivity of GSE to PV rating for various storage capacities, b) the sensitivity of the energy supplied by storage $(E_L + E_U)$ to variations in PV rating which is small for both small storage capacities and at large PV ratings

the sensitivity of $(E_L + E_U)$ to variations in PV rating is small for small storage capacities.

The result of this analysis is that the sensitivity of GSE to variations in PV rating in (4.14) is mostly due to the sensitivity of E_{g0} to variations in PV rating. This can be observed by plotting the sensitivity of GSE to variations in PV rating for different storage capacities in Fig. 4.8a and the sensitivity of the energy supplied

by storage $(E_L + E_U)$ to variations in PV rating.

Fig. 4.8a shows that the sensitivity of GSE to variations in PV rating for different storage capacities all have the same trend, i.e. the curve for zero storage could be shifted horizontally to approximate the curves for the other storage capacities. Fig. 4.8b shows that the energy $(E_L + E_U)$ supplied by a given storage capacity only has a major impact, relative to E_{g0}, when the PV rating is small (less than 1pu). However typically no storage or a small amount of storage is considered for small PV ratings since for these ratings the majority of generated energy is used to directly supply the load and there is insufficient excess to store. Note this assumes typical energy usage behavior, since it may be advisable to install storage for low PV ratings, in special cases, such as if the household has regular excess overnight demand.

Hence it is assumed that:

1. Storage installation will usually begin at 1 pu PV rating since at this PV rating annual generation and annual load are equal.

2. The sensitivity of GSE to PV rating curves for different storage capacities in Fig 4.8 all converge towards the curve of no storage capacity. Hence if the actual storage capacity is assumed to increase slowly as PV rating increases then the sensitivity of GSE for the given storage capacity is approximately by the sensitivity for no storage capacity.

Substituting the approximation in (4.14) into (4.13) yields the sensitivity of the benefit to variations in PV rating depending on the sensitivity of E_{g0} to PV rating as follows:

$$\begin{aligned} \frac{\partial B}{\partial P}\Big|_{E_s} &= G_1 c_f - \frac{\partial E_g}{\partial P}\Big|_{E_s}(c_g - c_f) \\ \frac{\partial B}{\partial P}\Big|_{E_s} &\approx G_1 c_f - \frac{\partial E_{g0}}{\partial P}\Big|_{E_s=0}(c_g - c_f) \end{aligned} \tag{4.15}$$

where:

$$E_{g0} = E_g[0, P] \approx \left(\sum_{i=1}^{N} c_i[P]\right)$$

which can be evaluated at the optimal point $[E_{s0}, P_0]$:

$$\frac{\partial B}{\partial P}\Big|_{E_s}[E_{s0}, P_0] \approx G_1 c_f - \frac{\partial E_{g0}}{\partial P}\Big|_{E_s=0}[E_{s0}, P_0](c_g - c_f) \tag{4.16}$$

where:

$$E_{g0} = E_g[0, P_0] \approx \left(\sum_{i=1}^{N[P_0]} c_i[P_0]\right)$$

Note that E_{g0} only depends on the list of critical capacities for a given PV rating.

4.5.3 Defining the n-index Equation and Optimal Storage Capacity for a Given PV Rating

The following is a collation of the various equations used to find the maximum benefit for a given investment:

$$B\big[\mathbf{E_g}[\mathbf{E_s},\mathbf{P}]\big] = P \times G_1 c_f - \mathbf{E_g}[\mathbf{E_s},\mathbf{P}](c_g - c_f) + L(c_g - c_f) \qquad \text{(4.1 Repeated)}$$

$$\left(\frac{\partial B}{\partial E_s}\Big|_P[E_{s0},P_0]\right)\frac{1}{C_E} = \left(\frac{\partial B}{\partial P}\Big|_{E_s}[E_{s0},P_0]\right)\frac{1}{C_P} \qquad \text{(4.8a Repeated)}$$

$$I_0 = P_0 \times C_P + E_{s0} \times C_E \qquad \text{(4.8b Repeated)}$$

where:

$$\frac{\partial B}{\partial E_s}\Big|_P[E_{s0},P_0] = n[P_0](c_g - c_f) \qquad \text{(4.12 Repeated)}$$

$$\frac{\partial B}{\partial P}\Big|_{E_s}[E_{s0},P_0] \approx G_1 c_f - \frac{\partial E_{g0}}{\partial P}\Big|_{E_s}[E_{s0},P_0](c_g - c_f) \qquad \text{(4.16 Repeated)}$$

where for a given PV rating (P_0) the optimal storage capacity (E_0) is found by solving (4.8a) which forms the optimal HES size $[E_{s0},P_0]$, and the investment (I_0) for this HES size is described by (4.8b). Then the maximum benefit B_0, described by (4.1), is found using the GSE at the optimal HES size. Hence the maximum benefit B_0 for the investment I_0 is found and repeating this process for different values of P_0 defines the MBI for a range of investments.

Hence the first step in finding the MBI is to find the optimal storage capacity. The optimal storage capacity can be found by substituting both (4.12) and (4.16) into (4.8a) and then re-arranging for $n[P_0]$. The term $n[P_0]$ discussed in Section 4.5.1 is both: i) the slope of the GSE to storage capacity curve for PV rating P_0, and ii) the n^{th} index in the list of critical capacities for P_0. The conditions on the index n is discussed in Section 4.5.4. The critical capacity at the n^{th} index is the optimal storage capacity for P_0 since the derivation in (4.8a) is for the maximum benefit and hence this index is called the optimal n-index for P_0, i.e. $n_{opt}[P_0]$.

$$\begin{aligned}
\left(\frac{\partial B}{\partial E_s}\Big|_P[E_{s0},P_0]\right)\frac{1}{C_E} &= \left(\frac{\partial B}{\partial P}\Big|_{E_s}[E_{s0},P_0]\right)\frac{1}{C_P} \\
n_{opt}[P_0](c_g - c_f)\frac{1}{C_E} &= \left(G_1 c_f - \frac{\partial E_{g0}}{\partial P}\Big|_{E_s=0}\Big(c_g - c_f\Big)\right)\frac{1}{C_P} \\
n_{opt}[P_0] &= \frac{C_E}{C_P}\frac{S[P_0]}{(c_g - c_f)}
\end{aligned} \qquad (4.17)$$

where:

$$S[P_0] = \left(G_1 + \frac{\partial E_{g0}}{\partial P}\Big|_{E_s=0}\right)c_f - \left(\frac{\partial E_{g0}}{\partial P}\Big|_{E_s=0}\right)c_g$$

The list of critical capacities is sorted in descending order and hence for example if n_{opt} is large then the optimal storage is likely small for that given PV rating.

Table 4.2: Separation of (4.17) into its four parts and each parts effect on the optimal storage capacity

n_{opt}	The optimal index in the critical capacity list for PV rating P_0. The higher the value of n_{opt} the lower the value of optimal storage capacity.
$\frac{C_E}{C_P}$	The cost ratio between the capital cost of storage capacity (C_E) and the capital cost of PV rating (C_P). The more expensive storage is in relation to PV rating the lower the value of optimal storage capacity.
$C_g - C_f$	The difference between grid energy and feed-in tariff. As grid supply price increases with respect to the feed-in tariff the higher the optimal value of storage capacity.
$S[P_0]$	The disincentive to store energy, as discussed below. The higher the value of $S[P_0]$ the lower the value of optimal storage capacity.

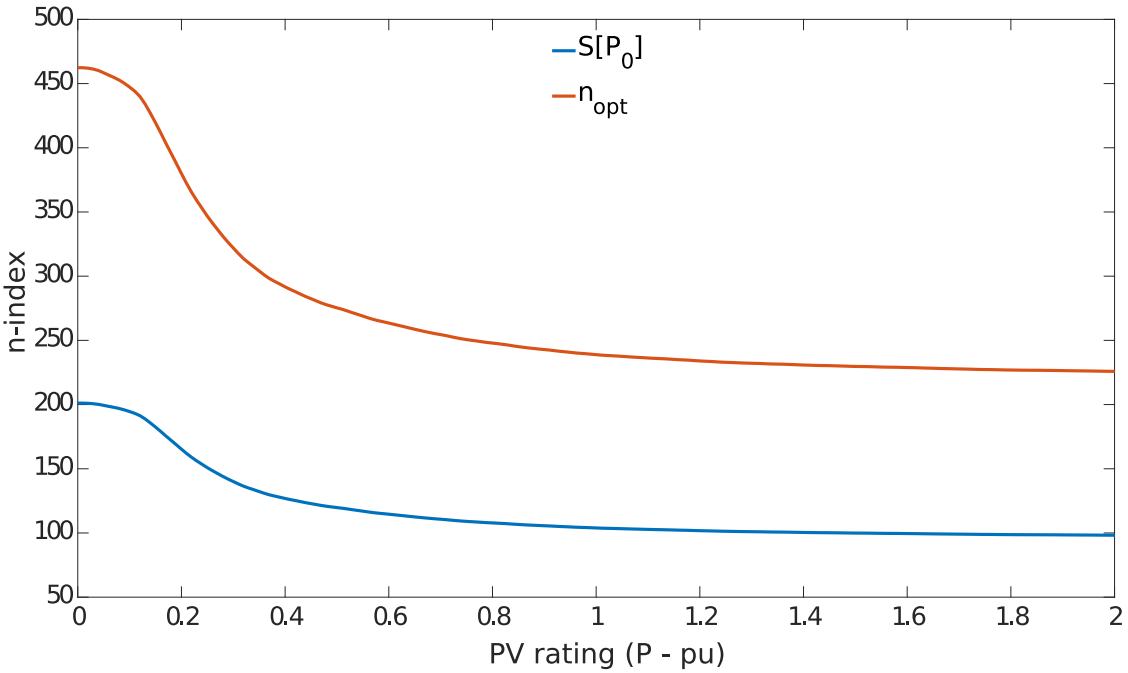

Figure 4.9: The disincentive to store energy $S[P_0]$ versus PV rating. This determines the value of n_{opt} and hence defines the optimal storage capacity. Note the case study data is used with the cost values in Table 1.3 hence 2.3 is the ratio between the two curves.

Equation (4.17) can be separated into four parts and the effect which each part has on the optimal storage capacity is discussed in Table 4.2.

The disincentive to store energy is the key component which defines how the n-index, hence optimal storage capacities, varies for different PV ratings. The $S[P]$ is plotted together with n_{opt} in Fig. 4.9 for a range of PV ratings. Note Fig. 4.9 uses the tariffs, c_f and c_g, from Section 1.6 and the sensitivity of GSE to PV rating from Fig. 4.8.

Hence this disincentive to store energy is directly related to the shape of the n-index versus PV rating curve and it is the only part of the n-index equation which

varies with PV rating since the other two parts are constants.

Calculating optimal storage capacity from optimal index n_{opt}

The n-index equation defines the optimal index n_{opt} at which the optimal storage capacity (E_{opt}) occurs for a given PV rating P_0 and hence from the critical capacities list of $\boldsymbol{C}[P_0] = \{C_1, ..., C_M\}$ the optimal storage capacity is found as follows:

$$E_{opt}[P_0] = C_{n_{opt}}[P_0]$$

Finding the optimal storage capacity is simple when n_{opt} is an integer between one and the critical capacity list length (M). However there are no constraints on the values which n_{opt} can take and hence there are three cases which must be considered:

1. When n_{opt} is not an integer
2. When $n_{opt} > M$, i.e. is greater than the critical capacity list length (M)
3. When $n_{opt} \leq 0$

4.5.4 Three Cases of Optimal n-Index

The first case, where n_{opt} is not an integer, is the most common case since the parameters in the n-index equation (4.17) are typically not integers. A non-integer n_{opt} means that the optimal storage capacity would occur between two adjacent critical capacities. For example consider, for a given PV rating, when $n_{opt} = 2.25$, $C_2 = 4$ days and $C_3 = 2$ days then the optimal storage capacity is 0.25 of the difference between C_2 and C_3, hence the optimal storage capacity is $E_{opt} \approx 3.5$ days.

In general, for non-integer values of n_{opt} the optimal storage capacity occurs between the critical capacity at $\lfloor n_{opt} \rfloor$ (the floor function) and the critical capacity at $\lceil n_{opt} \rceil$ (the ceiling function) such that:

$$E_{opt}[P] \approx C_{\lfloor n_{opt} \rfloor} - (n_{opt} - \lfloor n_{opt} \rfloor) \left(C_{\lfloor n_{opt} \rfloor} - C\lceil n_{opt} \rceil \right) \tag{4.18}$$

The second case occurs when the optimal storage index n_{opt} is greater than the critical capacity list length (M) and hence there is no value which can be indexed. In this case the resulting optimal storage capacity is zero since the last element in the critical capacity list is a storage capacity of zero. A n-index greater than the number of critical capacities suggests a negative optimal storage capacity. However this is not possible. The optimal storage capacity in this case is zero.

The third case, $n_{opt} \leq 0$, typically occurs when $c_g < c_f$ that is when selling energy to the grid provides a greater benefit than storing that energy or supplying

it to the load. Hence in this case, the maximum benefit would be only due to selling all PV generation and hence when $n_{opt} \leq 0$ the optimal storage capacity is also zero.

4.5.5 Advantage of n-estimation method

The n-estimation method is an improvement on previous search-based methods in both computational speed and in the analytical understanding of the factors affecting the MBI. The improved computational speeds in finding the MBI is achieved since, as shown in Fig. 4.4, the n-estimation method uses a closed-form equation to relate GSE to storage capacity for a given PV rating.

The n-estimation method also provides a closed-form equation to estimate the critical capacity list index corresponding to the MBI where the terms in this equation are the cost parameters which is a key advantage of this method. This equation means the sensitivity of the MBI to variations in the cost parameters can be easily computed compared to the search method since calculating the new n-index, finding the new storage and then finding the new benefit is much simpler when compared to searching a new range of HES sizes and making multiple comparisons to find the new MBI.

4.5.6 Summary of n-Estimation Derivation

This concludes the second part of this chapter which focused on deriving an estimation equation for the optimal HES size for a given investment. The result of this deriving is the development of the n-estimation equation (4.17) and the equation for optimal storage capacity (4.18).

The process to find the optimal storage capacity for a given annual load and annual solar irradiation time series is as follows:

Summary of n-estimation method

1. Select a range of PV ratings.
2. For each PV rating find the generation time series from the solar irradiation data.
3. Combine the above the generation time series for each PV rating with the load data and hence find the list of critical capacities for each PV rating.
4. Hence calculated $S[P_0]$ using the definition in (4.17) where E_{g0} which is calculated from the critical capacities.
5. Find the value of n_{opt} using (4.17).
6. The optimal storage capacity is then found for the range of PV rating using (4.18).

The final part of this chapter focuses on validating the n-estimation method

using the case study data and performs a sensitivity study. Details of the sensitivity study is provided in the following section.

4.6 Validating the n-Estimation Method

The n-estimation method is validated by comparing its estimated MBI to the search-based method's MBI. The same case study data from Chapter 3 is used for this comparison. First the base case is used to demonstrate that both methods can produce similar plots for: i) the optimal HES size, and ii) the investment to benefit trade-off. Then three case studies are selected where each case differs from the base case by considering: i) variations in the cost parameters (capital costs and energy tariffs), ii) variation in the load data by considering the load of six different households, and iii) variation in the year of generation data used. These three cases are chosen since they each impact a different part of the n-estimation equation.

4.6.1 Estimating the Base Case MBI

The optimal HES size for the base case is found using both the search method and the n-estimation method in Fig. 4.10. The n-estimation curve is shown to be a close approximation to the search method curve demonstrating both methods have similar optimal HES size, however note the runtime of the search method is an order of magnitude higher than the estimation method, that is if n-estimation has runtime of order N then the search method has runtime of order N^2.

There are two key points in Fig. 4.10, labeled (A) and (B), which are important to the MBI and can be found by both methods. The point labeled (A) is the PV rating at which the household should begin investing in storage and it is observed that for PV ratings below this point then the curves of both methods overlap. The point labeled (B) refers to the HES size at which the household should stop investing into storage and any further investment beyond this point should only go towards increasing the PV rating. It is observed that beyond point (B) the n-estimation method optimal HES sizes overlap with the search-based method optimal sizes. These two points provides the household owner with two easy to understand reference points about the optimal HES sizing under two given investment conditions (when to start and stop storage investment) and the expected benefit/investment at these points.

Between points A and B in Fig. 4.10 the estimated optimal HES sizes is less accurate due to estimation of the sensitivity of GSE due to variations in PV rating. For HES sizes smaller than at point A and larger than at point B, the estimated sensitivity of GSE to variations in PV rating is close to their true values seen in Fig. 4.8. For HES sizes between these points the estimated sensitivity of GSE to variations in PV rating is larger than its true value and this causes a slightly higher

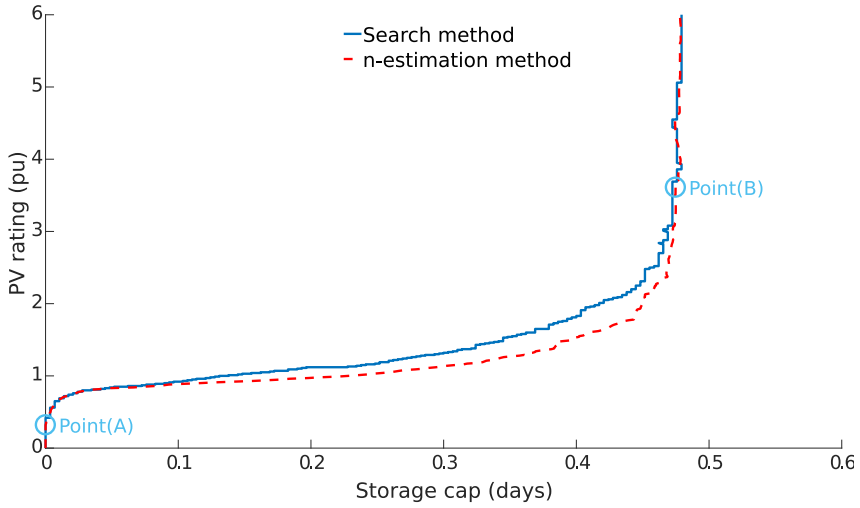

Figure 4.10: Comparison between the optimal HES size determined by the search and n-estimation methods, Note the optimal HES sizes are the combined PV rating and storage capacity which results in the MBI. Each point on the optimal trajectory correspond to an investment $I = C_P \times P + C_E \times E_s$,.

incentive to invest in storage. Hence the n-estimation's maximum benefit, for a given investment, has an optimal HES size comprising a larger storage capacity and a smaller PV rating when compared to the search method's optimal HES size. Hence the n-estimation method will be less accurate if the optimal HES size has a significantly large optimal storage capacity since as shown in Fig. 4.8 the estimate for the sensitivity of GSE to variation in PV rating is less accurate as storage capacity becomes significantly large.

Finding the HES Size at Which to Start and Stop Storage Investment

Both the search method and the n-estimation method can find the PV rating at which investment into storage should begin (point A) and the HES size when investment into further storage capacity is uneconomical (point B). However the n-estimation method is much faster at identifying these points.

Consider the optimal n-index (n_{opt}), which is the reference to the optimal storage capacity in the list of critical capacities, plotted against a range of PV ratings shown in Fig. 4.11 for the search method and the n-estimation method. The search method does not directly find n_{opt} however it does find the optimal storage capacity for a given PV rating which, combined with a list of critical capacities for that PV rating, can find an equivalent to n_{opt}. Note the dashed line labeled $M[P]$ is the total number of critical capacities for each PV rating and the critical capacity list is in descending order, i.e. for a given PV rating the larger the value of n_{opt} the smaller the optimal storage capacity.

In Fig. 4.11, the investment into storage should begin (point A) when the index n_{opt} is less than the number of critical capacities ($M[P]$), since the last element in the list is zero storage capacity and any index larger than the list length represents

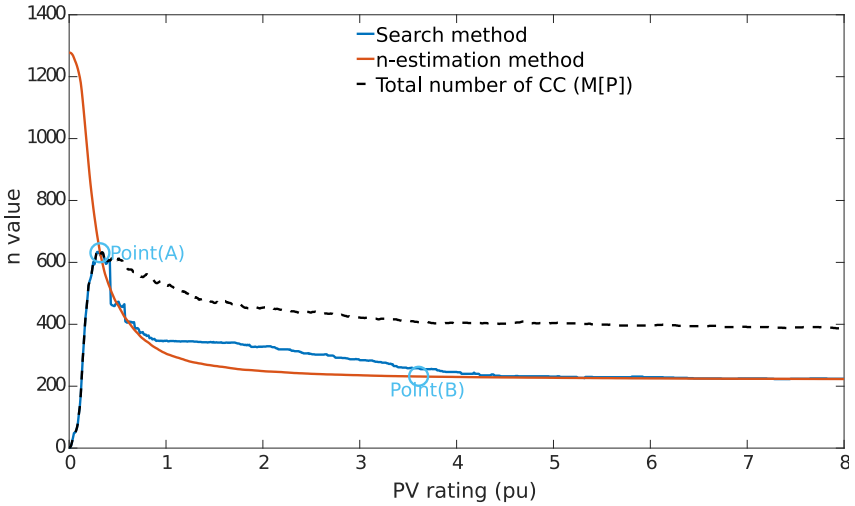

Figure 4.11: Comparing n_{opt} for both the search method and n-estimation method. Point (A) is the PV rating required to begin considering storage investment and Point (B) shows where the investment in storage should stop.

that no amount of storage capacity could improve the benefit. The investment into storage should stop (point B) when the optimal index n_{opt} is no longer influenced by the PV rating, i.e. when an increase in PV rating causes no change in n_{opt}. Finding these two points is possible using the n-estimation method since the n-index equation defines n_{opt} in Fig. 4.11.

Comparing the maximum benefit and investment trade-off for both n-estimation's MBI and search-based MBI

The maximum benefit to investment trade-off is plotted in Fig. 4.12 for the n-estimation and search-based methods, noting that both point (A) and point (B) refers to the same points from Fig. 4.10. Both methods produce nearly overlapping curves in Fig. 4.12 which suggest that the n-estimation method produces similar values of benefit as the search method when used to find the MBI.

In Fig. 4.12 there are two dashed curves, labeled B_h and B_f, which represent the slopes for two different parts of the MBI curve and these two slopes depend on the energy tariffs. The curve labeled B_h describes the benefit to investment if both: i) only PV is installed, and ii) if all generated energy is valued at the grid supply cost of c_g, i.e. if all generated energy could be supplied to the load. The curve B_h has the same slope as the MBI's curve for investment prior to point (A) and hence for investment prior to this point the majority of the benefit is a result of offsetting grid energy at the energy tariff price c_g.

The curve labeled B_f is the benefit to investment relationship if both: i) only PV is installed, and ii) if all generated energy is valued at the feed-in tariff of c_f, i.e. if all generated energy is sold to the grid. The B_f curve has the same slope as the MBI curve for investment greater than I_B since beyond this point the majority of the benefit is a result of GFI. Between the two points, (A) and (B), the benefit

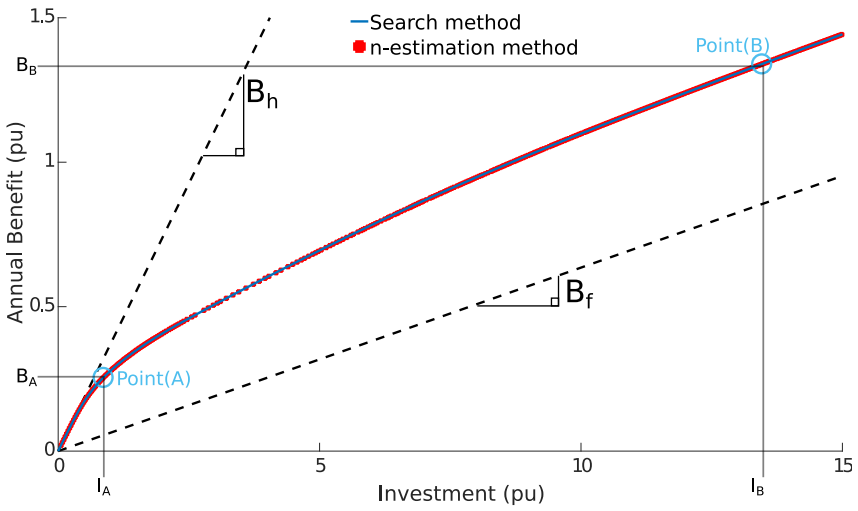

Figure 4.12: The benefit and investment trade-off curve for both the search method and estimation method. Point (A) is when investment begins into storage and point (B) is when investment in storage ends. B_h describes a slope at a rate c_g and B_f describes the slope at a rate c_f.

is provided through the combination of the GEO and GFI.

Sensitivity of the MBI to variation in HES size

The sensitivity of the n-estimation method to variation in HES sizes is examined by plotting in Fig. 4.14 for various contours representing a percentage of the optimal maximum benefit ([99.95, 99, and 95%]). These percentages are represented by two contours on each side of the optimal benefit. For instance in Fig 4.14 the investment I_0 has optimal benefit at the point labeled B_0 and the two points labeled $B_{0.95}$, where I_0 intersects the two 95% contours, represent HES sizes which have 95% of the optimal benefit.

The reason for these two contours is highlighted in Fig 4.13 where for the given investment I_0 the maximum benefit B_0 occurs with HES size $[P_0, E_{s0}]$. For the investment I_0 there are two HES sizes which can achieve 0.95% of this optimal benefit which are: i) $[P_1, E_{s1}]$, and ii) $[P_2, E_{s2}]$.

Fig. 4.14 shows that the benefit in the base case is not that sensitive to small errors in the MBI trajectory and that the n-estimation method's MBI trajectory produces better than 99.5% of the benefit of the optimal trajectory found by the search method. The other percentage contours show the sensitivity of the MBI to variations in the HES size, for example slightly over sizing the storage capacity for a given investment has a smaller impact on the benefit compared to under sizing storage. Note there are two contours for each percentage since the MBI has a convex shape as illustrated in Fig. 4.5.

Comparing the n-estimation method to the searched method in Fig. 4.14 shows the MBI for the estimated HES sizes are within 99.95% of the optimal benefit.

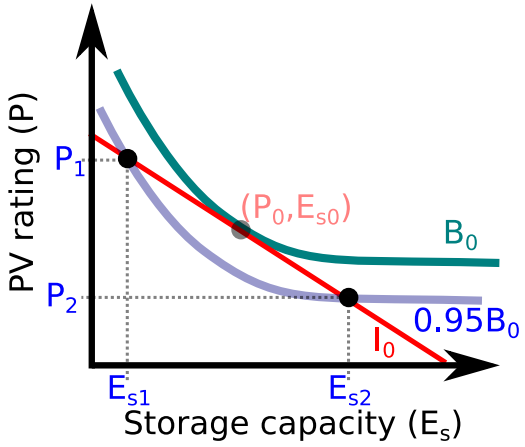

Figure 4.13: For investment I_0 there is one valid solution for optimal benefit B_0 at HES size $[P_0, E_{s0}]$ and two valid solutions for 95% of B_0, one at $[P_1, E_{s1}]$ and the other at $[P_2, E_{s2}]$. These two valid solution describes the two contours for each MBI percentage in Fig. 4.14.

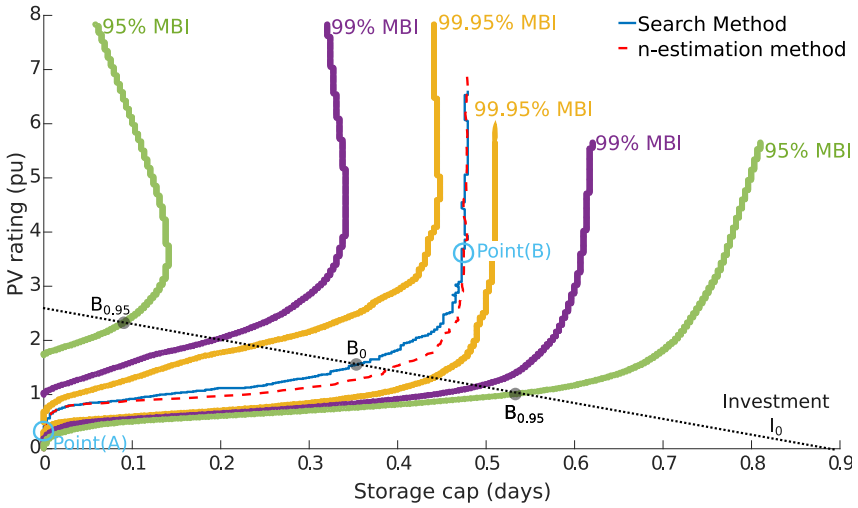

Figure 4.14: The accuracy of the n-estimation method is examined by considering different percentages of the ideal MBI benefit in the PV-E plane.

4.6.2 Sensitivity of the n-estimation Method with Cost Parameter Variations

The n-index equation in (4.17) contains four cost parameters: i) PV capital C_E per kW$_p$, ii) storage capital C_P per kWh, iii) Grid supply tariff c_g, and iv) Grid feed-in tariff c_g. The parameters are highlighted in blue in the following:

$$n_{opt}[P_0] = \frac{\boldsymbol{C_E}}{\boldsymbol{C_P}} \frac{S[P_0]}{(\boldsymbol{c_g} - \boldsymbol{c_f})} \qquad \text{(4.17 Repeated)}$$

where:

$$S[P_0] = \left(G_1 + \frac{\partial E_{g0}}{\partial P}\right) \boldsymbol{c_f} - \left(\frac{\partial E_{g0}}{\partial P}\right) \boldsymbol{c_g}$$

The n-index equation is further validated by comparing the optimal HES sizes and the investment to benefit trade-off for both the search-based method and esti-

mation method for each of the following list of cases where a given cost parameter is changed from the base case:

Case 1: The base case
Case 2: When storage capital is $0.5C_E$
Case 3: When PV capital is $0.5C_P$
Case 4: When grid supply tariff is $2c_g$
Case 5: When grid feed-in is $2c_f$

Fig. 4.15 demonstrates a reasonable agreement between the optimal HES sizes for the search MBI trajectory (solid) and the estimated MBI trajectory (dashed) for each of the cases.

Both case 2 and case 4 has a larger optimal storage capacity than the base case which can be explained using the n-index equation (4.17). The discuss of both cases is as follows:

1. In Case 2 the storage capital cost C_E is halved which results in a lower values of n_{opt} and hence a large value of optimal storage.

2. In Case 4 the GSE price c_g is increased which results in a smaller n_{opt} since both: i) the disincentive to store energy $S[P_0]$ will become smaller when compared to the base case, and ii) the difference between the energy tariffs $(c_g - c_f)$ will reduces the index n_{opt}.

The benefit to investment plot for each case in Fig 4.16 shows agreement between the search method and n-estimation method which validates the n-estimation method for variations in the cost parameters.

Finally the n_{opt} index is examined for each cost parameter change which provides insight into the two key points of: i) point (A), when to begin investing into storage, and ii) point (B), when to stop investing into storage. In Fig. 4.17, rather than showing the points for each case, the regions labeled A and B are used to provide a general range of PV ratings and n_{opt} at these points for all cases. Note for case 3 and case 5 the n_{opt} is always greater than the total length of the critical capacity list $M[P]$ hence no investment is made into storage in these cases. For the base case and case 4 there is minimal change in point (A) however case 2 has a smaller PV rating for point (A) since it has cheaper storage which means it invests into storage at a lower PV rating to achieve maximum benefit. The region labeled B shows that investment into storage should end at approximately the same PV rating for the base case, case 2 and case 4.

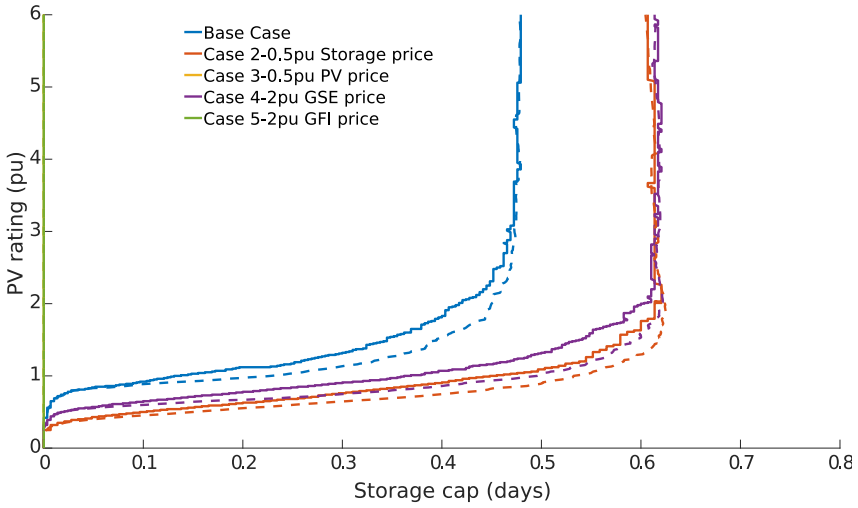

Figure 4.15: The n-estimation method's optimal HES sizes (dashed line) closely approximates the search sizes (solid line) for variations in the cost parameters. Note case 3 and case 5 overlap and are located on the y-axis.

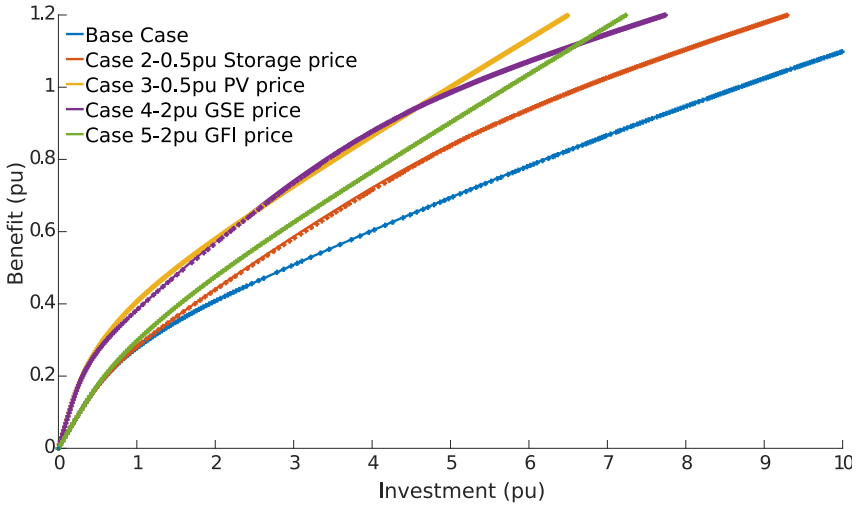

Figure 4.16: The benefit versus investment curve shows close agreement between the n-estimation MBI (dotted line) and search MBI (solid line) for each of the given cost cases. Note due to close agreement between methods their respective curves overlap for each case.

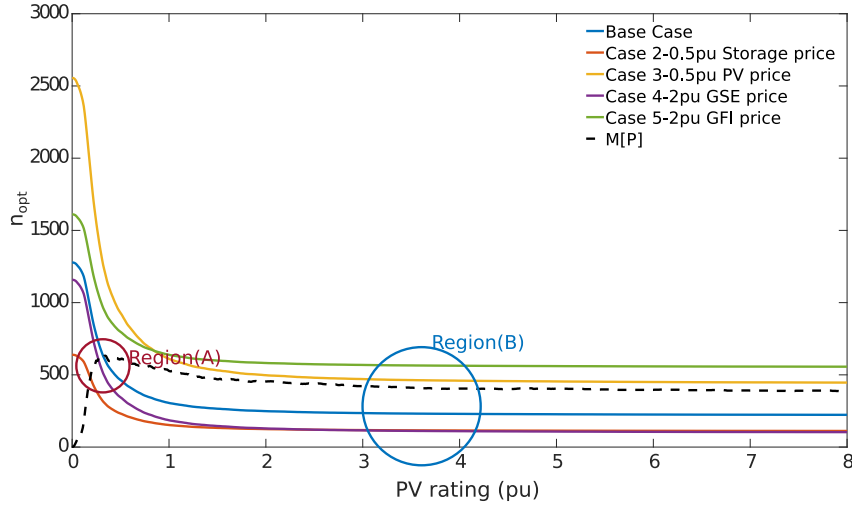

Figure 4.17: For the changes in cost parameters the estimated n_{opt} is plotted against PV rating to demonstrate region A and region B. Note Case 3 and Case 5 does not intersect with the dashed curve (number of critical capacities) and hence storage is not economical for these cases.

4.6.3 Sensitivity of the n-estimation Method with the Load of Various Households

The n-index equation in (4.17) contains two components which depend on the household load: i) the sensitivity of GSE to variations in PV rating, and ii) the list of critical capacities and hence the optimal storage capacity indexed by n_{opt}. The components are highlighted in blue in the following:

$$\boldsymbol{n_{opt}[P_0]} = \frac{C_E}{C_P}\frac{S[P_0]}{(c_g - c_f)} \qquad \text{(4.17 Repeated)}$$

where:

$$S[P_0] = \left(G_1 + \frac{\boldsymbol{\partial E_{g0}}}{\boldsymbol{\partial P}}\right) c_f - \left(\frac{\boldsymbol{\partial E_{g0}}}{\boldsymbol{\partial P}}\right) c_g$$

To validation the n-estimation method for various household loads, six households are selected and the search method's MBI is compared to the n-estimation's MBI. The load duration curve of the six households, labeled H1 to H6, is shown in Fig. 4.18 and each household's total annual load is listed. Further detail on the household daily load behavior is observed in Fig. 1.10. Note Household H3 has the largest annual load and the largest load for 50% of the year while household H2 has the smallest annual load and is the lowest curve in the load duration graphs.

In Fig. 4.19 the optimal HES size for the search method's MBI (solid line) is shown to agree with the estimation method's MBI (dashed line) for each of the different households. Note the PV rating and storage capacity of each household has been normalized by that household's annual load.

Comparing the maximum benefit to investment trade-off for each household in Fig. 4.20 also shows a good agreement between the search method and n-estimation method which verifies that the n-estimation method can provide an accurate MBI trajectory for a range of households with different load profiles.

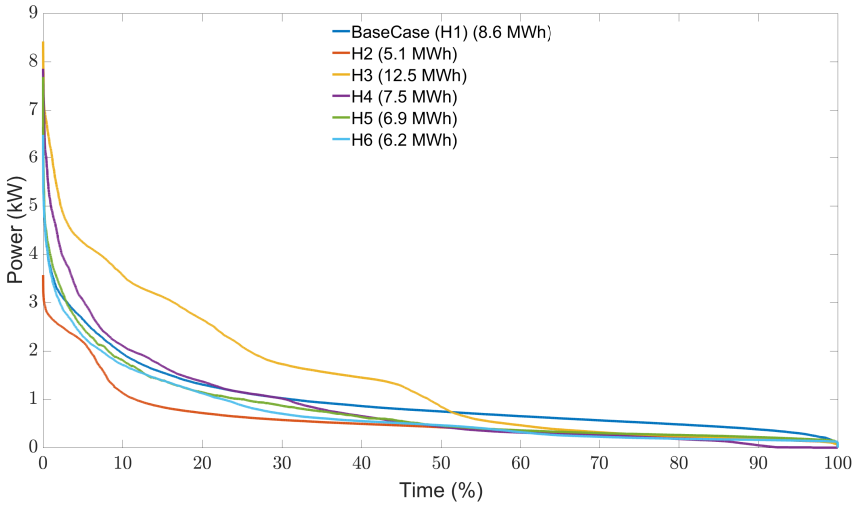

Figure 4.18: Load duration curves for the six household cases.

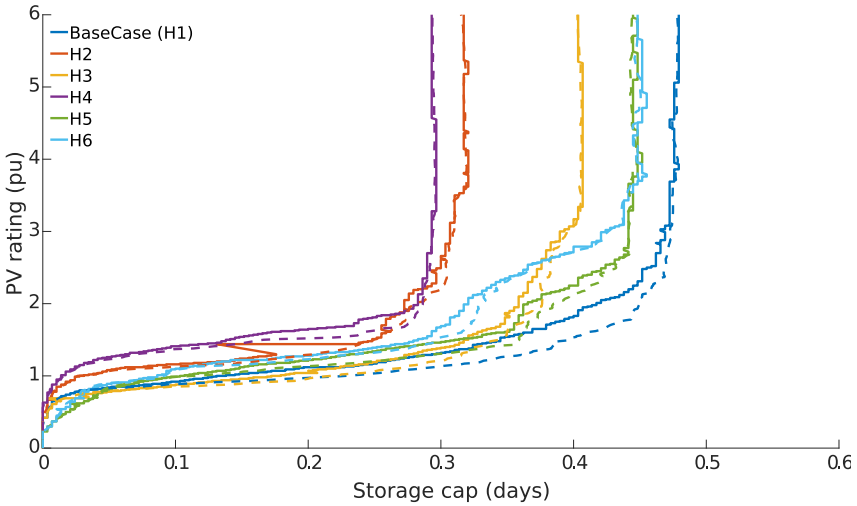

Figure 4.19: For the six households, the optimal HES size for the estimated MBI trajectory (dashed line) is a close approximation to the actual (search) MBI trajectory (solid line).

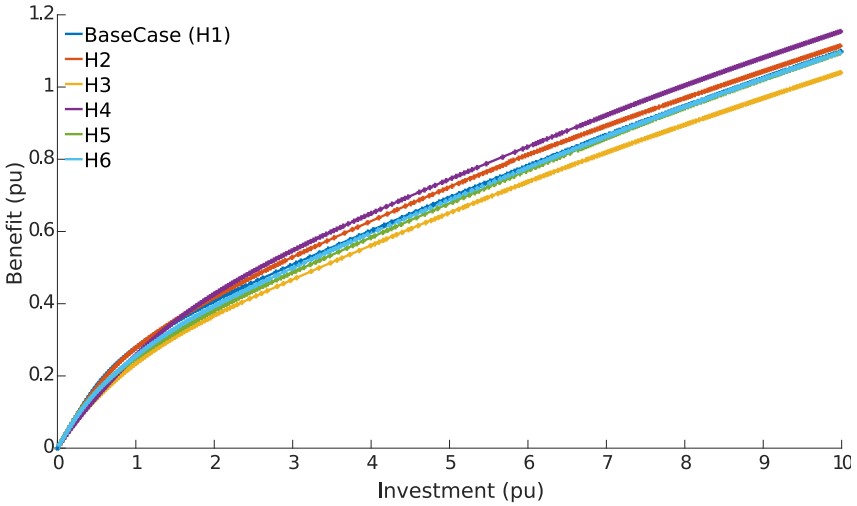

Figure 4.20: Benefit versus investment for the six households, comparing the searched MBI (solid line) and estimated MBI (dotted line).

4.6.4 Sensitivity of the n-estimation Method with Variation in PV Generation

The n-index equation in (4.17) contains three components which depend on the generation time series: i) the annual generation per kW$_p$ of PV (G_1), ii) the list of critical capacities and hence the optimal storage capacity indexed by n_{opt}, and iii) the sensitivity of GSE to variations in PV rating. The components are highlighted in blue in the following:

$$\boldsymbol{n_{opt}[P_0]} = \frac{C_E}{C_P}\frac{S[P_0]}{(c_g - c_f)} \qquad \text{(4.17 Repeated)}$$

where:

$$S[P_0] = \left(\boldsymbol{G_1} + \frac{\boldsymbol{\partial E_{g0}}}{\boldsymbol{\partial P}}\right) c_f - \left(\frac{\boldsymbol{\partial E_{g0}}}{\boldsymbol{\partial P}}\right) c_g$$

To validate the n-estimation method for various generation time series, six different years of generation data is used in combination with the load from the base case. A generation-duration curve for each of the six years of data is shown in Fig. 4.21 and the annual generation G_1 is listed for each year. Overall the generation duration curves have a similar shape, similar annual generation and similar kW/kW$_p$. The only notable difference is that the 2002 year having a slightly higher amount of generation.

For the different years of generation data, the optimal HES size for the search method's MBI and the n-estimation method's MBI shows agreement in Fig. 4.22 and there is also agreement in the benefit to investment trade-off in Fig. 4.23 for the various years of generation data.

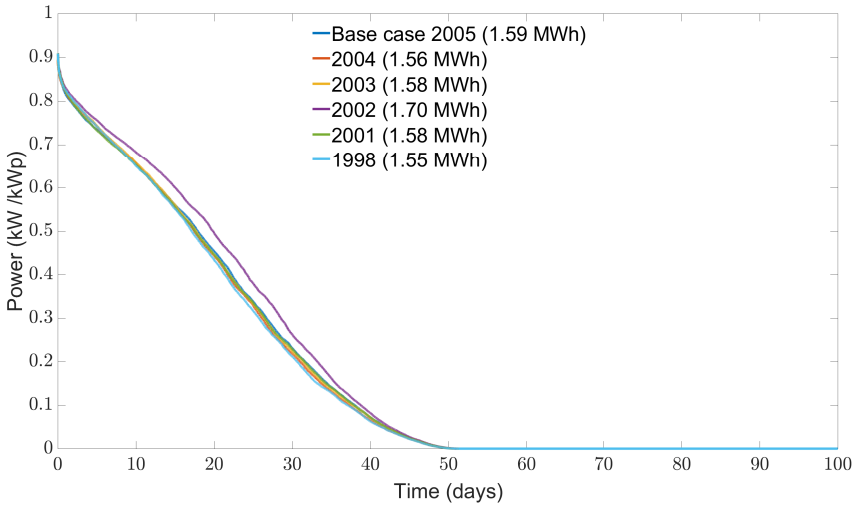

Figure 4.21: Generation duration curves for the six different years of solar irradiation.

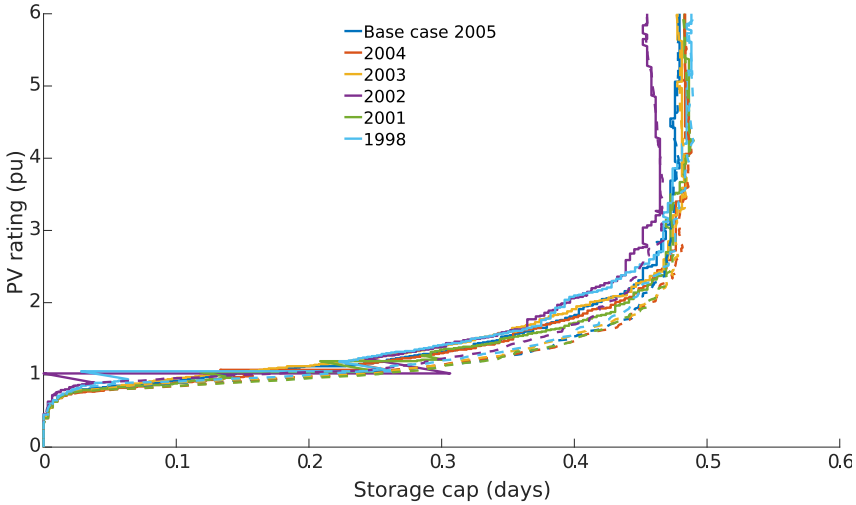

Figure 4.22: For the six years of generation, the optimal HES size (dashed line) for the estimated MBI trajectory is a close approximation to the actual (search) MBI trajectory (solid line).

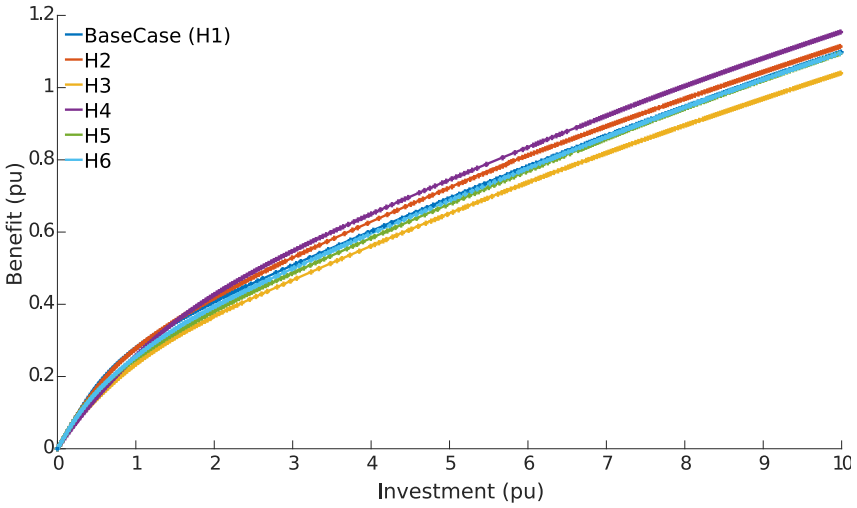

Figure 4.23: Benefit versus investment for the six years of generation, comparing the searched MBI (solid line) and estimated MBI (dotted line) which overlaps for all cases.

Chapter 5

Conclusions and Future Work

5.1 Conclusion

The goal of this thesis was to investigate the optimal sizing of a household energy system (HES), which contains PV generation (P) and energy storage (E_s), to provide the minimise the household's annual energy bill (i.e. maximise the benefit) for a given HES capital investment (maximum benefit for a given investment, MBI). The conventional approach to finding the optimal HES size is to compare the benefit for a number of HES sizes to find the maximum benefit however this provides minimal insight into the sensitivity of the maximum benefit to variations in HES size. A new method is proposed which analytically estimates the optimal HES size and provides greater insight into the maximum benefit. The new method, which depends on a number of simplifying assumptions, can be separated into two parts. The first part is to determine how the HES size affects the energy flow within the HES. The second part is to determine how the energy flows from the grid affects the maximum benefit and hence, when combined with the first part, how the HES size affects the maximum benefit.

A new method, called Critical Capacity Analysis (CCA), was developed in Chapter 2 to understand how the HES size, specifically how the storage capacity, affects the energy flows in the household. The HES size affects the grid energy required to satisfy the household's demand which is a major influence on the maximum benefit. The foundation of CCA is the recognition in this thesis that there is a piece-wise linear relationship between the storage capacity and the grid-sourced energy (hence benefit). The canonical form of a piece-wise linear function can be used to derive a closed-form relationship between storage capacity and grid-sourced energy. This equation depends on two key properties of a piece-wise linear function which are: i) its linear segments, and ii) its breakpoints. In a piecewise-linear plot the linear segments are lines of constant slope and the breakpoints are the points of intersection between two linear segments, where the slope changes. The CCA method provides an algorithm to find these breakpoints, which it calls critical capacities, for a given generation and load time-series.

A key property of CCA is that the number of critical capacities is equal to the number of time periods in the year when the net generation time series (difference of generation and load) is negative, hence for a typical year there is expected to be a minimum of 365 critical capacities due to the day/night cycle.

The CCA has computational benefits over the conventional method, where for $N \times N$ HES sizes the computation time using the CCA method is of approximately order N while the conventional method is of order N^2.

The key outcomes of the CCA method are two equations which are used to derive an estimation of the maximum benefit for a given investment. These two equations are:

1. The closed-form GSE equation for the grid-sourced energy in terms of storage

capacity for a given PV rating.

2. The decomposition of the GSE equation which describes the relationship between grid-sourced energy and the PV rating for a given storage capacity.

In Chapter 4 the maximum benefit for a given investment (MBI) is formulated as an optimisation problem where: i) the benefit is the function being maximised; ii) the constraint is the investment, and iii) the HES size is the variable. The trajectory of optimal HES size due to variations in capital investment (i.e. MBI trajectory) is found using the conventional search-based approach. This is done by selecting a number of HES sizes for a given capital investment, calculating the benefit at each HES size and searching the resulting benefits for the maximum. This procedure is repeated for a range of capital investments. An alternative approach, called the n-index estimation, is developed to provide a faster means of estimating the MBI trajectory using only the critical capacities for a range of PV ratings. The estimation method allows rapid calculation of the sensitivity of the MBI and optimal HES size to variations in the capital cost of PV and storage, and the grid energy and feed-in tariffs.

5.2 Future Work

Two areas of future work are identified:

1. Improvement of CCA to allow time-of-use analysis.

2. Application of CCA to a large power system case, such as the South Australian power system

5.2.1 CCA and Time of Use Analysis

In Chapter 4 the price of energy from the grid was assumed constant regardless of the time of day, which is standard for most households in South Australia. In the future 'time of use" tariffs will be more common, whereby the price of energy may change depending on time, typically defined by a peak time and an off-peak time. Typically peak times are defined by high demand for energy e.g. during the early evening, and the off-peak time is defined by low demand for energy. It is also possible that the household may be charged an additional fee based on their maximum power demand during specific times. These conditions add a higher degree of complexity to the overall sizing problem, since the relation between the storage capacity and the benefit obtained from storage (for a given PV rating) would vary depending on the time, e.g. applying a storage capacity of 1 kWh during an off-peak time would be of smaller benefit than during a peak time.

If CCA is adapted to include time of use tariffs, it may be possible to provide insight into how these tariffs affect the optimal HES size. The key feature of CCA is to identify loops in the power-energy plane and the resulting time series which occur would provide a means to include time of use information in the trade-off curve between storage capacity and grid energy offset GEO .

5.2.2 CCA and the South Australian Power System

The key elements of a HES could be considered as a simplified representation of the South Australian (SA) power system. The parallels between the devices installed in the HES and their corresponding equivalence in the SA power system is seen in Table 5.1. For example a household's PV generation time series is equivalent to the aggregation of all intermittent generation in the SA power system scenario. Note for the HES that the usage of the grid connection is separated into providing a sink for excess power (feed-in) and a source of power (grid sourced). In the power system case there is a slight difference between energy supplied to/from the SA power system as shown in Table 5.1.

Table 5.1: Comparison between HES and the SA power system

HES	**SA Power System**
Energy storage	Energy storage
PV system	Intermittent generators (e.g. wind/PV etc)
Grid Connection (energy from the grid)	Fossil fueled generators and power supplied from other states through interconnectors
Grid Connection (energy to the grid, feed-in)	Power supplied to other states through interconnectors

Note to find the maximum benefit and optimal HES sizing of the SA power system would require CCA to be usable with time-varying tariffs as the price of energy for the SA power system would depend on time. However, determining the storage requirements for a given renewable generation capacity does not require time-varying tariffs.

The analysis of the SA power system would examine the trade-off between: i) the energy required from the combination of the conventional generation and the interconnectors, and ii) the energy storage requirement. The use of CCA could provide a faster means to evaluate a number of future grid scenarios where the amount of intermittent generation increases and also provides insights to aid in predicting the benefits that increased levels of storage would have on the system.

Bibliography

Note the number(s) at the end of a entry is the page that entry appears in this thesis.

[1] "Residential solar PV system prices for September 2017 - Solar Choice," https://www.solarchoice.net.au/blog/residential-solar-system-prices-september-2017, Sep. 2017. 2

[2] SolarChoice, "What are the best cities for home solar battery storage? (August 2017 update)," https://www.solarchoice.net.au/blog/best-australian-city-for-battery-storage-2017, Aug. 2017. 2

[3] Origin Energy, "Solar Batteries & Tesla powerwall," https://www.originenergy.com.au/for-home/solar/systems-batteries/tesla-powerwall.html, Sep. 2017. 2

[4] D. M. Greenwood, N. S. Wade, P. C. Taylor, P. Papadopoulos, and N. Heyward, "A Probabilistic Method Combining Electrical Energy Storage and Real-Time Thermal Ratings to Defer Network Reinforcement," *IEEE Transactions on Sustainable Energy*, vol. 8, no. 1, pp. 374–384, Jan. 2017. 7, 8, 9, 11, 14, 15, 31, 32

[5] Y. K. SUN, Q. DING, H. XING, P. P. ZENG, and F. F. SUN, "Optimal Placement and Sizing of Grid-scale Energy Storage in Distribution Networks with Security Constrains," in *2018 International Conference on Power System Technology (POWERCON)*, Nov. 2018, pp. 1477–1482. 7, 8, 9, 11

[6] G. Pulazza, N. Zhang, C. Kang, and C. A. Nucci, "Transmission Planning With Battery-Based Energy Storage Transportation For Power Systems With High Penetration of Renewable Energy," *IEEE Transactions on Power Systems*, vol. 36, no. 6, pp. 4928–4940, Nov. 2021. 7, 8, 9, 11

[7] E. Tsioumas, N. Jabbour, M. Koseoglou, D. Papagiannis, and C. Mademlis, "Enhanced Sizing Methodology for the Renewable Energy Sources and the Battery Storage System in a Nearly Zero Energy Building," *IEEE Transactions on Power Electronics*, vol. 36, no. 9, pp. 10 142–10 156, Sep. 2021. 7, 8, 11

[8] M. R. Narimani, B. Asghari, and R. Sharma, "Optimal Sizing and Operation of Energy Storage for Demand Charge Management and PV Utilization," in *2018 IEEE/PES Transmission and Distribution Conference and Exposition (T D)*, Apr. 2018, pp. 1–5. 7, 8, 11

[9] K. Koiwa, K.-Z. Liu, and J. Tamura, "Analysis and Design of Filters for the Energy Storage System: Optimal Tradeoff Between Frequency Guarantee and Energy Capacity/Power Rating," *IEEE Transactions on Industrial Electronics*, vol. 65, no. 8, pp. 6560–6570, Aug. 2018. 7, 8, 11

[10] J. Martinez-Rico, I. R. de Argandoña, E. Zulueta, U. Fernandez-Gamiz, and M. Armendia, "Energy Storage Sizing Based on Automatic Frequency Restoration Reserve Market Participation of Hybrid Renewable Power Plants," in *2021 International Conference on Smart Energy Systems and Technologies (SEST)*, Sep. 2021, pp. 1–6. 8, 11, 12

[11] A. Bera, M. Abdelmalak, S. Alzahrani, M. Benidris, and J. Mitra, "Sizing of Energy Storage Systems for Grid Inertial Response," in *2020 IEEE Power Energy Society General Meeting (PESGM)*, Aug. 2020, pp. 1–5. 8, 11, 13

[12] H. Bitaraf, S. Rahman, and M. Pipattanasomporn, "Sizing Energy Storage to Mitigate Wind Power Forecast Error Impacts by Signal Processing Techniques," *IEEE Transactions on Sustainable Energy*, vol. 6, no. 4, pp. 1457–1465, Oct. 2015. 8, 11

[13] B. S. Borowy and Z. M. Salameh, "Methodology for optimally sizing the combination of a battery bank and PV array in a wind/PV hybrid system," *Energy conversion, ieee transactions on*, vol. 11, no. 2, pp. 367–375, 1996. 8, 11, 31, 32

[14] H. Delavaripour, H. Karshenas, A. Bakhshai, and P. Jain, "Optimum battery size selection in standalone renewable energy systems," in *Telecommunications Energy Conference (INTELEC), 2011 IEEE 33rd International*, Oct. 2011, pp. 1–7. 8, 11, 14, 15, 31

[15] Z. Y. Gao and P. Wang, "Reliability evaluation of power systems with WTGs and energy storage," in *IPEC, 2010 Conference Proceedings*. IEEE, 2010, pp. 654–659. 8, 11, 15, 31, 33, 34

[16] Z. Guo, W. Wei, L. Chen, M. Shahidehpour, and S. Mei, "Economic Value of Energy Storages in Unit Commitment With Renewables and Its Implication on Storage Sizing," *IEEE Transactions on Sustainable Energy*, vol. 12, no. 4, pp. 2219–2229, Oct. 2021. 8, 11, 13

[17] S. Guo, A. Kurban, Y. He, F. Wu, H. Pei, and G. Song, "Multi-objective sizing of solar-wind-hydro hybrid power system with doubled energy storages under

optimal coordinated operation strategy," *CSEE Journal of Power and Energy Systems*, pp. 1–11, 2021. 8, 11

[18] D. Sidorov, Q. Tao, I. Muftahov, A. Zhukov, D. Karamov, A. Dreglea, and F. Liu, "Energy balancing using charge/discharge storages control and load forecasts in a renewable-energy-based grids," in *2019 Chinese Control Conference (CCC)*, Jul. 2019, pp. 6865–6870. 8, 11

[19] M. T. Elsir, M. A. Abdulgalil, A. T. Al-Awami, and M. Khalid, "Sizing and Allocation for Solar Energy Storage System Considering the Cost Optimization," in *2019 8th International Conference on Renewable Energy Research and Applications (ICRERA)*, Nov. 2019, pp. 407–412. 8, 11, 12

[20] F. Zhang, G. Wang, K. Meng, J. Zhao, Z. Xu, Z. Y. Dong, and J. Liang, "Improved Cycle Control and Sizing Scheme for Wind Energy Storage System Based on Multiobjective Optimization," *IEEE Transactions on Sustainable Energy*, vol. 8, no. 3, pp. 966–977, Jul. 2017. 8, 11

[21] L. Tian, J. Guo, and L. Cheng, "A novel method for energy storage sizing based on time and frequency domain analysis," in *2016 International Conference on Probabilistic Methods Applied to Power Systems (PMAPS)*, Oct. 2016, pp. 1–6. 8, 11

[22] J. Li, W. Wei, and J. Xiang, "A Simple Sizing Algorithm for Stand-Alone PV/Wind/Battery Hybrid Microgrids," *Energies*, vol. 5, no. 12, pp. 5307–5323, Dec. 2012. 8, 11, 31, 32

[23] L. H. Koh, G. Z. Yong, W. Peng, and K. J. Tseng, "Impact of Energy Storage and Variability of PV on Power System Reliability," *Energy Procedia*, vol. 33, pp. 302–310, 2013. 8, 11, 14, 31

[24] J. M. Santos, P. S. Moura, and A. T. de Almeida, "Technical and economic impact of residential electricity storage at local and grid level for Portugal," *Applied Energy*, vol. 128, pp. 254–264, Sep. 2014. 8, 11, 31

[25] U. B. Irshad, M. S. H. Nizami, S. Rafique, M. J. Hossain, and S. C. Mukhopadhyay, "A Battery Energy Storage Sizing Method for Parking Lot Equipped With EV Chargers," *IEEE Systems Journal*, vol. 15, no. 3, pp. 4459–4469, Sep. 2021. 8, 9, 11

[26] V. Sharma, M. H. Haque, and S. M. Aziz, "Annual Electricity Cost Minimization for South Australian Dwellings through Optimal Battery Sizing," in *2019 IEEE Milan PowerTech*, Jun. 2019, pp. 1–6. 8, 9, 11, 16

[27] R. Khezri, A. Mahmoudi, and M. H. Haque, "Optimal Capacity of PV and BES for Grid-connected Households in South Australia," in *2019 IEEE Energy Conversion Congress and Exposition (ECCE)*, Sep. 2019, pp. 3483–3490. 8, 11

[28] L. Zhou, Y. Zhang, K. Li, and X. Xie, "Optimal Sizing of PV System and BESS for Smart Household under Stepwise Power Tariff," in *2018 International Conference on Power System Technology (POWERCON)*, Nov. 2018, pp. 1314–1319. 8, 11, 12

[29] F. Hafiz, D. Lubkeman, I. Husain, and P. Fajri, "Energy Storage Management Strategy Based on Dynamic Programming and Optimal Sizing of PV Panel-Storage Capacity for a Residential System," in *2018 IEEE/PES Transmission and Distribution Conference and Exposition (T D)*, Apr. 2018, pp. 1–9. 8, 11

[30] C. Park, V. Knazkins, F. S. Sevilla, P. Korba, and J. Poland, "On the estimation of an optimum size of Energy Storage System for local load shifting," in *2015 IEEE Power Energy Society General Meeting*, Jul. 2015, pp. 1–5. 8, 11

[31] H. Shin and J. Hur, "Optimal Energy Storage Sizing With Battery Augmentation for Renewable-Plus-Storage Power Plants," *IEEE Access*, vol. 8, pp. 187 730–187 743, 2020. 8, 11

[32] M. Li, L. Wang, Y. Wang, and Z. Chen, "Sizing Optimization and Energy Management Strategy for Hybrid Energy Storage System Using Multiobjective Optimization and Random Forests," *IEEE Transactions on Power Electronics*, vol. 36, no. 10, pp. 11 421–11 430, Oct. 2021. 8, 9, 11

[33] S. Majumder, S. A. Khaparde, A. P. Agalgaonkar, P. Ciufo, S. Perera, and S. V. Kulkarni, "DFT-Based Sizing of Battery Storage Devices to Determine Day-Ahead Minimum Variability Injection Dispatch With Renewable Energy Resources," *IEEE Transactions on Smart Grid*, vol. 10, no. 1, pp. 626–638, Jan. 2019. 8, 11, 13

[34] P. Arun, "Sizing Curve for Isolated Photovoltaic-Battery Systems using Artificial Neural Networks," in *2018 2nd International Conference on Green Energy and Applications (ICGEA)*, Mar. 2018, pp. 147–151. 8, 11

[35] T. Kerdphol, Y. Qudaih, and Y. Mitani, "Battery energy storage system size optimization in microgrid using particle swarm optimization," in *IEEE PES Innovative Smart Grid Technologies, Europe*, Oct. 2014, pp. 1–6. 8, 11

[36] T. Jiang, H. Chen, X. Li, R. Zhang, X. Kou, and F. Li, "Optimal Sizing and Operation Strategy for Hybrid Energy Storage Systems Considering Wind Uncertainty," in *2018 IEEE Power Energy Society General Meeting (PESGM)*, Aug. 2018, pp. 1–5. 8, 11

[37] K. Baker, G. Hug, and X. Li, "Energy Storage Sizing Taking Into Account Forecast Uncertainties and Receding Horizon Operation," *IEEE Transactions on Sustainable Energy*, vol. 8, no. 1, pp. 331–340, Jan. 2017. 8, 11

[38] I. N. Moghaddam and B. Chowdhury, "Optimal sizing of Hybrid Energy Storage Systems to mitigate wind power fluctuations," in *2016 IEEE Power and Energy Society General Meeting (PESGM)*, Jul. 2016, pp. 1–5. 8, 11

[39] L. Chua and S. M. Kang, "Section-wise piecewise-linear functions: Canonical representation, properties, and applications," *Proceedings of the IEEE*, vol. 65, no. 6, pp. 915–929, Jun. 1977. 14, 33, 34

[40] D. M. W. Leenaerts and W. M. G. van Bokhoven, *Piecewise Linear Modeling and Analysis*. New York; London: Springer, 1998. 14, 33, 34

[41] Endo Tatsuo, "Damage Evaluation of Metals for Random or Varying loading," in *Proceedings Of The 1974 Symposium On Mechanical Behaviour Of Materials*, vol. 1. Society of Material Science, 1974, pp. 371–380. 16, 31, 38

[42] C. Amzallag, J. P. Gerey, J. L. Robert, and J. Bahuaud, "Standardization of the rainflow counting method for fatigue analysis," *International Journal of Fatigue*, vol. 16, no. 4, pp. 287–293, Jun. 1994. 16, 38

[43] I. Rychlik, "A new definition of the rainflow cycle counting method," *International Journal of Fatigue*, vol. 9, no. 2, pp. 119–121, Apr. 1987. 16, 51

[44] Y. Yang, S. Bremner, C. Menictas, and M. Kay, "Battery energy storage system size determination in renewable energy systems: A review," *Renewable and Sustainable Energy Reviews*, vol. 91, pp. 109–125, Aug. 2018. 16

[45] Y. Ru, J. Kleissl, and S. Martinez, "Storage Size Determination for Grid-Connected Photovoltaic Systems," *IEEE Transactions on Sustainable Energy*, vol. 4, no. 1, pp. 68–81, Jan. 2013. 16

[46] H. Hesse, R. Martins, P. Musilek, M. Naumann, C. Truong, and A. Jossen, "Economic Optimization of Component Sizing for Residential Battery Storage Systems," *Energies*, vol. 10, p. 835, Jun. 2017. 16

[47] R. Arghandeh, J. Woyak, A. Onen, J. Jung, and R. P. Broadwater, "Economic optimal operation of Community Energy Storage systems in competitive energy markets," *Applied Energy*, vol. 135, pp. 71–80, 2014. 16

[48] Department of Industry, "Smart-Grid Smart-City Customer Trial Data," https://data.gov.au/dataset/smart-grid-smart-city-customer-trial-data. 20, 24

[49] Australian Government Bureau of Meteorology, "About the one minute solar data product," http://www.bom.gov.au/climate/data/oneminsolar/about-IDCJAC0022.shtml. 20

[50] National Renewable Energy Laboratory. Golden, CO, "System Advisor Model Version 2015.1.30 (SAM 2015.1.30)," https://sam.nrel.gov/content/downloads, Mar. 2015. 20

[51] K. Bataineh and D. Dalalah, "Optimal Configuration for Design of Stand-Alone PV System," *Smart Grid and Renewable Energy*, vol. 03, no. 02, pp. 139–147, 2012. 31

[52] V. Sharma, M. H. Haque, and S. M. Aziz, "Energy cost minimization for net zero energy homes through optimal sizing of battery storage system," *Renewable Energy*, vol. 141, pp. 278–286, Oct. 2019. 32

[53] A. T. C. de Freitas Silva, "Design of the storage capacity of artificial reservoirs," Ph.D. dissertation, University of Libson, 2010. 37, 44, 45

[54] B. Alamri and A. Alamri, "Technical review of energy storage technologies when integrated with intermittent renewable energy," in *SUPERGEN*, Apr. 2009, pp. 1–5. 38

[55] M. Chawla, R. Naik, R. Burra, and H. Wiegman, "Utility energy storage life degradation estimation method," in *2010 IEEE Conference on Innovative Technologies for an Efficient and Reliable Electricity Supply*, Sep. 2010, pp. 302–308. 38

[56] Adam Nieslony, "Rainflow Counting Algorithm - File Exchange - MATLAB Central," Apr. 2010. 53

Appendix A

Defining the Rules-based Approach to Identify Critical Capacities

The rules-based method was summarised in Section 2.4.1 using both an example time series and a discussion on how each rule was applied to determine the Critical Capacities in the provided example. The following will discuss how each rule identifies the critical capacity and are validated by comparing the GSE at different storage capacities using: i) the critical capacities found by the rule and ii) the simulation of the state of charge (SoC) for each storage capacity.

The rules can be categorised into two main groups, rule 1 which identifies critical capacities which originate from the need to supply future loads, and rule 2 which identifies critical capacities which originate, only after applying rule 1, from the need to transfer energy forward. The rules were developed from the notion that the net generation time series required two passes to identify how it and storage can cause GSE. The first pass examines how the load causes GSE and the second pass examines how the generation causes GSE.

Note in the development of the rules-based method, the storage capacity is assumed to start empty which is different from the assumptions listed in Section 1.6. However this does not affect the development of the rules.

A full-page summary of the five rules is shown in Fig. 2.17 in Section 2.4.1.

A.1 Rules Development: Example time series

The example power and energy time series from Section 2.4.1 is shown in Fig. A.1. The net generation power time series is integrated to produce the net generated energy time series. In Section 2.4.1 the Rippl's method was used to separate the net generation energy time series into six segments shown in Fig. A.1b.

The first four periods are used to demonstrate the five rules; note Period four demonstrates two rules which must exist together. The final two periods (five and six)

A.2 Period One

The first rule (Rule 1a) is demonstrated using the first period, Fig. A.2a, from the example net generation power time series.

The first period contains a single interval of positive net generation (20 kW) and a single interval of negative net generation (10 kW). Since the net generation time series assumes a constant power for each one hour interval, the power time series can be expressed as a row matrix (called the power row matrix) of [20 -10] kW where each element represents the average power in a given hour. This representation allows the example to be discussed using simple operations on a row matrix rather than using operations on the time-series.

The base rule (Rule 1a) states that for a period containing one positive and one negative interval the critical capacity is the energy within the negative interval, for

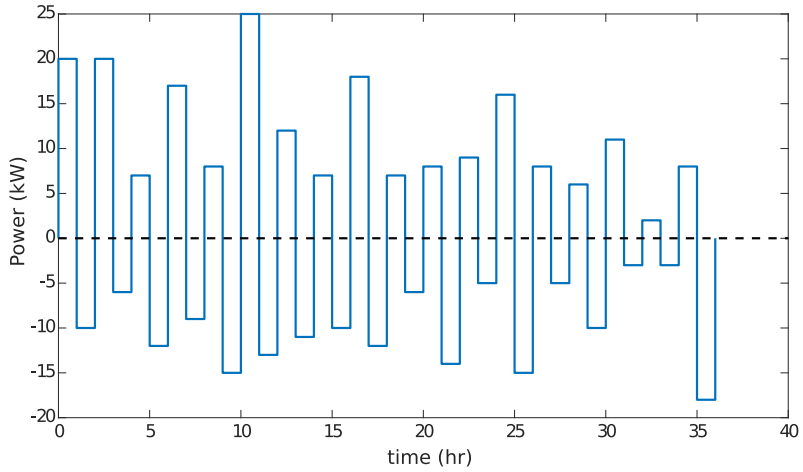

(a)

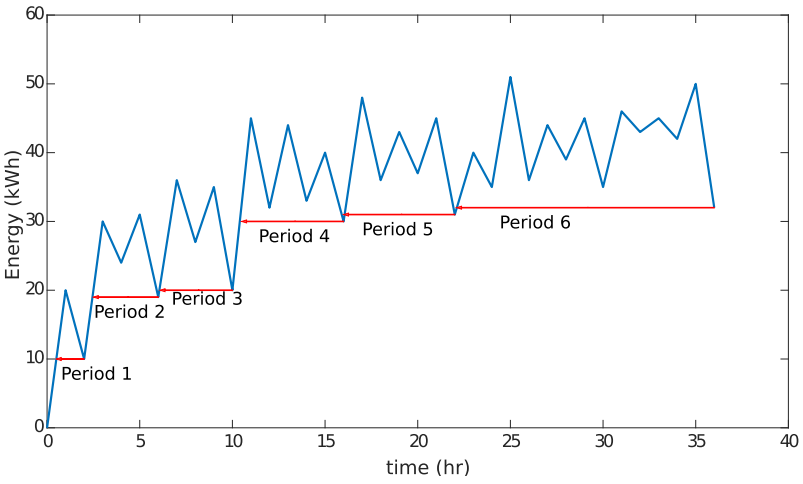

(b)

Figure A.1: (Fig. 2.16 Repeated) Example time series for the rules based approach, a) net generation power time series, b) net generated energy time series

this example it is 10 kWh. This rule is validated using the SoC simulation for three storage capacities (10 kWh, 9 kWh, 8kWh) in Fig. A.2b. Note the dotted line shows where and the amount of GSE (negative energy) which would occur for the given storage capacities.

When the storage capacity is equal to the critical capacity (10 kWh) then no GSE occurs. For storage capacities below the critical capacity the GSE is shown by the dotted lines where the GSE is the difference between the storage capacity and the critical capacity. For example the 9 kWh storage capacity has 1 kWh of GSE and the 8 kWh has 2 kWh of GSE. The source of the GSE for storage capacities below 10 kWh is a result of storage being unable to store sufficient energy before the load at time of one hr.

Rule 1a. For a simple period of only one negative interval, the critical capacity is the energy within the negative interval.

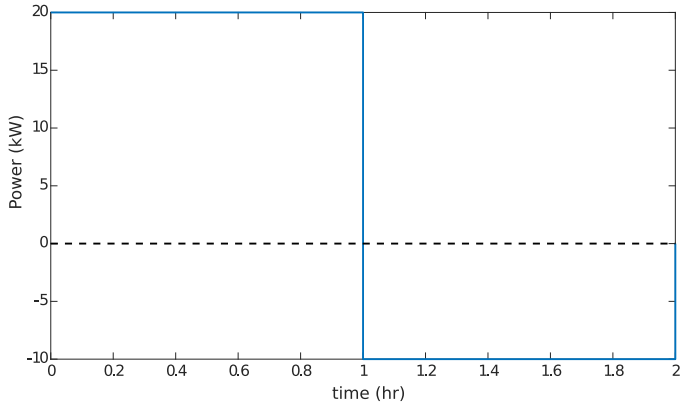

(a)

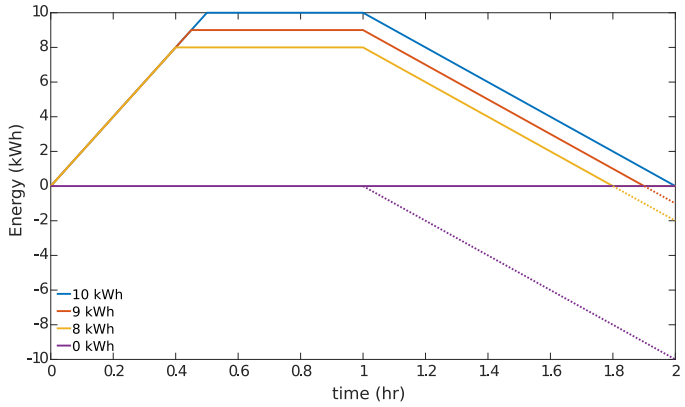

(b)

Figure A.2: Example period 1

A.3 Period Two

The second period, represented by its power row matrix [20 -6 7 -12] kW, has two negative intervals and two positive intervals where each interval is an element in the row matrix. For periods containing two or more positive and negative intervals, the critical capacities are found by integrating the net generation power from the end of the period to the start of the period and this process is called the reverse integral. This reverse integral can also be written as an energy row matrix similar to the power row matrix. By starting the integral at the end of the time series this reverse integral represents the deficit (negative reverse integral) or surplus (positive reverse integral) in energy at a given time in the interval and the time at the end of that period. A deficit at a given time in the reverse integral represents that energy is required from earlier in the period to supply the load between the given time and the end of the period. A surplus represents that there is sufficient energy between a the given time and the end of the period such that no energy is required from an earlier time to the supply the load.

The purpose of the reverse integral is to find the largest deficit which represents the required storage capacity to ensure load within the period can be supplied by storing the generated energy. The time of the largest deficit, called the negative-critical time, is also significant since there may be a further critical capacities in both

the time prior to and the after the time of largest deficit. Note for each period, the total generated energy equals the total demanded load energy and hence when the reverse integral reaches the start of the period there should be no deficit in energy (e.g. the last element in the reverse integral should be positive).

The reverse integral for period two is represented by the energy row matrix [-12 -5 -11 9] kWh where reading this matrix left to right represents moving backwards in time. The first element -12 kWh occurs during a negative interval and represents 12 kWh of deficit which must be stored from an earlier time to supply the load. The second element of -5 kWh occurs during a positive interval and it is smaller than first element however there is still a deficit of 5 kWh. The third element of -11 kWh occurs during a negative interval (-6 kWh) and the 11 kWh of deficit results from: i) the load during this interval (6 kWh) and ii) the deficit of 5 kWh from the second element. Finally the last element of 9 kWh means that there is both i) sufficient energy to supply the future load and ii) there is 9 kWh surplus energy within this period, which is not needed to supply the load and can be sold to the grid.

Hence Rule 1b.1 finds the critical capacity by finding the largest deficit in the reverse integral and so for period two the critical capacity is 12 kWh. The second part of Rule 1b is to create a sub-period between the start of the time series and the negative-critical time (not including the negative-critical time). For period two the negative-critical time is at the 5 hr point in Fig. A.3a and hence the created sub-period is [20 -6 7] kWh. Then Rule 1 is applied to this sub-period and since this sub-period only contains one negative interval then Rule 1a identifies the critical capacity of 6 kWh. Hence period two has two critical capacities; 12 kWh and 6 kWh

Rule 1b.1 is validated in Fig. A.3b which simulates the SoC for storage capacities of: i) 1 kWh below the first and second critical capacities, ii) 1 kWh above the second critical capacity, and iii) at each of the critical capacities. Note the first critical capacity occurs between the times 5 to 6 and the second critical capacity occurs between the times 3 to 4. These times refers to the interval over which GSE would occur when storage is sized below a critical capacity e.g. if storage is sized below 12 kWh then the first critical capacity loses load between time 5 and time 6.

For storage capacities between the first critical capacity (12 kWh) and the second critical capacity (6 kWh) the GSE is linearly related to the difference between 12 kWh and the storage capacity, e.g. for the 11 kWh storage simulation there is GSE of 1 kWh and for the 7 kWh storage simulation there is 5 kWh ofGSE.

Below the second critical capacity, the relationship of the GSE to storage capacity changes as seen by the 5 kWh storage simulation where there is 8 kWh of GSE. This GSE is comprised of 7 kWh from the first critical capacity (between hour 5 and hour 6) and 1 kWh from the second critical capacity (between hour 2 and hour 4). This separation of GSE for 5 kWh of storage is marked in Fig. A.3b.

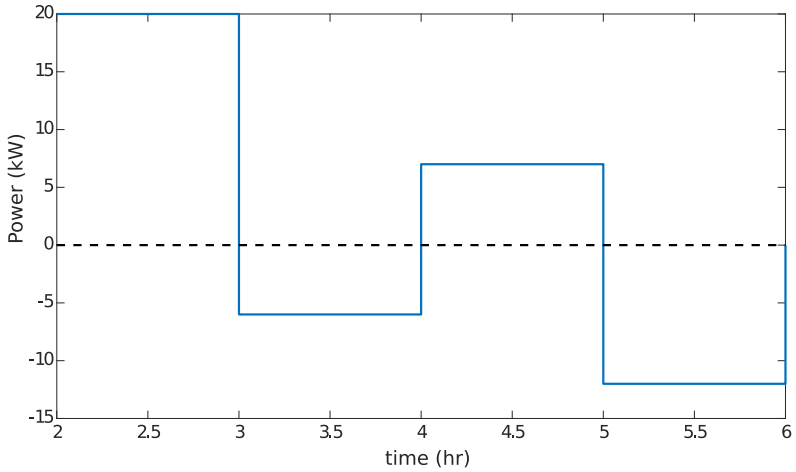

(a)

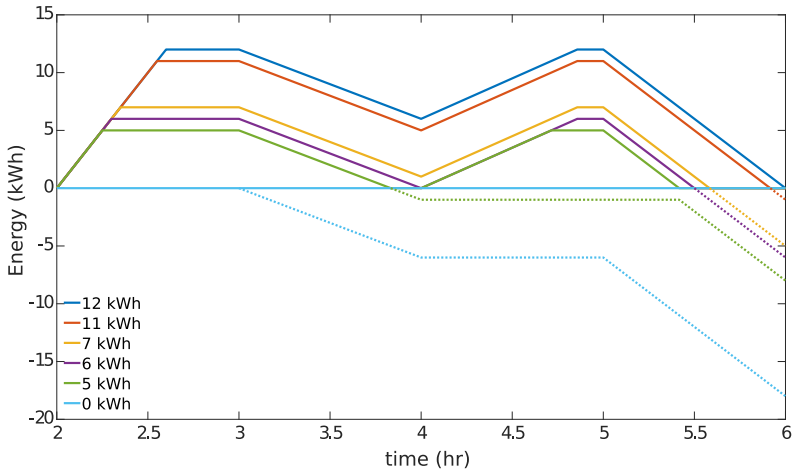

(b)

Figure A.3: Example period two

Rule 1b.1 For periods containing more than one negative interval, energy may need to be stored across multiple positive and negative intervals. Hence the reverse integral (the integral beginning at the end of the period and moving towards the start) is performed which represents the deficit/surplus of net generated energy between a given time and the end of the period. A deficit at a given time represents that energy is required from earlier in the period to supply the load between that given time and the end of the period. The largest deficit in the reverse integral is a critical capacity and the time of the deficit is called the negative-critical time. Between the start of the period and the negative-critical time (not including the negative-critical time), a sub-period is formed which is then examined using Rule 1.

A.4 Period Three

In the discussion of Rule 1b.1, in period two the negative-critical time occurred at the last load interval in the period and hence after the negative-critical time there is

no positive/negative intervals. Period three presents a case where positive/negative intervals occur after the negative-critical time which may contain further critical capacities.

The third period has a power row matrix [17 -9 8 -15] kW and by following Rule 1b.1 has a reverse integral of [-15 -7 -16 17] kWh. Hence the critical capacity of 16 kWh is found and the negative-critical time occurs at the third index in the reverse integral which corresponds to the second index in the power row matrix (hour 7 to 8 in Fig. A.4a). From Rule 1b.1 the sub-period between the start of the period and the negative-critical time would be the sub-period [17] which does not contain a critical capacity. It can be shown by simulation (Fig. A.4b) there there exists another critical capacity between the negative-critical time and the end of the period.

Rule 1b.2 creates a sub-period between the negative-critical time (not including the negative-critical time) and the end of the period. Rule 2a is then applied to this sub-period which states that if a sub-period created by Rule 1b.2 contains only one generation interval then the critical capacity in that sub-period is equal that generation interval's energy. For period three the sub-period created by Rule 1b.2 has a power row matrix of [8 -15] kW which contains only one positive interval with energy 8 kWh and Rule 2a states this energy is a critical capacity. Hence period three contains two critical capacities: 16 kWh and 8 kWh.

Rule 1b.2 and Rule 2a are validated using the storage SoC simulation in Fig. A.4b which considers storage capacities of: i) 1 kWh below the first and second critical capacity, ii) 1 kWh above the second critical capacity, and iii) at each of the critical capacities. Note the first critical capacity occurs between times 6 to 10 and the second critical capacity occurs between the times 8 to 10.

When storage is sized below the first critical capacity (16 kWh) but above the second critical capacity then GSE occurs at the expected rate (1:1) between the times of 6 to 10. When storage is sized at the second critical capacity of 8 kWh, the first critical capacity has 1 kWh of GSE at times 8 and 7 kWh of GSE at time 10, for a total 8 kWh of GSE. When storage is 7 kWh (below the second critical capacity) then an additional 1 kWh of GSE occurs between times 8 to 10 such that the period has 10 kWh of GSE. The separation of GSE between the critical capacities is: i) the first critical capacity has 2 kWh of GSE at times 7 to 8 and 7 kWh of GSE at times 9 to 10, and ii) the second critical capacity has 1 kWh of GSE at time 10.

Rule 1b.2 The reverse integral is performed as described in Rule 1b.1 and if after the negative-critical time there are additional positive/negative intervals of time then this rule creates a different sub-period. The sub-period is between the negative-critical time and the end of the period and Rule 2 is then applied to this sub-period.

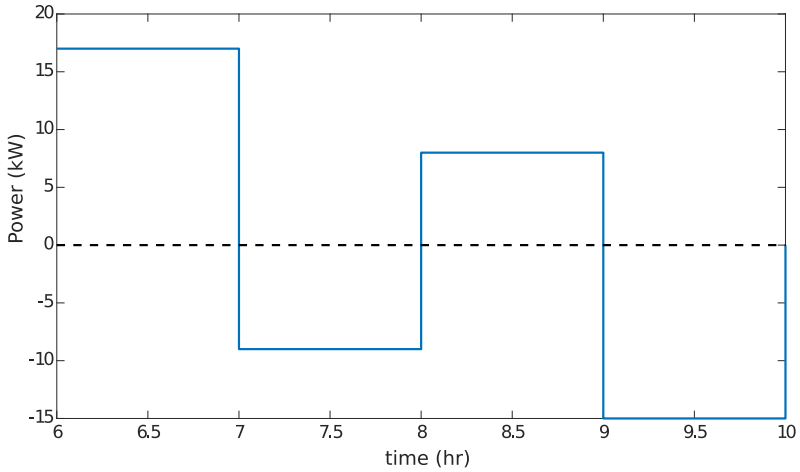

(a)

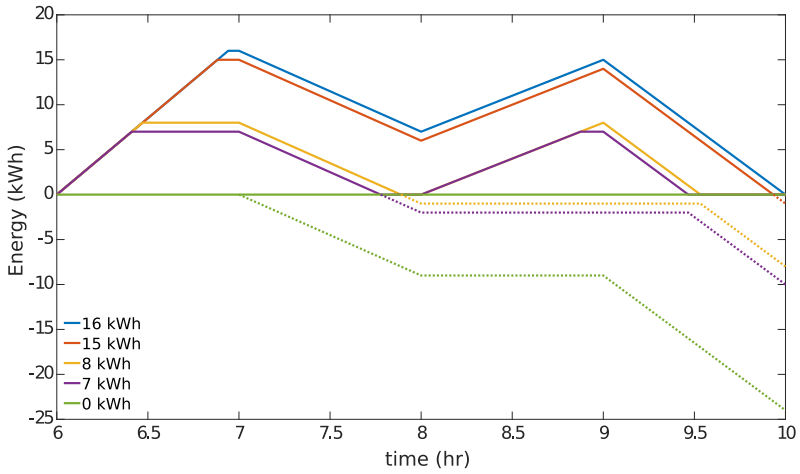

(b)

Figure A.4: Example period 3

Rule 2a For the sub-periods created by Rule 1b.2, if the sub-period contains only one positive interval than the energy in that interval is a load critical capacity.

A.5 Period Four

Since Rule 2a is the base case for the second rule there also exists a Rule 2b to consider when the sub-period created by Rule 1b.2 contains more than one positive interval. Period four is used to demonstrate this case by first applying the previously discussed sets of rules.

Period four has a power row matrix of [25 -13 12 -11 7 -10] kW. Beginning with Rule 1 the reverse integral is [-10 -3 -14 -2 -15 10] kWh with critical capacity of 15 kW. Applying Rule 1b.2 creates the sub-period of [12 -11 7 -10] kW which contains multiple positive intervals (12 kW and 7 kW). The critical capacity within this sub-period results from the inability to store sufficient energy across the multiple periods of positive load which causes a critical capacity. There are two cases: i) the inability

to transfer energy across the entire sub-period, e.g. [12 -11 7 -10] kW or ii) the inability to transferring energy across the end of the period, e.g. [7 -10] kW.

Hence the forward integral is considered for the two cases: i) [12 1 8 -2] kWh and ii) [7 -2] kWh. Rule 2b states the largest of these forward integrals is a critical capacity, which occurs at a time called the positive-critical time. Hence for this sub-period the critical capacity is 12 kWh and the critical time is the period 3 index (or time 12 in Fig. A.5a). Rule 2b creates two sub-periods and applies Rule 2 to them: i) between the critical time and the end of the current sub-period and ii) between the start of the current sub-period and the critical time. Hence the new sub-period is [7 -10] and which Rule 2a identifies has a critical capacity of 7 kWh. To summarise, period four has critical capacities of 15 kWh, 12 kWh and 7 kWh.

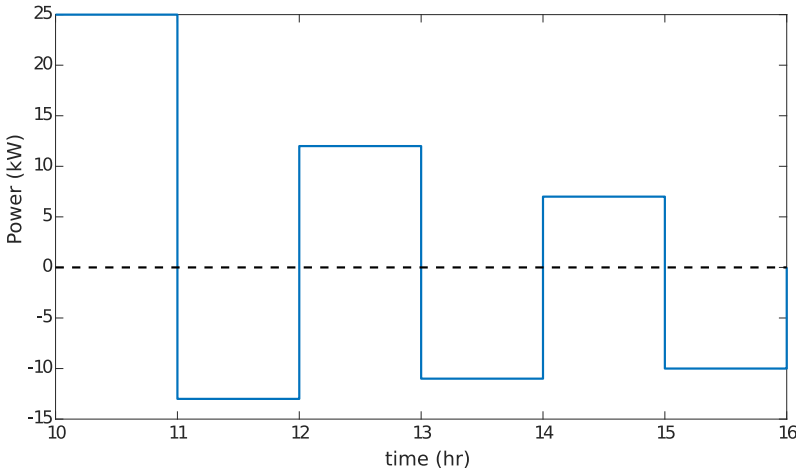

(a)

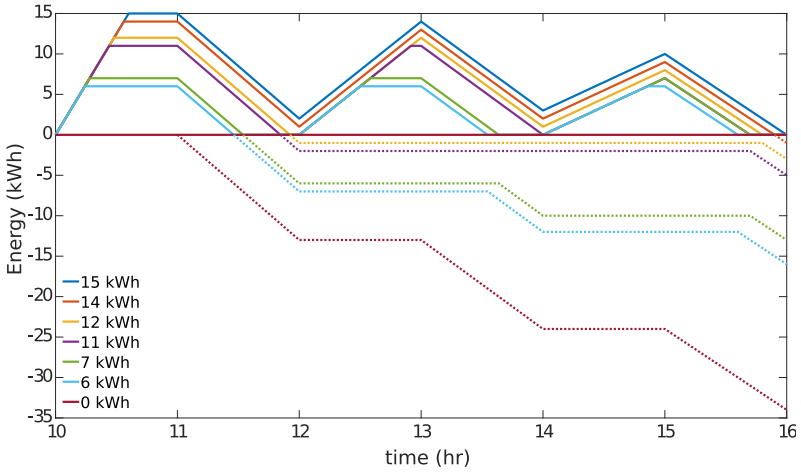

(b)

Figure A.5: Example period 4

Rule 2b is validated using the storage SoC simulation for period four in Fig. A.5b which considers storage capacities of: i) 1 kWh below the first and second critical capacity, ii) 1 kWh above the second critical capacity, and iii) at each of the critical capacities. The outcome is that Rule 2b identifies the critical capacity of 12 kWh at time 12 hr and 7 kWh at time 14 hr. When storage is below 11 kWh (below the

second critical capacity) it is seen that an additional 1 kWh of GSE occurs after time 12 hr, where an additional 1 kWh is added per kWh reduction in storage. Similarly when storage is below 6 kWh (below the third critical capacity) an additional 1 kWh of GSE occurs after time 14 hr.

Period four did not consider the second part of Rule 2b since the sub-period in Period four had a positive-critical time at the start of the sub-period. When the critical capacity is found via the forward integral, if then Rule 2b creates two sub-periods, i) one mentioned previously between the positive-critical time and the end of the current sub-period which is examined starting with Rule 2, and ii) the second is between the beginning of the forward integral (which contained the critical capacity) and the positive-critical time which is examined starting with Rule 1. An example of the second sub-period created will be seen in Period five.

Rule 2b For the sub-periods created by Rule 1.b.2, when there are multiple positive intervals in the sub-period, the forward integrals from each positive interval of time to each future positive intervals of time is considered. The forward integral with the largest energy defines a load critical capacity and the time this occurs is called the positive-critical time. Two sub-periods are created: i) the first is between the positive-critical time and the end of the current sub-period which is examined starting with Rule 2, and ii) the second is between the beginning of the forward integral (which contained the critical capacity) and the positive-critical time which is examined starting with Rule 1.

A.6 Period Five

Period five can be represented by the power row matrix [18 -12 7 -6 8 -14] kW and beginning with Rule 1 the reverse integral is [-14 -6 -12 -5 -17 1] kWh which contains a critical capacity of 17 kWh with a sub-period of [7 -6 8 -14] kW. Applying Rule 2 to this sub-period, the forward integral is [7 1 9 -5] kWh which identifies a critical capacity of 9 kWh. Following Rule 2b, a sub-period is created between the beginning of the forward integral containing the critical capacity and the positive-critical time, hence creating a sub-period of [7 -6] kW. Applying Rule 1 to this latest sub-period reveals the final critical capacity of 6 kWh. To summarise the critical capacities are 17 kWh, 9 kWh and 6 kWh.

Fig. A.6b shows the storage SoC simulation for period five which considers storage capacities of: i) 1 kWh below the first and second critical capacity, ii) 1 kWh above the second critical capacity, and iii) at each of the critical capacities. The key point here is that period five has demonstrated the second type of sub-period created by Rule 2b, hence for 6 kWh below the third critical capacity then an additional 1 kWh of GSE should occur after time 13 hr. This is demonstrated in Fig. A.6b.

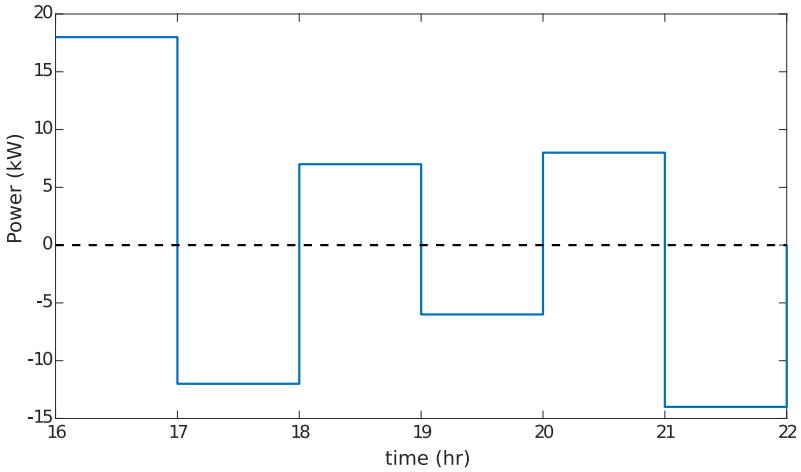

(a)

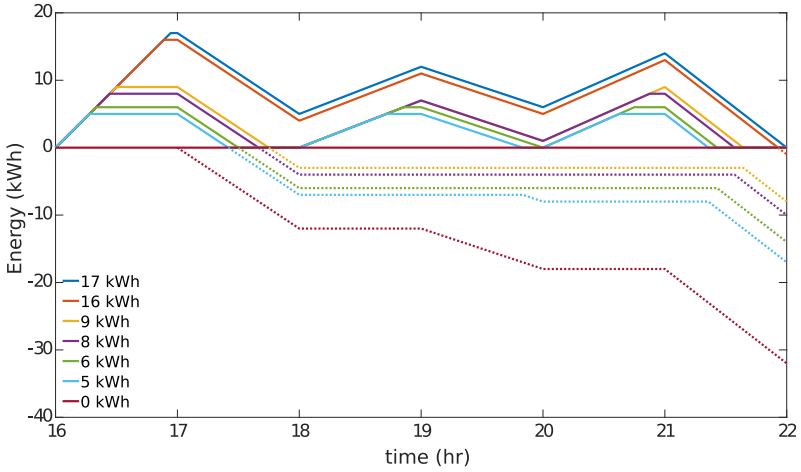

(b)

Figure A.6: Example period 5

A.7 Period Six

Period six provides an example of all rules being implemented, it has the two base case rules (Rule 1a and Rule 2a) and demonstrates both, i) the two sub-periods created by combining both Rule 1b.1 and Rule 1b.2, and ii) the two sub-periods created by both Rule 2b.

Period six has the power energy row matrix of [9 -5 16 -15 8 -5 6 -10 11 -3 2 -3 8 -18] kW. The rules are applied such that:

1. Beginning with Rule 1, the reverse integral is [-18 -10 -13 -11 -14 -3 -13 -7 -12 -4 -19 -3 -8 1] kWh with a critical capacity of 19 kWh and there are two sub-periods which occur.

2. The first sub-period created by Rule 1b.1 is p_1 =[9 -5] kW contains one positive interval hence Rule 1a finds a critical capacity of 5 kWh

3. The second sub-period created by Rule 1b.2 is p_2 =[8 -5 6 -10 11 -3 2 -3 8 -18] kW which then applies Rule 2.

4. The forward integral of the second sub-period, p_2, is summarised in Table A.1 which using Rule 2a identifies the critical capacity of 15 kWh and creates two additional sub-periods.

5. The additional sub-periods (from above) are labeled p_3 =[11 -3 2 -3] kW, which then applies Rule 1, and p_4=[8 -5 6 -10] which then applies Rule 2.

6. The above sub-period p_3 using Rule 1b has reverse integral [-3 -1 -4 11] kWh which has critical capacity 4 kWh and then Rule 1b.1 creates the sub-period [2 -3] and applies Rule 2 which identify a critical capacity of 2 kWh.

7. The remaining sub-period of p_4 when applying Rule 2 has two forward integrals of [8 3 9 -1] and [6 -10]. Hence by Rule 2b it has critical capacity of 9 kWh and creates a sub-period of [8 -5] which applying Rule 1 has a critical capacity of 5 kWh.

To summarise, the list of all critical capacities within this period is: [19 15 9 5 5 4 2] kWh. Note there is a repeated critical capacity of 5 kWh hence storage capacities below 5 kWh will have additional GSE of twice the regular rate.

Fig. A.7b shows the storage SoC simulation for period five which considers storage capacities of: i) 1 kWh below the first and second critical capacity, ii) 1 kWh above the second critical capacity, and iii) at each of the critical capacities. The key point here is that each rule has identified: i) where GSE will occur and ii) when GSE will occur for a given storage capacity. To summarise for sizing storage capacities less than each critical capacity, noting that sizing below each critical capacity adds 1 kWh of GSE per 1 kWh difference between the critical capacity and storage:

1. Below the first critical capacity (19 kWh) causes GSE between times 25 to 36 hrs.

2. Below the second critical capacity (15 kWh) causes GSE between times 30 to 36 hrs.

3. Below the third critical capacity (9 kWh) causes GSE between times 26 to 30 hours.

4. Below the fourth/fifth critical capacity (5kWh) causes two instances of GSE the first between times 22 to 24 hr and the second between times 26 to 28 hr.

5. Below the sixth critical capacity (4 kWh) causes GSE between times 30 to 34 hrs.

6. Below the seventh critical capacity (2kWh) causes GSE between times 32 to 34 hrs.

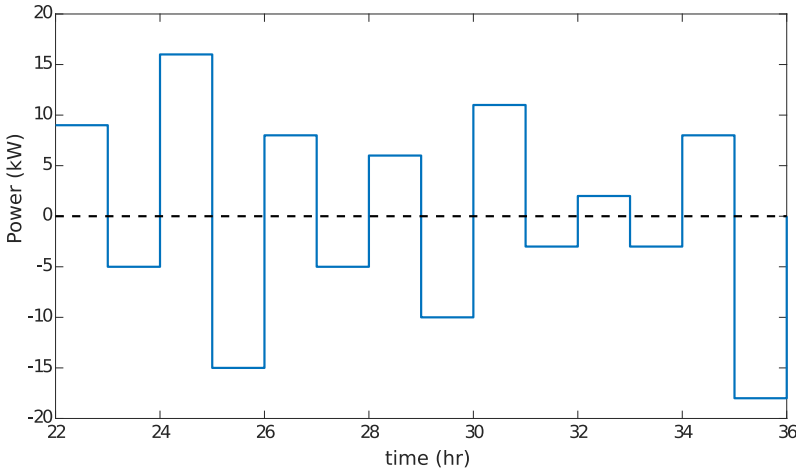

(a)

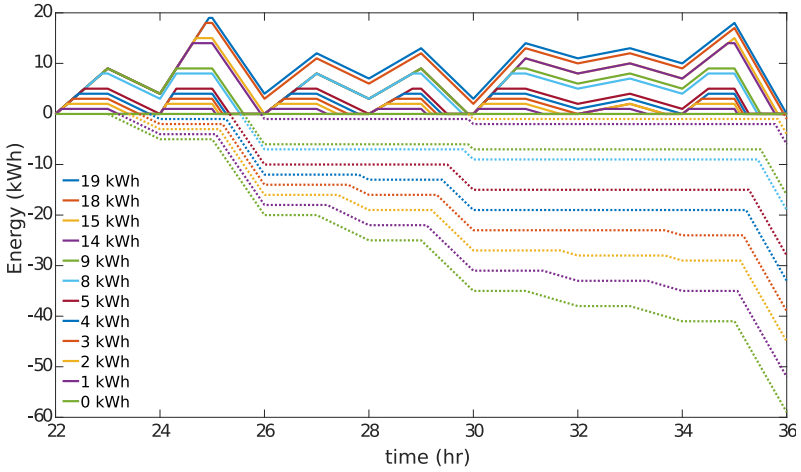

(b)

Figure A.7: Example period 6

A.8 Algorithm of Rules

The algorithm 3 is pseudocode describing the rules-based method, highlighting where the rules are applied.

Table A.1: Demonstrating Rule 2.b for the given original sub-period, each column represents a time step for the sub period and each row represents the forward integral starting at a given time step.

	t_1	t_2	t_3	t_4	t_5	t_6	t_7	t_8	t_9	t_{10}
Original	8	-5	6	-10	11	-3	2	-3	8	-18
t_1	8	3	9	-1	10	7	9	6	14	-4
t_3			6	-4	7	4	6	3	11	-7
t_5					11	8	10	7	**15**	-3
t_7							2	-1	7	-11
t_9									8	-10

Algorithm 3 Pseudo code for rules based load critical capacity identification

Notation: The input is the Time series (T) with one or more alternating positive negative periods and the output is the list of critical capacities (CC)

Function - Rule 1:

if T contains only 1 negative period **then** [**Rule 1a - The BaseCase**]
    The Negative period is a CC
    Return
else [**Rule 1b**]
    Find the CC between last negative period and first negative period and identify its beginning and end times [t_a, t_b]
    if if [t_a] occurs after the first negative period **then** [**Rule 1b.1**]
        Create a sub-period between the start of the time series and the negative time interval before t_a
        Call Rule 1 on the sub-period
    end if
    if There exists any positive time periods in the series between [t_a, t_b] **then** [**Rule 1b.2**]
        Create a sub-period between the first positive period after t_a to t_b
        call Rule 2 on the sub-period
    end if
end if

SubFunction-Rule 2:

if T contains 1 positive period **then** [**Rule 2a - The BaseCase**]
    The Positive period is a CC
    Return
else [**Rule 2b**]
    Find the CC between the first positive period and last positive period and identify its beginning and end times [t_c, t_d]
    if if [t_d] occurs before the end of the time series **then**
        Create a sub-period between the first positive interval after t_d and the last positive period in the time series
        Call Rule 2 on the sub-period
    end if
    if There exists any negative time periods in the series between [t_c, t_d] **then**
        Create a sub-period between the first negative period after t_c to t_d
        Call Rule 1 on the sub-period
    end if
end if

Appendix B

Critical Capacity Analysis: Matlab Code

The following is the matlab code used to perform the CCA analysis. There are two major adaption to the code. The first is seen on lines 32 to 50 where cycles are separated into load critical capacity and generation critical capacity. The second is seen on lines 89 to 113 where the residues are separated into load critical capacity and generation critical capacity.

```
1  function [LoadCC, LoadCC_Time, GenCC, GenCC_Time,
       AdditionalInjected, AdditionalInjectedInterval,
       CycleType]=CCA_Matlab(NetGenPower)
2
3  %First seperate netgenpower into each positive/negative
       sections, andrecord the time of each positive/negative
        interval
4      [PeakTroughs, TimePT]=AccumPeakTrough(NetGenPower);
5
6      %Determine the accumulated peak/trough data (to be
           rainflow counted)
7      if(PeakTroughs(1)~=0)
8          PeakTroughs=[0 PeakTroughs];
9          TimePT=[0 0; TimePT];
10     end
11         APT=cumsum(PeakTroughs);
12
13         s=nan(1,length(APT));
14
15     % Application of rainflow counting algorithm
16         n=0; NumLoadCC=0; NumGenCC=0; NumAI=0;
17
18         Init=nan(1,length(APT));
19
20         CT=Init; GenCC=Init; LoadCC=Init; GenCC_Time=[
               Init Init];LoadCC_Time=[Init Init];
21         AdditionalInjected=Init;
               AdditionalInjectedInterval=Init;
22
23     CycleType=nan(2,length(APT));
24       for index=1:length(APT)
25         n=n+1; s(n)=APT(index); %Constructs the stack
               list which the rainflow algorithm is applied
               to.
26         CT(n)=index; %building the time list
```

```
27          while((n>=3) && abs(s(n-1)-s(n-2)) <= abs(s(n)-s(n
               -1)))
28            ampl=abs(s(n-1)-s(n-2));
29            if(n==3) %in Rainflow method this is called a
                 halfcycle
30              StartT=CT(1); EndT=CT(2);
31
32              if(s(n-1)-s(n-2)>0 && s(n)-s(n-1)<0) %
                   found a value on the right hand (Gen CC
                   ) side of the rainflow plot
33                NumGenCC=NumGenCC+1;
34                GenCC(NumGenCC)=ampl; %half
35                CycleType(2,NumGenCC)=0.5;
36                GenCC_Time(NumGenCC,:)=[TimePT(StartT
                     ,2) TimePT(EndT,2)];
37                if s(n-2)<0
38                  NumAI=NumAI+1;
39                  AdditionalInjected(NumAI)=s(n-2);
40                  AdditionalInjectedInterval(NumAI)
                       =TimePT(StartT,2);
41                end
42
43              else % found a value on the left hand (
                   Load CC) side of the rainflow plot
44                NumLoadCC=NumLoadCC+1;
45                LoadCC(NumLoadCC)=ampl;
46                StartT=CT(n-2); EndT=CT(n-1);
47                LoadCC_Time(NumLoadCC,:)=[TimePT(StartT
                     ,1) TimePT(EndT,2)];
48                CycleType(1,NumLoadCC)=0.5;
49              end
50                s(1)=s(2); s(2)=s(3);n=2; %remove the
                     first point and move back 1 step
51                CT(1)=CT(2); CT(2)=CT(3);
52
53            else %This is a full cycle in the rainflow
                 method. These values exist on both the left
                  hand side and right hand side of rainflow
                 plot (Value is both a gen. & load CC)
54                StartT=CT(n-2); EndT=CT(n-1);
55                NumLoadCC=NumLoadCC+1;
```

```
56                LoadCC(NumLoadCC)=ampl;
57                CycleType(1,NumLoadCC)=1;
58                 NumGenCC=NumGenCC+1;
59                 GenCC(NumGenCC)=ampl; %full
60                 CycleType(2,NumGenCC)=1;
61
62                   if(s(n-1)-s(n-2)>0) %transition Low to
                         High - correct time index
63                        LoadCC_Time(NumLoadCC,:)=[TimePT(
                             StartT,2) TimePT(EndT,2)];
64                        GenCC_Time(NumGenCC,:)=[TimePT(
                             StartT,2) TimePT(EndT,2)];
65                   else % transition from high to low -
                        time index is fine.
66                             LoadCC_Time(NumLoadCC,:)=[
                                TimePT(StartT,1) TimePT(
                                EndT,2)];
67                             GenCC_Time(NumGenCC,:)=[TimePT
                                (StartT,1) TimePT(EndT,2)];
68                   end
69
70                s(n-2)=s(n);CT(n-2)=CT(n);n=n-2; %remove
                     the previous two points and move back
                     two steps
71             end
72          end
73       end
74
75       %sort the Generation CC values before the residues
            are considered.
76       if APT(2)<0
77           NumGenCC=NumGenCC+1;
78
79           IndexFirstNeg=0;
80            for j=1:length(APT)
81               IndexFirstNeg=j;
82               if(APT(j)>0)
83                  IndexFirstNeg=IndexFirstNeg-1; %step back
84                  break;
85               end
86           end
```

```
87          FirstNegative=min(APT(1:IndexFirstNeg));MFNTime=
               min(APT(1:IndexFirstNeg))==(APT(1:
               IndexFirstNeg));
88          GenCC(NumGenCC)=abs(FirstNegative); %First Time
89          MFNFirstTime=TimePT(MFNTime',:);
90          GenCC_Time(NumGenCC,:)=[MFNFirstTime(1)
               MFNFirstTime(2)];
91          CycleType(2,NumGenCC)=-1;
92      end
93
94      % Dealing with residues,  positive to negative
           residues are Load CC and neg->pos are Gen CC
95      for index=1:n-1
96          ampl=s(index)-s(index+1);
97          StartT=CT(index); EndT=CT(index+1);
98          if(ampl>0) % left hand side of rainflow plot
99              NumLoadCC=NumLoadCC+1;
100             LoadCC(NumLoadCC)=ampl;
101             LoadCC_Time(NumLoadCC,:)=[TimePT(StartT,1)
                   TimePT(EndT,2)];
102             CycleType(1,NumLoadCC)=0;
103         else % Right hand side of rainflow plot
104             NumGenCC=NumGenCC+1;
105
106             GenCC(NumGenCC)=abs(ampl); %res
107             GenCC_Time(NumGenCC,:)=[TimePT(StartT,1)
                   TimePT(EndT,2)];
108             CycleType(2,NumGenCC)=0;
109             if s(index)<0
110                 NumAI=NumAI+1;
111                 AdditionalInjected(NumAI)=s(index);
112                 AdditionalInjectedInterval(NumAI)=TimePT(
                       StartT,1);
113             end
114         end
115     end
116
117     %Original values were the same length as the peak/
           through vector. This reduces the output to only
           the required size.
```

```
118     LoadCC=LoadCC(1:NumLoadCC); LoadCC_Time=LoadCC_Time
           (1:NumLoadCC,:);
119     GenCC=GenCC(1:NumGenCC); GenCC_Time=GenCC_Time(1:
           NumGenCC,:);
120
121     AdditionalInjected=AdditionalInjected(1:NumAI);
           AdditionalInjectedInterval=
           AdditionalInjectedInterval(1:NumAI);
122
123     %sorting all outputs
124     [LoadCC, CCIndex_sort]=sort(LoadCC,'descend');
125     LoadCC_Time=LoadCC_Time(CCIndex_sort,:);
126     CycleType(1,1:NumLoadCC)=CycleType(1,CCIndex_sort);
127     CycleType=CycleType(:,1:max(NumLoadCC,NumGenCC));
128 end
129
130 function [PeakTroughs, TimePT]=AccumPeakTrough(
       DataToSeperate)
131     % seperate data into each positive/negative sections,
           and record the time of each positive/negative
           interval
132     Pos=DataToSeperate; Neg=DataToSeperate;
133         %Dealing with inital value ==0
134         if DataToSeperate(1)==0
135             if(DataToSeperate(2)>0) %if the first period
                   is positve so neg list should ignore
136              Pos(Pos<0)=nan; Neg(Neg>=0)=NaN;
137             else %First period negative so Pos list
                   should ignore
138                     Pos(Pos<=0)=nan; Neg(Neg>0)=NaN;
139             end
140         else %Any other zero values are added to the neg?
141            Pos(Pos<=0)=nan; Neg(Neg>0)=NaN;
142         end
143
144     %seperating the positive and negative period
145     [PosPeriod, PosTime]=SepNaN(Pos,1);[NegPeriod,
           NegTime]=SepNaN(Neg,1);
146
147     %The group of positive and negatives can now be sumed
           and constructed into [p n p n] ect similar for
```

```
        the time series [p p; n n; p p; n n]
148     PeakValue=cellfun(@sum,PosPeriod)';TroughValue=
          cellfun(@sum,NegPeriod)';
149
150     PeakTroughs=NaN(1,length(PeakValue)+length(
          TroughValue));TimePT=NaN(length(PeakValue)+length(
          TroughValue),2);
151
152     % Check if input data was troughs or peaks only
153     if isempty(PosTime)
154         PeakTroughs=TroughValue;
155         TimePT=NegTime;
156     elseif isempty(NegTime)
157         PeakTroughs=PeakValue;
158         TimePT=PosTime;
159     %Which comes first? peak or trough?
160     elseif PosTime(1,1)==1 %peak first than trough [p n p
          n]
161         PeakTroughs(1:2:end)=PeakValue;PeakTroughs(2:2:
              end)=TroughValue;
162         TimePT(1:2:end,:)=PosTime;TimePT(2:2:end,:)=
              NegTime;
163     elseif NegTime(1,1)==1 %trough first than peak [n p n
          p]
164         PeakTroughs(1:2:end)=TroughValue;PeakTroughs(2:2:
              end)=PeakValue;
165         TimePT(1:2:end,:)=NegTime;TimePT(2:2:end,:)=
              PosTime;
166     else
167         error('Could not determine if positive or
              negative period is first')
168     end
169
170 end
171
172 function [SepCell, TimeSeperated]=SepNaN(A,option)
173 %configuring default options
174 if(nargin<2)
175    option=1;
176 end
177    if ~isnan(A(end))
```

```
178             A=[A NaN];
179     end
180
181       idx2=find(isnan(A)); idx1=[1 idx2(1:end-1)+1];  n=
            numel(idx1);
182      Sep=cell(n,1);p=1;TimeRecord=nan(n,2);
183
184     if(option~=1)% including the nan's
185      for k=1:n
186        ExtractedSec=A(idx1(k):idx2(k)-1);
187        if(~isempty(ExtractedSec))
188            Sep{p}=(ExtractedSec);
189            Sep{p+1}=NaN;
190            TimeRecord(p,:)=[idx1(k) idx2(k)-1];
191            TimeRecord(p+1,:)=[idx2(k) idx2(k)];
192            p=p+2;
193        else
194            Sep{p}=NaN;
195            TimeRecord(p,:)=[idx1(k) idx2(k)];
196            p=p+1;
197        end
198      end
199      SepCell=Sep;
200      TimeSeperated=TimeRecord;
201
202      else  %Removing the NaNs
203          for k=1:n
204            ExtractedSec=A(idx1(k):idx2(k)-1);
205            if(~isempty(ExtractedSec))
206                Sep{p}=(ExtractedSec);
207                TimeRecord(p,:)=[idx1(k) idx2(k)-1];
208                p=p+1;
209            end
210          end
211          SepCell= Sep(1:p-1);
212          TimeRecord(p:end,:)=[];
213          TimeSeperated=TimeRecord;
214     end
215 end
```